COPYRIGHT

TRIBHUVAN UNIVERSITY

INSTITUTE OF ENGINEERING

PULCHOWK CAMPUS,LALITPUR

DEPARTMENT OF CIVIL ENGINEERING

The undersigned certify that they have read, and recommended to the Institute of Engineering for acceptance, a thesis entitled **"Analysis of double curvature arch dam and abutment stability using three dimensional nonlinear finite element numerical modeling in MATLAB R2013a of Budhigandaki Hydroelectric Project**" submitted by **Aanand Kumar Mishra** in partial fulfilment of the requirements for the degree of Master in Geotechnical Engineering.

_____

Supervisor, Prof. Dr. Akkal Bahadur Singh

Department of Civil Engineering

Master Programme in Geotechnical Engineering
Pulchowk Campus, Lalitpur

_____

External Examiner:

Er. Prakash Shrestha

_____

Dr. Indra Prashad Acharya
Co-ordinator
Master Programme in Geotechnical Engineering
Pulchowk Campus, Lalitpur

ACKNOWLEDGEMENT

First of all, I would like to express my gratefulness to my supervisor **Prof. Dr. Akal Bahadur Singh**; for his invaluable advices, patience and encouragement throughout this work.

. Throughout the work with the arch dam on Budhigandaki River, Budhigandaki Hydroelectric Development Committee, Tripureshwar Marga has helped out with valuable information and knowledge about the structural, geological and geotechnical data.

I'm grateful to Late **Prof. Padma Khadka**, former Coordinator of M.Sc. in Geotechnical Engineering, Pulchowk Campus,Lalitpur for his constant support, motivation and management. I'm grateful to **Dr. Indra Prashad Acharya**, Coordinator of M.Sc. in Geotechnical Engineering, Pulchowk Campus, Lalitpur for his motivation, support and management in crucial moments of this work.

I'm thankful to my friends and family for their continuous support and motivation for the achievement of this work.

At last but not the least, I would like to thank all known and unknown persons and events which motivated me during complex of times and provided strings to attach me with this work.

Er. Aanand Kumar Mishra

Kathmandu

November, 2016

TABLE OF CONTENTS

LIST OF TABLES

LIST OF FIGURES

ABBREVATIONS

HIDCL	Hydro electricity Investment and Development Company
INPS	Integrated Nepal Power System
HEP	Hydro Electric Project
HPP	Hydro Power Project
GON	Government of Nepal
NEA	Nepal Electricity Authority
U/S	Up stream
D/S	Down Stream
GSI	Geological Strength Index
RMR	Rock Mass Rating
RQD	Rock Quality Designation
JRC	Joint Roughness Coefficient
JCS	Joint wall Compressive Strength
FEM	Finite Element Method
FDM	Finite Difference Method
BEM	Boundary Element Method
PDE	Partial Differentiation Equation
DEM	Distinct Element Method
DDA	Discontinuous Displacement Analysis
FOS	Factor of Saftey
FSL	Full supply level
MOL	Minimum operation level
RL	Reduced level

SYMBOLS

λ_E	Factor of safety
λ_ϕ	Factor of safety
τ_{max}	Shear strength of joint
τ	Shear stress at joint
σ_{ci}	Uniaxial compressive strength
m_i	Material constant of intact rock
m_b	Material constant of rock mass
a	Hoek and Brown parameter
s	Hoek and Brown parameter
σ	Stress
ε	Strain
{a}	nodal displacement vector
{ }	Vector
u	Displacement
A	Transformation matrix
N	Shape function
B	Strain function
D	Constitutive matrix
F	Force vector
K	Stiffness matrix
P	Concentrated force
Γ	Surface area
V	Volume
Δ	Small increment
E_i	Modulus of elasticity of intact rock

E_{rm}	Modulus of elasticity of rock mass
E_o	Modulus of elasticity of infilling
Gi	Shear modulus of intact rock
G_{rm}	Shear modulus of rock mass
Φ_r	Residual frictional angle
Φ_b	Basic frictional angle
I	Identity matrix
$[\ ]^{'}$	Transpose of matrix
$\delta/\delta x$	Partial differentiation
f	Yield function
g	Plastic potential function

ABSTRACT

As Nepal needs peaking type electric plant to solve the current deficiency during dry season, storage type hydroelectric plant is very promising option for this problem. For construction reservoir of dam is required and in context of Nepal where geology is young and construction of large scale dams are not in practice till date, stability analysis of such large scale dam along with its foundation is important job, so this thesis is dedicated towards the three dimensional finite element analysis of double curvature arch dam, abutment and foundation. This thesis includes preparing the solid deformable model representing the purposed dam for the Budhi Gandaki hydroelectric project in Budhi Gandaki River near Benighat and its foundation, generation of hexahedral elements for continuum portion and interface element for the discontinuity in foundation, developing partial deferential equations representing the three dimensional finite element solution for the model which considers the elastic plastic behaviour of rock mass in foundation through return field method and study of variation in the deformation and stresses in dam and foundation with different foundation rock mass properties . To perform pure mathematical modelling of problem, MATLAB is used as programming language, which gives the understanding of analysis process and numerical techniques that is not achieved by using commercial applications based on finite element analysis.

Identification of potential failure plane or surface is performed and factor of safety is evaluated for sliding through plane or wedge formed at abutment or beneath concrete arch dam in foundation rock mass. Evaluation of safety is done at different stages of loading (excluding dynamic loading and seismic loading) which includes hydrostatic loads, gravitational loads and pore pressure as major loadings. Different states of discontinuities (with and without filling material, weathered and unweathered condition) are considered for safety for potential failure. Failure of rock mass is evaluated according to failure criterion and deformation of rock mass is evaluated.

1. INTRODUCTION

1.1 Background

According to figures of 2011 provided by hydroelectricity investment and development company limited (HIDCL) in Integrated Nepal Power System (INPS) annual peak demand was 946.10 MW and dry season generation was 450 MW giving deficiency of 450 MW, which will rise by 8.85% annually, as a result INPS will continue to be a sub-optimal system in the absence of peaking plants, resulting in the spilling of water during the wet season and capacity deficit during the dry season.[1,3] A storage project of sufficient capacity is an ideal remedy for such a situation. To address this situation, NEA is looking into implementing a storage hydropower plant to firm up the overall generation capacity in the INPS. Kulekhani I and Kulekhani II totalling to 92 MW are the only storage hydropower plants capable of seasonal regulation in the 705MW capacity INPS. As result Government of Nepal (GON) is planning to develop storage projects in the near future and Budhi Gandaki HEP is considered one of the best candidate project for the development due to its location very near to the load centre and is right sized and located storage project which has capability to cope with this heavy load shedding and varying demand.

1.2 Project description

1.2.1 General

The Budhi Gandaki Hydroelectric Project is a storage type of project located between boundary of Gorkha and Dhading district on the Budhi Gandaki River in Central/ Western Developmentregion of Nepal. The Budhi Gandaki Hydropower Project is located on the Budhi Gandaki River, approximately 2km from its confluence with Trishuli River at Benighat. Benighat can be accessed by the Prithivi Highway linking Kathmandu and Pokhara about 80 km from Kathmandu. The prefeasibility study of Budhi Gandaki Hydropower Project found the project with the option of 1200 MW.

1.2.2 Geology and geotechnical description

The Dam is located in the most favourable stretch of the river. The bedrock consists of quartzite, phyllite and siliceous dolomite of the Nourpul formation. Quartzite and alternant quartzite-phyllite are predominant in the upstream part, where

the dam is located. The structural setting is characterized by overturned stratigraphic sequence, with bedding strike near perpendicular to the river and dip towards upstream. The bedding dip is very steep at the river level and decreases in the upper part of the abutments.

The project site is delimited by two zones figure 1.1 of intense tectonic deformation: to the north, the contact between the Nourpul and the Dandagaon formations; to the south, a regional fault zone identified during the Inception phase and named Budhi Gandaki Mauwa Khola fault. Between the two deformation zones, the tectonic stress was accommodated mostly by second order fractures and shear zones, with different orientations and variable persistence. The resulting rock mass assembly consists of well interlocked blocks.

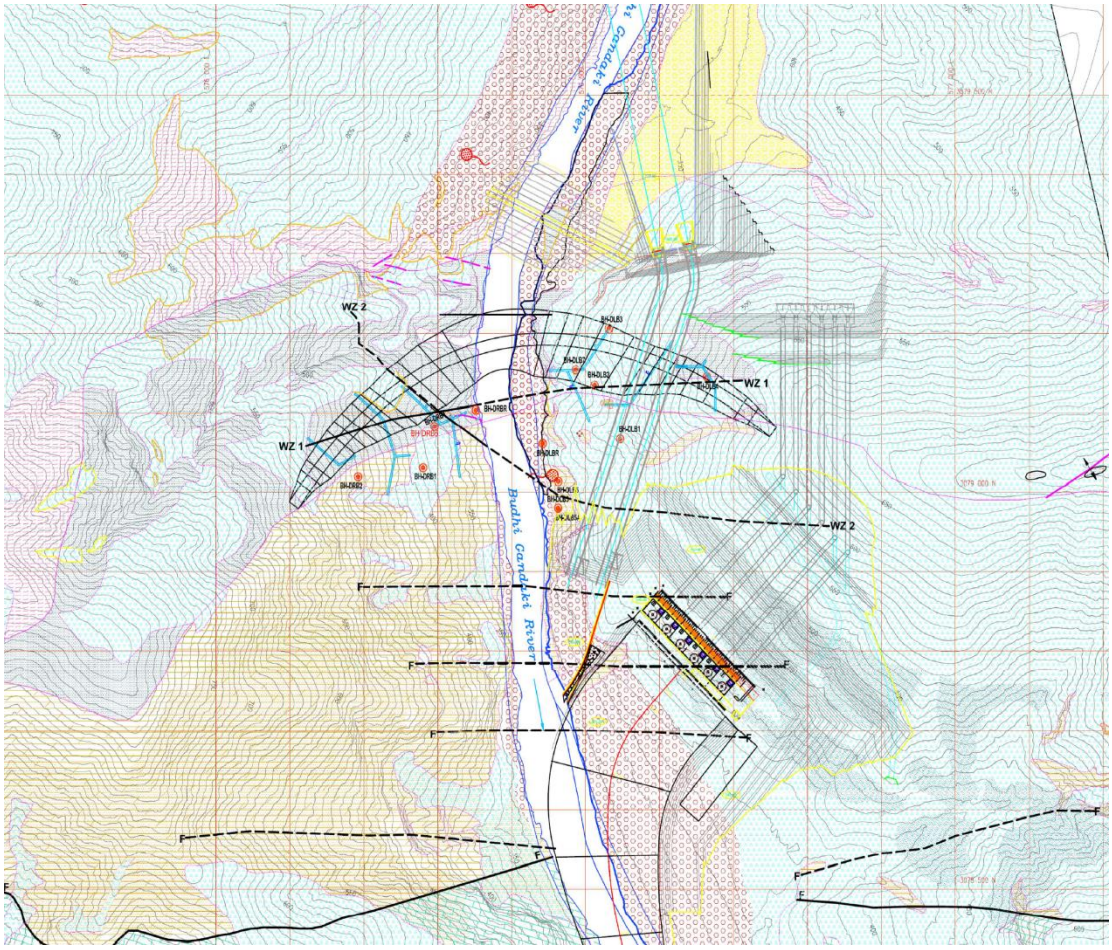

Figure 1-1 Geological condition of Budhi Gandaki dam site (after feasibility study and detailed design of BudhiGandaki HEP)

Two noticeable weakness zones are found on upstream and downstream of dam. These weak zones will require specific treatment but, it has not been considered in this work. One of the discontinuity sets identified at the dam site, including shears, features low dip to the SW. This attitude is unfavourable for the stability of the Left Abutment. The amplitude of the potential instability depends on the persistence of these discontinuities, which is difficult to apprehend precisely at the present stage. The unfavourable discontinuities were dully identified in the exploratory galleries, in particular in the GLM and GLL galleries. Their strength characteristics at various scales were evaluated based on field observations and strength tests of the sheared infill. Finally, potential failure scenarios involving these discontinuities have been considered for stability calculations according to "Londe wedge" method. The analysis performed for pseudo static conditions corresponding to the design earthquakes, OBE and SEE, concluded that the wedge stability is not critical.In the Left Bank, former slope instabilities are inferred from the morphological pattern, considerable thickness of the overburden and the presence of open discontinuities in the upper part of the dam abutment.

1.2.3 Dam features

According to feasibility study and detailed design of Budhi Gandaki HPP four dam types were analysed i) Clay core rock fill dam, ii) Concrete face rock fill dam, iii) Arch-gravity dam and iv) Double curvature arch dam. In report it has been concluded double curvature arch dam is most cost effective. Total volume of dam will be 5753000 m^3 of concrete, with total height of dam between deepest foundation level (EL 280m) and the crest parapet (EL 543) is 263m. The dam width at the base is 80m and the developed dam crest length is 760m. According to feasibility report drawing of dam purposed is as in fig 1.2 and 1.3.[3]

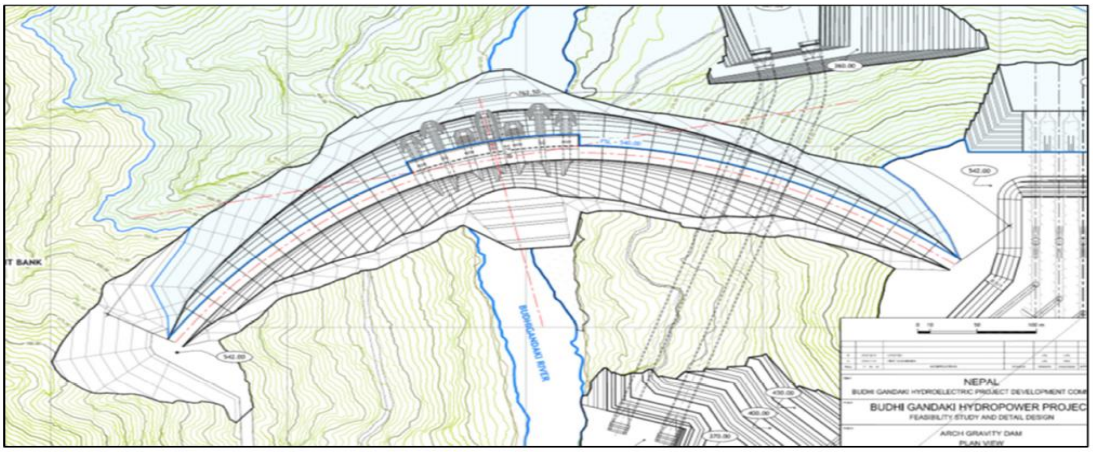

Figure 1-2 plan double curvature arch dam over Budhigandaki River (feasibility study and detailed design of Budhigandaki HEP)

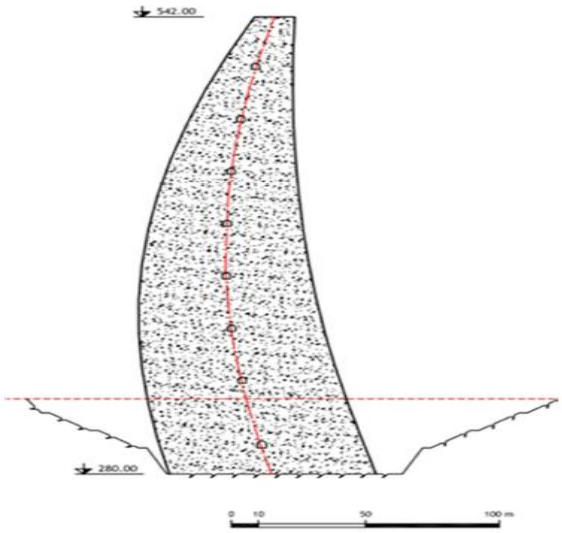

Figure 1-3 cross section of arch dam

1.3 Historical Cases

Historically, arch dam failures have resulted primarily from foundation deficiencies. Sliding of large blocks (bounded by geologic discontinuities) within the foundation or abutments of an arch dam resulted in some of the biggest civil engineering disasters of the 20th Century. Typically, these failures were sudden, brittle, and occurred on first-filling of the reservoir. The abutment stability analysis evaluation considers potential for rock block wedges in the foundation to become unstable due to loads from the dam. Potential rock blocks are formed by intersecting discontinuities (i.e. joints, faults, bedding planes) in the rock mass. Certain notable examples of such type of failure are:

1.3.1 St. Francis Dam: 1928

St. Francis Dam was a curved concrete gravity dam constructed in San Francis Quito Canyon approximately 45 miles north of Los Angeles California. The dam was 205 feet high, 16 feet thick at the crest, and 175 feet thick at the base. The crest length of the main dam was about 700 feet. Analysis of the disaster indicated that failure initiated by sliding along weak foliation planes in the left abutment, perhaps on a remnant of an old Paleo-landslide (Anderson et al, 1998).

1.3.2 Malpasset Dam: 1959

Malpasset Dam was a 216-foot-high thin concrete arch structure completed in 1954 in southern France. The dam was 5 feet thick at the crest and 22 feet thick at the base. The dam was founded on gneiss. The failure was attributed to sliding of a large block of rock in the left abutment of the dam formed by an upstream dipping fault on the downstream side, and a foliation shear on the upstream side. Experiments suggested that the arch thrust acting parallel to the foliation decreased the permeability perpendicular to the foliation to the point where large uplift pressures could have built up behind a sort of underground dam. The uplift forces in combination with the dam thrust were sufficient to cause the block to slide, taking the dam with it (Anderson et al 1998).

1.3.3 El Fraile :

The dam experienced a major slide on one of the abutments during filling. The dam did not collapse. A concrete thrust block abutment was constructed and the dam was saved.

1.4 Objective

The objective of this study is to carry out stress strain analysis of the dam and its foundation of arch dam through numerical finite element modelling. In general the objectives are listed as below:

i) To use MATLAB R2013 as fourth generation programming language for analysis and modelling.

ii) To perform the non-linear finite element numerical modelling of arch dam and its foundation.

iii) Numerical modelling of geometric nonlinearity or discontinuity using interface element.

iv) Use of return field method for elastic-plastic analysis of rock mass.

v) Analysis of variation in the deformation and stress with in dam and foundation for different properties of rock mass.

vi) To identify the possible mode of sliding of plane or wedge at abutments or foundation.

vii) Stability analysis of abutments and foundation of arch dam over Budhi Gandaki River.

viii) Implementation of Hoek-Brown yield criterion and Barton's shear strength criteria for rock mass.

ix) Determination of factor of safety for rock mass and wedge abutment failure at different loading condition.

1.5 Scope

This thesis covers the implementation of finite element analysis for numerical modelling of double curvature arch dam and its foundation. Hexahedral element is used for the three dimensional modelling of continuous portion and zero thickness interface element is used for modelling of discontinuities. Linear Elastic and perfectly plastic analysis is performed through use of return field method. Dam over Budhi Gandaki River near Benighat for a hydroelectric project is considered for analysis. Analysis is performed for empty to full reservoir level at different stages are performed. Dead load, hydrostatic load, pore pressure are considered as loading cases. Relationship of change in foundation properties and deformation in both foundation and dam is tried to achieve. A multi-paradigm numerical computing environment and a fourth generation programming language MATLAB is used as platform for numerical modelling. After recognition of potential failure modes and surfaces at abutments and foundation, factor of safety for those potential modes are computed. Validation of work is done by the analytical numerical solution and results from previous works on this project.

1.6 Limitation

Limitations of this thesis are as below:

i) Material non-linearity is only considered for foundation rock mass.
ii) Interface element is not used for the dam foundation contact.
iii) Dynamic loading of reservoir and seismic loading are not considered.
iv) Geological data are obtained through previous investigations.
v) Unavailable geological data are assumed.
vi) Validation is done through analytical analysis.
vii) Safety factor is only computed for certain potential failure modes.

2. LITERATURE REVIEW

The aim with this literature study is to evaluate the present state of knowledge for stability analyses of large structures founded on rock, and the features necessary to consider. In order to obtain this the calculated or expressed safety is in general determined from knowledge about the load and the resistance. The process to get it starts with the development of the geological model. This model is mainly developed from the results of site investigations. However, which investigations those are necessary, or how it should be developed, will not be investigated in this study. From the geological model, possible failure modes are identified. Different modes of failure can be possible, and it is necessary to analyse them all to find the weakest link. A material model of the rock mass is chosen which can model the characteristics necessary for the analysis. For large structures, or for rock masses of complex nature, several types of models may be necessary for different parts of the foundation.

2.1 Fundamental principles of stability analysis

Stability of dam foundation is represented by assessment of factor of safety for stability, and it is useful to define a global safety measure, that can be ascribed to potential failure mechanism. All stability analyses are associated with certain amounts of uncertainty. Regarding rock masses, the uncertainty is larger than for manufactured materials, such as steel and concrete. They have been formed under millions of years and have a natural spatial variation of its properties. In addition to this, the information is always limited. It is hidden in the rock mass, revealing its properties cost time and money. Stability analyses are therefore to a large extent a question of finding the right balance between the load, the resistance, the uncertainties, and also the consequences of a failure. To find this balance, two components are in general used. The first is an expression for the calculated safety. The calculated safety can be expressed in several different ways. The ones most frequently used are:

- Total factor of safety
- Probability of failure
- Limit states with partial factors of safety

The second component is the acceptance requirement. It determines which magnitude the calculated safety should have for an acceptable risk.

There are two alternative definitions for safety factor, ratio of maximum external load which is able to induce the sliding instability of a portion of jointed rock mass and actual load applied to the structure (λ_E) and ratio between the shear strength of joints bounding the mechanism and the average shear stress during equilibrium under externally applied load (λ_Φ) [4]. Safety factor λ_E, is unrealistic since it is difficult to think of actual circumstances which are capable of increasing load over maximum ones(1), so λ_Φ is used as factor of in this thesis for realistic approach.

$$\lambda_\Phi = \frac{Shear\ strength\ of\ joint\ (\tau max)}{shear\ stress\ during\ equilibrium(\tau)} \quad (2.1)$$

Where,

τ_{max}= strength of joint where potential sliding may occur it is obtained using Barton's equation

τ= shear stress at joint where potential sliding may occur obtained through FEM analysis

All stability analyses are associated with certain amounts of uncertainty. Regarding rock masses, the uncertainty is larger than for manufactured materials, such as steel and concrete. They have been formed under millions of years and have a natural spatial variation of its properties. In addition to this, the information is always limited. It is hidden in the rock mass, revealing its properties cost time and money. Stability analyses are therefore to a large extent a question of finding the right balance between the load, the resistance, the uncertainties, and also the consequences of a failure.

2.2 Safety evaluation of rock foundation

Safety evaluation of rock foundation problems can be basically categorized in two types as represented by E.Hoek and P.Londe(1974), which are

- Rupture of rock or resistance to failure
- Deformations and their effect on foundation rock and the structure

Rupture of rock considers failure of rock mass through over stressing, such as tensile compressive or shear stress, which can be evaluated using appropriate failure criterion

of rock mass, due to loads imposed after construction of structure. Rupture of rock also includes failure of rock through formation of wedge or plane from discontinuities present in foundation trigged by pore pressure and other loads from structure. For rupture of rock prominent failure modes are identified and proper analysis method is used for evaluation of safety factor.

In consideration of rock deformations it is necessary to differentiate between deformation with in the rock mass and surface displacements. Deformation with in rock mass is used for understanding intrinsic behaviour of foundation whereas surface deformation is adequate for analysing the engineering structure built upon it. For surface deformation rock mass can be considered as equivalent continuous medium resulting similar surface displacement where as for the deformation with in rock discontinuity should be considered. The equivalent continuous medium can be defined by Young's modulus and Poison's ratio, giving the same displacements at the surface as those of the actual site. Comparisons between the results of analyses and measurement of foundation deformations on many dams have shown this approximation to be valid according to E.Hoek and P.Londe(1974).

2.3 Failure criteria

At which stress levels failure occur is defined with a failure criterion. For continuum materials in foundations, the failure mechanism is shear failure. This mechanism creates a shear zone, with an angle, α, to the principal stress direction. This angle depends on the relation between major and minor principal stresses. The development of the shear zone occurs since propagation of cracks in the major principal stress direction is prevented by the confining stress.[5]

Rock, in its natural state, is a complex material the matrix of which usually contains interconnected pores and micro-fissures. Especially at low stress levels where there is a nonlinear load and deformation response, these fissures and pores reduce the tensile strength of the rock. Furthermore, rock foundations exhibit planes of weakness, which include joints, bedding planes, faults and stratifications. A single joint in a rock

mass decreases the shear strength in the tangential direction and reduces the tensile strength to practically zero in the perpendicular direction.

It occurs a significant inhomogeneity and anisotropy in the rock mass strength. In rock mechanics, the use of empirical failure criteria is widely accepted. Until now, theoretical failure criteria have been limited in their scope and application, due to a complex rock mass behavior. Some rock failure criteria allow for adjustments of rock strength based on rock type classifications. Because of physical limitations on the experimental set-up, most failure criteria are two-dimensional, i.e. they are described in terms of major and minor principal stresses. The effect of intermediate principal stress is generally ignored, though there exists some experimental evidence that it may influence failure to some extent (Sheorey, 1997). Empirical failure criteria that have been proposed so far use stress, and no strain, as their determining parameters (e.g. Balmer, 1952, Bieniawski, 1974, Hoek & Brown, 1980, and Sheorey, 1989). This is because determining a strain value for failure proves to be difficult and also because it is easier to measure stress in experiments. Brief descriptions of empirical and theoretical failure criteria can be found in Sheorey (1997). The Hoek-Brown failure criterion (Hoek & Brown, 1997) presents a widely accepted tool to evaluate the performance of the foundation rock at a dam site. The Hoek-Brown criterion is used extensively in practice and is applicable to jointed rock masses without significant anisotropy. It has been developed from regression analysis of tri-axial test data of different rock types and has been continuously evolved, since it was first published in 1980, to include a wide variety of rock characteristics. The criterion, which relates the rock mass strength to a widely accepted rock mass classification, is relatively simple to implement in a finite element analysis.

For discontinuity materials, shear failure occurs along discontinuities or through intact rock. As a consequence, failure criteria valid for discontinuities are necessary in order to model the complex behaviour of a discontinuity rock masses. Over the years, many different criteria have been proposed for intact rock, rock masses, and discontinuities. A description of the most significant is made by Sheorey (1997) and Edelbro (2003) among others. Here, three of the most common ones used in rock mechanics will be described; the Mohr-Coulomb criterion applicable for intact rock, fractured rock masses, and discontinuities; the Hoek-Brown (1980) failure criterion

applicable for intact rock and fractured rock masses; and Barton's (1973) criterion for estimating the shear strength of rough unfilled discontinuities.

2.3.1 Failure criteria of continuous mass

The material parameters for the rock mass are derived from two parameters relating to the intact rock material, coupled with two parameters which characterise the quality of the in-situ rock mass. The intact rock parameters are the uniaxial compressive strength of the intact rock material, σ_{ci}, and the petrographic constant, m_i, Examples of the latter can be found in e.g. (Rocscience Inc. 2006; Marinos and Hoek 2000). The first in-situ parameter is the Geological Strength Index, *GSI*, which is a qualitative classification number for rock masses, see e.g. (Marinos, Marinos, and Hoek 2005). A tool in estimating the *GSI (*Geological strength Index) index is the chart in Figure 2.1. The second in-situ parameter is the disturbance factor, D, which ranges from 0 to 1, for undisturbed rock masses D = 0.

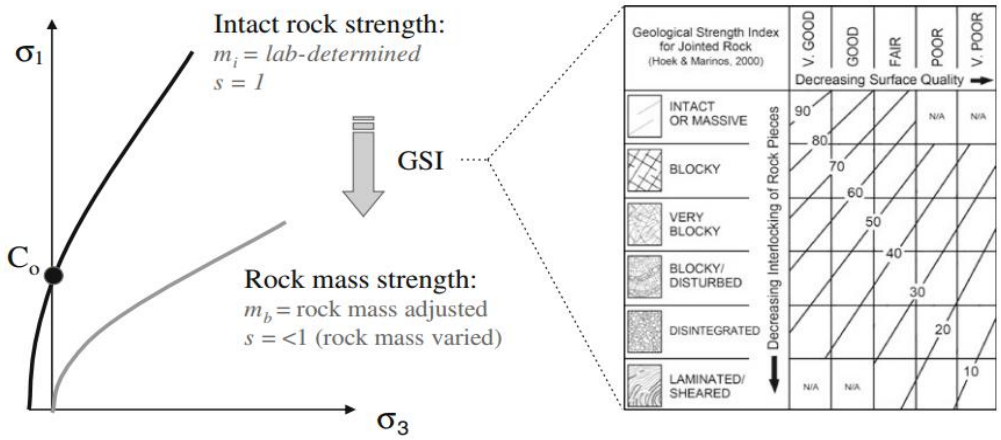

Figure 2-1 Scaling of Hoek–Brown failure envelopes for intact rock to that for rock mass strength. Marinos et al. (2005)

In rock mechanics and geotechnical engineering compressive stresses are most often taken as positive. With this convention and with the parameters outlined above the failure criterion is written as and failure envelop is given in fig2.1.

$$\sigma 1=\sigma 3+\sigma ci\ (mb\frac{\sigma 3}{\sigma ci}+s)^{a} \qquad (2.2)$$

Where σ1> σ2> σ3 are the effective principal stresses positive in compression. The empirically determined parameters m_b, s and a are given by

$$m_b = m_i \, e^{(GSI-100)/(28-14D)} \quad (2.3)$$

$$s = e^{(GSI-100)/(9-3D)} \quad (2.4)$$

$$a = \frac{1}{2} + \frac{1}{6}\left(e^{-\frac{GSI}{15}} - e^{-\frac{20}{3}}\right) \quad (2.5)$$

The rock mass modulus of elasticity, E_{rm}, can be estimated from

$$Erm = \frac{1-D/2}{1+e^{(75+25D-GSI)/11}} \, 10^5 \, MPa \quad (2.6)$$

Or, if intact rock modulus, E_i , is known

$$Erm = Ei \left(0.02 + \frac{1-\frac{D}{2}}{1+e^{\frac{60+15D-GSI}{11}}}\right) \quad (2.7)$$

2.3.2 Failure criteria of discontinuity

Before the 1960's, it was customary to describe the shear strength of discontinuities with the linear Mohr-Coulomb failure criterion. In the sixties it was recognized by a number of researchers that the failure envelope was curved. One of the most important contributions was made by Patton (1966). A development of Patton's work was presented by Barton (1973). Later Barton and Choubey (1977) revised the criteria presented by Barton (1973) after direct shear test on 130 weathered rock samples. They presented an empirical curved failure criterion, which estimated the peak shear strength of discontinuities. It accounted for the roughness of the discontinuity, and the compressive strength of the discontinuity surface. The criterion was expressed according to equation 2.8.

$$\tau max = \sigma n . \tan[JRC \log 10(\frac{JCS}{\sigma n}) + \phi r \,] \quad (2.8)$$

Where,

τ_{max} is the peak shear strength,

σn is the effective normal stress,

JRC is the joint roughness coefficient of wall,

JCS is the joint wall compressive strength

Φ_r is the residual friction angle. Barton and Choubey (1977) suggest that it can be estimated from equation 2.9.

$$\phi r = (\phi_b - 20) + 20(r / R) \quad (2.9)$$

Where r is the Schmidt rebound number wet and weathered fracture surfaces and *R* is the Schmidt rebound number on dry un-weathered sawn surfaces.

2.4 Method of analysis

There exist three main approaches; the Finite Difference Method (FDM); the Finite Element Method (FEM); and the Boundary Element Method (BEM). The difference between them is the solution technique for solving the PDEs (Partial Differential Equations) of the problem. Due to the differences in solution techniques, each of these methods has special characteristics which make one method more suitable for a certain type of problem and unsuitable for another. In a review paper, Jing (2003) says that FEM has advantages in handling material in-homogeneity and non-linearity, while BEM is the best tool for simulating fracturing processes. FDM on the other hand, due to its conceptual simplicity, is a useful tool for coupled Thermo Hydro Mechanical (THM) problems.

Due to its maturity, the possibility of modelling continuum rock masses, interaction between foundation and structure, interaction between different material through interface elements and elastic-plastic behaviour, FEM has become one of the most widely used tools for rock mechanical problems. When FEM is used to analyze a rock mechanical problem, it is generally performed in six steps, including (Stille et al. 2005):

- Description of reality (description of geological conditions etc.).
- Idealization (simplification of reality).
- Discretization (Division of the system into finite elements).
- Element analysis (Selection of material model).
- Structural analysis (Running the program).
- Interpretation of result.

The stresses and strains in elastic-plastic materials are dependent on the loading history. As a consequence, when the FEM is used in rock-mechanical problems with elastic-plastic material properties, the analysis must follow the true loading sequence

in order to obtain relevant values on stresses and deformations. All rock mechanical problems are three-dimensional in nature.

A problem with the FEM is that it does not model infinite boundaries well. To handle this, the common technique is to discretize beyond the zone of influence from the structure. A study performed by Foster et al. (1994), on the effects of foundation depth in the model versus vertical stresses, concludes that a finite element grid should include a foundation depth of at least three times the base width of the structure. With this ratio between the foundation depth and base width of the dam, the difference from theory of elasticity is less than 10 percent. To achieve accurate stress results within the dam, Foster et al. (1994) conclude that a foundation model of depth and width equal to 1.5 and 3.0 times the base width of the dam are sufficient to achieve accurate stress results.

For analysis of discontinuities different methods are developed, such methods are the Distinct Element Method (DEM) (Cundall 1980), and the Discontinuous Displacement Analysis (DDA) (Shi et. al. 1988). In these methods, forces between the rock blocks are transferred through contacts at their boundaries. But application of interface element suggested by Goodman (1977) and A. Jens et al.(1995), made the application of FEM very convenient.

2.5 Elastic-plastic analysis

For the plastic analysis of rock mass non-linear finite element method is used considering return field method. In order to model this non-linear stress-strain behaviour of rock masses, the linear elastic model is not sufficient. The theory of elastic-plasticity has to be used, since it has the ability to model these behaviours. It has been the subject for a number of books, for example by Hill (1950), Mendelson (1968), and Desai and Siriwardane (1984). The following account of the basic concepts of elastic plasticity is mainly from Nordal (2004).

The theory of elastic-plasticity assumes that the strains in the rock mass can be divided into elastic and plastic strains, as described in figure 2.2.

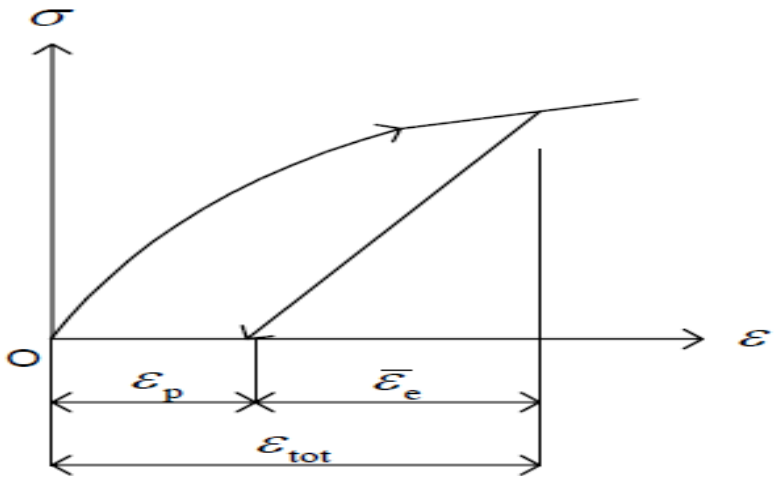

Figure 2-2 Elastic and plastic strains

The basic relation in small strain plasticity is that a strain is composed of elastic and a plastic part.

$$\Delta\varepsilon=\Delta\varepsilon^{e}+\Delta\varepsilon^{p} \tag{2.10}$$

In perfect plasticity, plastic strain occurs during yielding when

$$f(\sigma)=0 \text{ and } \left(\frac{\delta f}{\delta\sigma}\right)^{T}\delta\sigma=0 \tag{2.11}$$

f is yield function, here Hoek and Brown criteria is used as yield function for the rock mass and σ is principle stress vector. Considering D as elastic constitutive stiffness matrix then finite strain increment yields the finite stress increment of

$$\Delta\sigma= D\Delta\varepsilon^{e} - D\Delta\varepsilon^{p} = \Delta\sigma^{e} - \Delta\sigma^{p} \tag{2.12}$$

For calculation of plastic stress and strain there are two method, which are forward Euler procedure and stress update by return mapping, return mapping method is used in this thesis. As presented by Clausen, Johan Christian.[11] According to which for Hoek-Brown criterion can be used as elasto-plastic analysis in finite element calculations yield surface equation can be written in equation 2.13 where $\sigma_1 > \sigma_2 > \sigma_3$ are principle stress tensile stress taken positive and rest of terms are as defined in equations 2.3,2.4 and 2.5.

$$f=\sigma_1-\sigma_3-\sigma_{ci}\left(s-m_b\frac{\sigma 1}{\sigma ci}\right)^{a} \tag{2.13}$$

Plastic potential function for non-associated material behaviour for perfectly plastic is chosen similar as yield function, so

$$g= \sigma_1-\sigma_3-\sigma_{ci}(s-m_b\frac{\sigma 1}{\sigma ci})^a \quad (2.14)$$

Component $\Delta\sigma^p$ plastic corrector stress of equation 2.12 can be obtained from equation below

$$\Delta\sigma^p=\Delta\lambda\frac{\partial g}{\partial \sigma} \quad (2.15)$$

Gradient of yield surface and plastic potential with respect to stress is given in equations below

$$\frac{\partial f}{\partial \sigma} = \begin{Bmatrix} \frac{\partial f}{\partial \sigma 1} \\ \frac{\partial f}{\partial \sigma 2} \\ \frac{\partial f}{\partial \sigma 3} \end{Bmatrix} \quad (2.16)$$

$$\frac{\partial g}{\partial \sigma} = \begin{Bmatrix} \frac{\partial g}{\partial \sigma 1} \\ \frac{\partial g}{\partial \sigma 2} \\ \frac{\partial g}{\partial \sigma 3} \end{Bmatrix} \quad (2.17)$$

During return mapping stress after increment of load is obtained by constitutive relationship of deformable solid, and principle stress of stress obtained be σ^B , if it lies out of yield surface i.e. value of equation 3.16 greater than 1 for σ^B , then updated stress σ^c should be computed and slope of line connecting σ^B and σ^C should be equal to slope of plastic corrector which is slope of vector $D^*\frac{\partial g}{\partial \sigma}$, $s= D^*\frac{\partial g}{\partial \sigma}$, then slope of plastic corrector $\alpha_s=s_3/s_1$ and slope of line connecting σ^B and σ^C be α_r, return mapping is expressed in figure 2-3

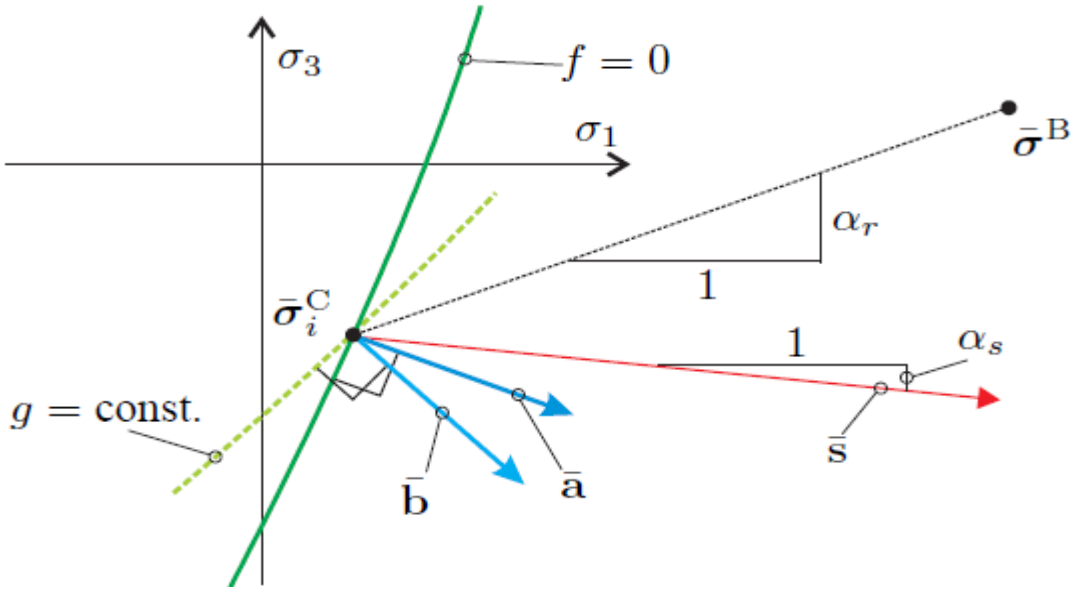

Figure 2-3 Return to yield surface

$$\alpha_r=\frac{\sigma_3^C-\sigma_3^B}{\sigma_1^C-\sigma_1^B} \quad (2.18)$$

$$h_f=\alpha_r-\alpha_s \quad (2.19)$$

Above equation should value zero and is solved Newton-Raphson method and σ_1^C is obtained by iteration process and σ_3^C is obtained using equation 3.16, and

$$\sigma_2^C=t_f s_2+\sigma_2^B \quad (2.20)$$

$$t_f=(\sigma_1^C-\sigma_1^B)/s_1 \quad (2.21)$$

Where s_1 ,s_2 and s_3 are first, second and third component of s.

After updating stress constitutive matrix should also be modified for next increment of load, updated constitutive matrix D^{epc} is obtained using following relations.

$$D^{epc}=D^c\frac{D^c\frac{\partial g}{\partial\sigma}\frac{\partial f}{\partial\sigma}^T D^c}{\frac{\partial f}{\partial\sigma}^T D^c\frac{\partial g}{\partial\sigma}} \quad (2.22)$$

Where D^c is modified elastic stiffness matrix given by

$$D^c=DT \quad (2.23)$$

Modification matrix T is given by

$$T=(I+\Delta\lambda D\frac{\delta^2 g}{\delta\sigma^2})^{-1} \quad (2.24)$$

Plastic strain $\Delta\varepsilon^p$ can be obtained using constitutive matrix and plastic strain.

2.6 Vector analysis of wedge stability

Stability analysis of wedge can be done by different methods like Graphical analysis of slopes using stereo nets, Londe method of analysis and Vector analysis of slopes. For verification of some work done in this thesis is done by Vector analysis of slopes. Vector analysis is performed as suggested by E.T Cording, Hendron [1980], which is as described in following paragraphs.

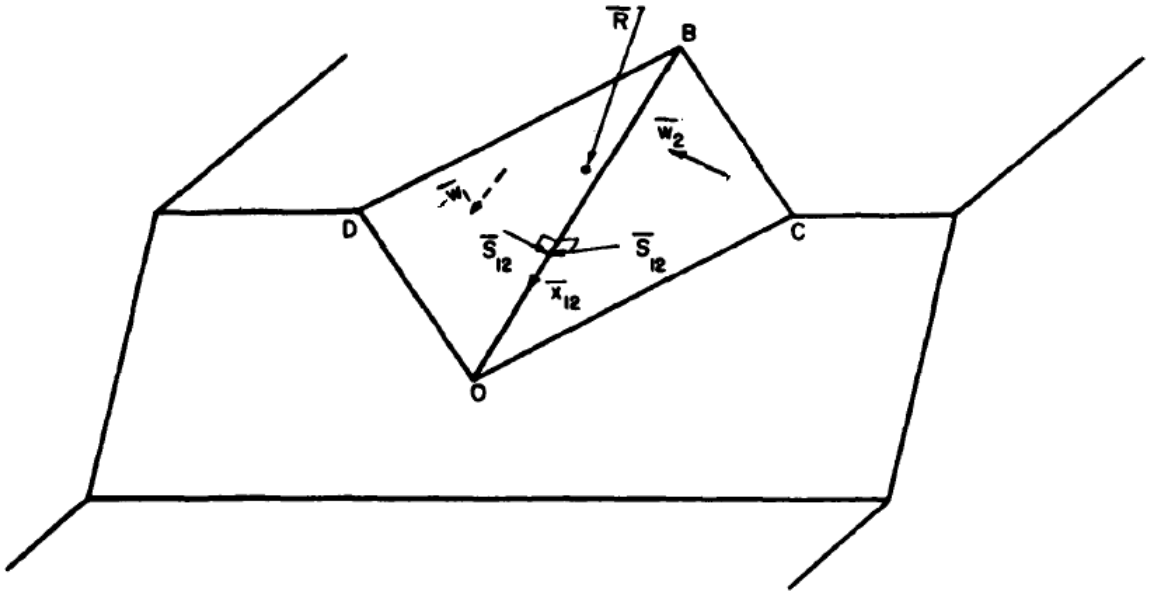

Figure 2-4 Planes of wedge, their vectors and force vector acting on wedge

If R be total force vector acting on wedge which consists dead load vector D, pore water pressure forces U_1 and U_2 acting on planes 1 and 2 respectively and Q thrust from dam.

w_1 and w_2 be the normal unit vector of planes 1 and 2 respectively, x_{12} be the unit vector of intersection line of plane 1 and 2. $_1S_{12}$ and $_2S_{12}$ are vector normal to vector w_1 and x_{12} and vector w_2 and x_{12} respectively.

Modes of sliding of wedge can be uplift of wedge on both plane, sliding on one plane only and sliding on both plane along intersection of planes. Among these sliding modes most prominent can be identified by following approaches.

- If R . w_1 >0 then uplift on plane 1 will occur and if R. w_2 >0 then uplift occurs on plane 2. If both condition satisfies then uplift will occurs on both plane and wedge will be unstable.
- If R. w_1 <0 and R. w_2 >0 then sliding will occur on plane 1 only, similarly if R. w_1 >0 and R. w_2 <0 then sliding will occur on plane 2 only.
- If R. w_1 <0 and R.w_2 <0, R. x_{12} >0 then sliding will occur along the intersection line of wedge.

Factor of safety for stability of wedge can be obtained after identifying mode of sliding and failure condition is used as recommended by Barton (1973). Factor of safety if

- Sliding occurs at any one plane then F.O.S can be obtained using equation 2.25

$$F.O.S = Ni * \tan(\phi_i)/T_i \quad (2.25)$$

Where 'i' represents plane 1 and 2,

N_i is normal force on plane i,

T_i is shear force acting on plane i,

ϕ_i is resisting friction angle of plane i, which is obtained using Barton (1973).

- Sliding occurs at intersection then .O.S can be obtained using equation 2.26,

$$F.O.S = (N_1 * \tan\phi_1 + N_2 * \tan\phi_2)/T_{12} \quad (2.26)$$

Where ,T_{12} is component of R along $x_{12,}$

N_1 and N_2 are component of normal force acting on plane 1 and 2.

3. METHDOLOGY

3.1 Introduction

The finite element method is nowadays the most frequently used computational method in engineering problems. In this numerical technique all complexities of a problem such as shape, boundary and loading conditions are kept the same but the results obtained are approximate. When using this method, calculations are robust due to the large number of unknowns leading to a large pile of simultaneous equations for the user to solve. Hence the use of computer programs to take care of these equations is one face of the method. The evaluation of these simultaneous equations is done by using one of the matrix methods of solving simultaneous equations. The MATLAB programming language is useful in illustrating how to program the Finite element method due to the fact that it allows one to very quickly code Numerical methods and has a vast predefined mathematical library suitable for handling matrices.

There are different numerical methods for analysis and modelling of geotechnical problem, for continuous model Finite element method (FEM), Finite difference method (FDM) and Boundary element method (BEM) can be used, and for discontinuous model Distinct element method (DEM) and Discontinuous deformation analysis (DDA) can be used. Among all these methods FEM is used along with zero thickness boundary elements

3.2 Modelling a continuum

The first step in the finite element analysis involves the division of the body into smaller Pieces, known as finite elements. This is equivalent to replacing the body with an infinite number of degrees of freedom by a system having finite number of degrees of freedom.

3.2.1 Selection of element, nodes and degree of freedom

In finite element analysis there are different types of element according to shape of the structure, dimension of analysis, such as for one dimensional member bar elements (Two-Nodded Linear Element, Three-Nodded Quadratic Element) are used whereas for plane stress and strain analysis two dimensional elements are used (Four-Nodded Bilinear Quadrilateral, Eight-Nodded Quadratic Quadrilateral, Three-Nodded Linear Triangle, Six-Nodded Quadratic Triangle) are used. As in this study three

dimensional modeling is to be performed so, eight node hexahedron element as shown

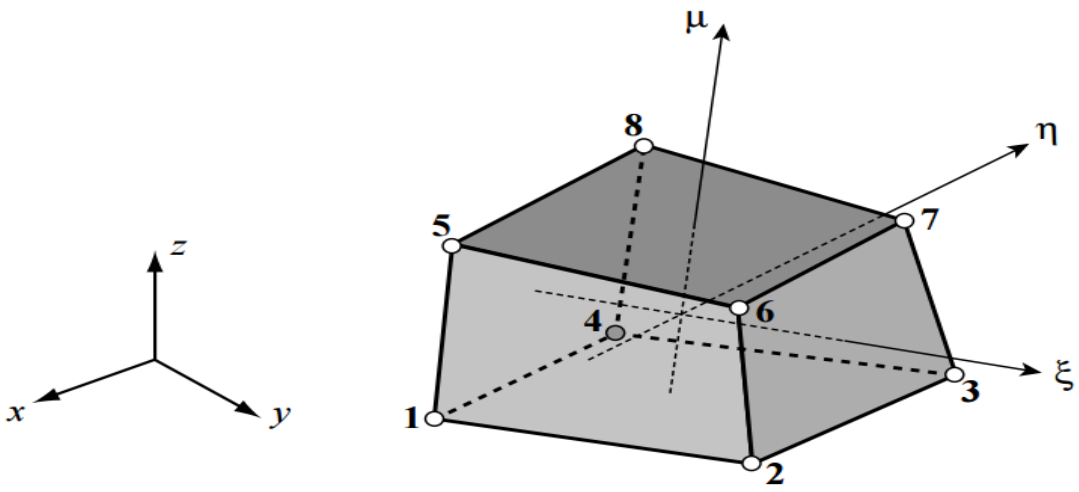

Figure 3-1 Hexahedral element used for finite element modelling

in fig 3.1 is used. Degree of freedom is defined according to the number of unknowns parameters in a model, and in an element at a node degree of freedom is defined according to unknown parameters, in case of this thesis deformation are considered as unknown parameter and as for three dimensional analysis three degree of freedom is considered at each node of an element, there will 24 degree of freedom in an element which is adopted.

3.2.2 Generation of mesh and size of element

Size of an element is taken non uniform according to the sensitivity of different portions of model, such as the contact of dam and foundation, abutments, and probable surface of failure is finely meshed with smaller sized elements, size of element also depends up on shape of boundary of model so to provide smooth surface at curved surface of dam and possible realistic consideration of contact between rock-dam and rock-rock finer elements are used.

3.2.3 Developing Constitutive relations

For three dimensional modelling of continuum component of dam and rock foundation is done using eight nodded hexahedral element as shown in fig 3-1, having nodal displacement represented by displacement vector {a}, elemental displacement vector {u} , elemental strain vector {ε} and elemental stress vector {σ}, which are as below.

$\{a\}'=\{ u_{x1} ,u_{y1} ,u_{z1},u_{x2} u_{y2} u_{z2} u_{x3} u_{y3} u_{z3} u_{x4} u_{y4} u_{z4} u_{x5} u_{y5} u_{z5} u_{x6} u_{y6} u_{z6} u_{x7} u_{y7} u_{z7} u_{x8} u_{y8} u_{z8}\}$ (3.1)

$\{u\}'=\{u_x ,u_y, u_z\}$ (3.2)

$\{\varepsilon\}'=\{\varepsilon_{xx} ,\varepsilon_{yy}, \varepsilon_{zz}, \varepsilon_{xy}, \varepsilon_{xz}, \varepsilon_{yz} \}$ (3.3)

$\{\sigma\}'=\{\sigma_{xx} ,\sigma_{yy} ,\sigma_{zz} ,\sigma_{xy} ,\sigma_{xz}, \sigma_{yz} \}$ (3.4)

Relationship between above vectors can be defined as below

$u_x=N_1* u_{x1}+ N_2* u_{x2}+ N_3* u_{x3}+ N_4* u_{x4}+ N_5* u_{x5}+ N_6* u_{x6}+ N_7* u_{x7}+ N_8* u_{x8}$

$u_y=N_1* u_{y1}+ N_2* u_{y2}+ N_3* u_{y3}+ N_4* u_{y4}+ N_5* u_{y5}+ N_6* u_{y6}+ N_7* u_{y7}+ N_8* u_{y8}$

$u_z=N_1* u_{x1}+ N_2* u_{z2}+ N_3* u_{z3}+ N_4* u_{z4}+ N_5* u_{z5}+ N_6* u_{z6}+ N_7* u_{z7}+ N_8* u_{z8}$

Hence in matrix form above equations can be written as

$\{u\}=[N]\{a\}$ (3.5)

Strain displacement relation of deformable solid can be written as

$\varepsilon_{xx}=\frac{\partial ux}{\partial x}$; $\varepsilon_{yy}=\frac{\partial uy}{\partial y}$; $\varepsilon_{zz}=\frac{\partial uz}{\partial z}$

$\varepsilon_{xy}=\frac{\partial ux}{\partial y}+\frac{\partial uy}{\partial x}$

$\varepsilon_{xz}=\frac{\partial ux}{\partial z}+\frac{\partial uz}{\partial x}$

$\varepsilon_{yz}=\frac{\partial uy}{\partial z}+\frac{\partial uz}{\partial y}$

Above equations can be represented in matrix form by

$\{\varepsilon\}=[d]*\{u\}$ (3.6)

$\{\varepsilon\}=[d]*[N]*\{a\}$ (3.7)

$\{\varepsilon\}=[B]\{a\}$ (3.6)

From generalize Hoek's law constitutive relation for deformable solids

$\{\sigma\}=[D]\{\varepsilon\}$ (3.7)

$$[D]=\frac{E}{(1+\nu)(1-2\nu)}\begin{bmatrix} 1-\nu & \nu & \nu & 0 & 0 & 0 \\ \nu & 1-\nu & \nu & 0 & 0 & 0 \\ \nu & \nu & 1-\nu & 0 & 0 & 0 \\ 0 & 0 & 0 & 0.5-\nu & 0 & 0 \\ 0 & 0 & 0 & 0 & 0.5-\nu & 0 \\ 0 & 0 & 0 & 0 & 0 & 0.5-\nu \end{bmatrix} \quad (3.8)$$

Where [N] and [B] are shape matrix and strain matrix as defined (in Finite Element Analysis Using MATLAB® and Abaqus by Amar Khennane) for hexahedral element .Applying virtual work method small increment of stress and strain in adopted element

$$\int_{vol}\{\delta\,\varepsilon\}'\{\delta\sigma\}\mathrm{dv}=\int_{vol}\{\delta u\}'\{b\}dv+\int_{\Gamma}\{\delta u\}'\{t\}d\Gamma+\sum\{\delta u\}'\{p\} \quad (3.9)$$

Where,

{ε} represents the strain vector

{σ} is the stress vector

{U} is the displacements vector

{b} is the body forces vector

{t} is the traction forces vector

{P} is the vector of concentrated forces applied

dv is an element of volume

dΓ is an element of the boundary of the element on which the traction forces{t}are applied

After substituting values from equations 3.5, 3.6, and 3.7 in equations 3.9, following relation is obtained

$$[k]\{a\}=\{f\} \quad (3.10)$$

Where [k] is elemental stiffness matrix and {f} is elemental force matrix and

$$[k]=\int_{vol}[B][D][B]\,\mathrm{dv} \quad (3.11)$$

$$\{f\}=\int_{vol}[N]^{T}\{b\}\mathrm{dv}+\int_{area}[N]^{T}\{t\}\mathrm{dA}+\sum[N]^{T}\{P\}_{I} \quad (3.12)$$

For numerical integration of equations 3.10, 3.11and3.12 Gauss quadrature integration is used.

$$[k]=\sum_{i=1}^{n1}\sum_{j=1}^{n2}\sum_{k=1}^{n3}wi.wj.wk.d.[B]'.[D].[B] \quad (3.13)$$

$$\int_{vol}[N]^{T}\{b\}dv=\sum_{i=1}^{n1}\sum_{j=1}^{n2}\sum_{k=1}^{n3} wi.wj.wk.d.[N]'.\{b\} \quad (3.14)$$

Here $n1$, $n2$ and $n3$ are the number of Gauss points in the ξ, η and μ direction, respectively, w_i, w_j and w_k are Gauss weight value at gauss point i, j, and k. 'd' is determinant of Jacobian matrix [J] of x, y and z w.r.t ξ, η and μ.

$$[J]=\begin{bmatrix} \frac{\partial N1}{\partial \xi} & \frac{\partial N2}{\partial \xi} & \frac{\partial N3}{\partial \xi} & \frac{\partial N4}{\partial \xi} & \frac{\partial N5}{\partial \xi} & \frac{\partial N6}{\partial \xi} & \frac{\partial N7}{\partial \xi} & \frac{\partial N8}{\partial \xi} \\ \frac{\partial N1}{\partial \eta} & \frac{\partial N2}{\partial \eta} & \frac{\partial N3}{\partial \eta} & \frac{\partial N4}{\partial \eta} & \frac{\partial N5}{\partial \eta} & \frac{\partial N6}{\partial \eta} & \frac{\partial N7}{\partial \eta} & \frac{\partial N8}{\partial \eta} \\ \frac{\partial N1}{\partial \mu} & \frac{\partial N2}{\partial \mu} & \frac{\partial N3}{\partial \mu} & \frac{\partial N4}{\partial \mu} & \frac{\partial N5}{\partial \mu} & \frac{\partial N6}{\partial \mu} & \frac{\partial N7}{\partial \mu} & \frac{\partial N8}{\partial z} \end{bmatrix} * \begin{bmatrix} x1 & y1 & z1 \\ x2 & y2 & z2 \\ x3 & y3 & z3 \\ x4 & y4 & z4 \\ x5 & y5 & z5 \\ x6 & y6 & z6 \\ x7 & y7 & z7 \\ x8 & y8 & z8 \end{bmatrix} \quad (3.15)$$

Components of matrix [B] is obtained from following equation,

$$\begin{Bmatrix} \frac{\partial Ni}{\partial x} \\ \frac{\partial Ni}{\partial x} \\ \frac{\partial Ni}{\partial x} \end{Bmatrix} = inv(J) * \begin{Bmatrix} \frac{\partial Ni}{\partial \xi} \\ \frac{\partial Ni}{\partial \xi} \\ \frac{\partial Ni}{\partial \xi} \end{Bmatrix} \quad (3.16)$$

Where x_i, y_i and z_i are coordinates of nodes 'i' of hexahedral element and 'i'=1,2,…8

Gauss abscissa and weights as given in table given below at different gauss point.

Number of points, n	Points, x_i	Weights, w_i
1	0	2
2	$\pm\sqrt{\frac{1}{3}}$	1
3	0	$\frac{8}{9}$
	$\pm\sqrt{\frac{3}{5}}$	$\frac{5}{9}$
4	$\pm\sqrt{\frac{3}{7}-\frac{2}{7}\sqrt{\frac{6}{5}}}$	$\frac{18+\sqrt{30}}{36}$
	$\pm\sqrt{\frac{3}{7}+\frac{2}{7}\sqrt{\frac{6}{5}}}$	$\frac{18-\sqrt{30}}{36}$
5	0	$\frac{128}{225}$
	$\pm\frac{1}{3}\sqrt{5-2\sqrt{\frac{10}{7}}}$	$\frac{322+13\sqrt{70}}{900}$
	$\pm\frac{1}{3}\sqrt{5+2\sqrt{\frac{10}{7}}}$	$\frac{322-13\sqrt{70}}{900}$

Shape function

The values of the field variable computed at the nodes are used to approximate the values at non-nodal points (that is, in the element interior) by interpolation of the nodal values. And that interpolation matrix is defined as shape function [N], shape function used for the hexahedra element is as:

$$\begin{Bmatrix} N_1(\xi,\eta,\zeta) \\ N_2(\xi,\eta,\zeta) \\ N_3(\xi,\eta,\zeta) \\ N_4(\xi,\eta,\zeta) \\ N_5(\xi,\eta,\zeta) \\ N_6(\xi,\eta,\zeta) \\ N_7(\xi,\eta,\zeta) \\ N_8(\xi,\eta,\zeta) \end{Bmatrix} = \frac{1}{8} \begin{Bmatrix} (1-\xi)(1-\eta)(1-\zeta) \\ (1+\xi)(1-\eta)(1-\zeta) \\ (1+\xi)(1+\eta)(1-\zeta) \\ (1-\xi)(1+\eta)(1-\zeta) \\ (1-\xi)(1-\eta)(1+\zeta) \\ (1+\xi)(1-\eta)(1+\zeta) \\ (1+\xi)(1+\eta)(1+\zeta) \\ (1-\xi)(1+\eta)(1+\zeta) \end{Bmatrix}$$

Where, ξ , η and ζ are ideal coordinates of hexahedron element.

When the finite-element method is used for solving elastic-plastic problems, the load and/or the forced displacement are applied in increments. In each increment equilibrium is sought by minimizing the force residual, i.e. the difference between the external and internal forces. Global equilibrium iterations are then carried out until the norm of the residual is smaller than a described number. A popular method for establishing equilibrium is the Newton-Raphson scheme. With the Newton-Raphson scheme the stiffness matrix is updated in each equilibrium iteration. The stresses and the constitutive matrices are updated according to the constitutive law. This is the method which has been used for all finite element calculations in this thesis. A schematic presentation of the Newton-Rapson in the elastic plastic finite element method is presented in the flow chart below after, Johan Clausen.[11]

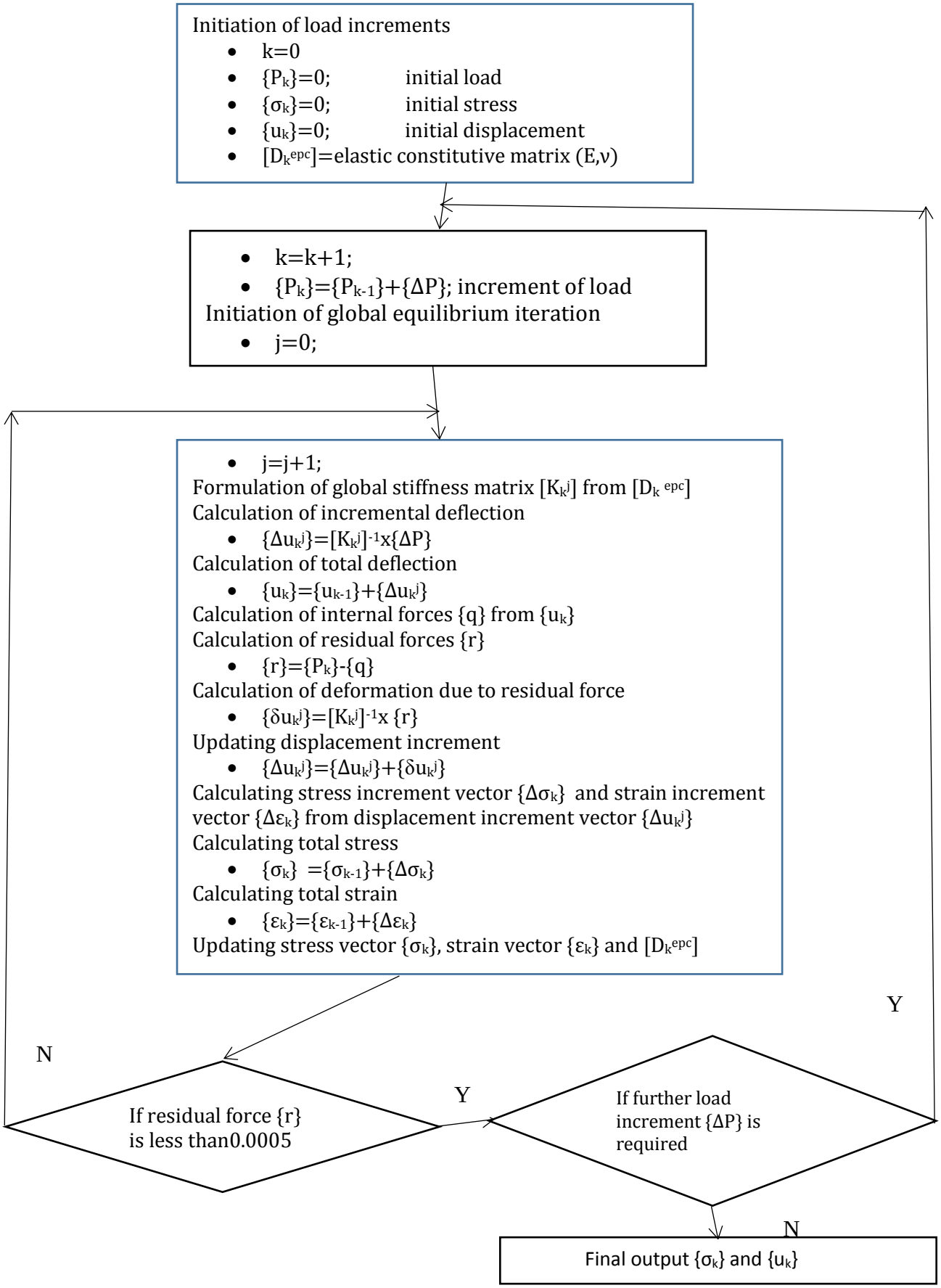
Initiation of load increments
k=0
{Pk}=0; initial load
{σk}=0; initial stress
{uk}=0; initial displacement
[Dkepc]=elastic constitutive matrix (E,ν)
k=k+1;
{Pk}={Pk-1}+{ΔP}; increment of load
Initiation of global equilibrium iteration
j=0;
j=j+1;
Formulation of global stiffness matrix [Kkj] from [Dk epc]
Calculation of incremental deflection
{Δukj}=[Kkj]-1x{ΔP}
Calculation of total deflection
{uk}={uk-1}+{Δukj}
Calculation of internal forces {q} from {uk}
Calculation of residual forces {r}
{r}={Pk}-{q}
Calculation of deformation due to residual force
{δukj}=[Kkj]-1x {r}
Updating displacement increment
{Δukj}={Δukj}+{δukj}
Calculating stress increment vector {Δσk} and strain increment vector {Δεk} from displacement increment vector {Δukj}
Calculating total stress
{σk} ={σk-1}+{Δσk}
Calculating total strain
{εk}={εk-1}+{Δεk}
Updating stress vector {σk}, strain vector {εk} and [Dkepc]
N
If residual force {r} is less than0.0005
Y
If further load increment {ΔP} is required
Y
N
Final output {σk} and {uk}

3.3 Modelling of discontinuity

The deformations of discontinuities in rock masses have been studied by Goodman (1974) and Bandis et al. (1983) among several others. For foundations, the deformations in discontinuities can constitute the main part of the total deformation. As a consequence, the deformation characteristics of the discontinuities are an important parameter in order to model the stress strain response of a jointed rock mass. The deformation characteristics can be divided into properties in the normal direction, and in the tangential direction. The characteristics are also different before, and after the peak shear stress. The discontinuity is modelled by interface element. An isoparametric zero thickness interface element (Goodman et al. 1968, Ghaboussi et al., 1973; Carol and Alonso, 1983; Wilson, 1977; Desai et al. 1984, Beer, 1985).Which has also been used for jointed rock slopes (Graves et. Al 1987)and other discontinuous structures [Tzamtzis, A.D. 1994,Tzamtzis et al. 1992 and Goodman et al. 1972].

An interface finite element for three-dimensional analysis has been previously developed [Goodman 1968, Zienkiewicz, O. C. 1970]. Mahtab and Goodman 1968 extended the jointed rock model to three-dimensions, and developed a two-dimensional (plane) joint element of zero thickness. A more sophisticated joint/interface element applicable to two and three-dimensional finite element analysis was presented by Beer [Beer, G., 1985], based on assumptions similar to those of References [Ghaboussi et al. 1937] & [Van Dillen et al. 1981], but a general isoparametric formulation was used instead and the element was of zero thickness, particularly suited to the modelling of rock joints and fractures. Three dimensional zero thickness interface element used for this thesis is presented in fig (3.3), its purpose is to permit large relative movements to occur between adjacent blocks, and the transfer of shear stresses across the interfaces. With reference of figure displacement at any point with in element can be represented as:

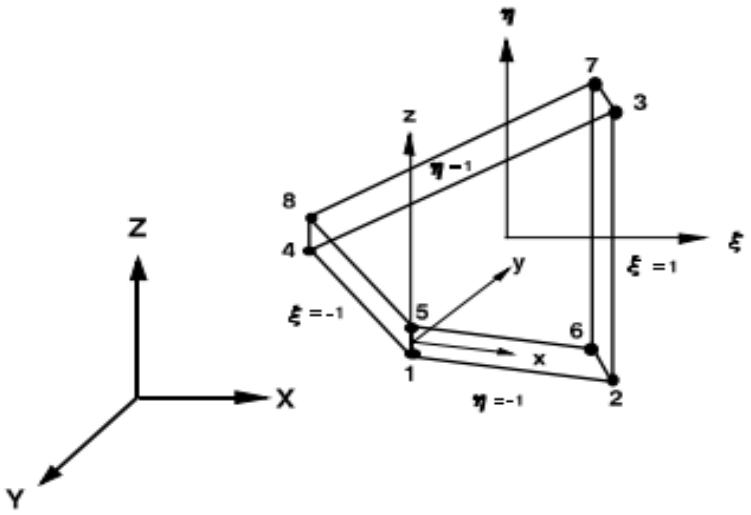

Figure 3-2 Interface element for three dimensional modelling

$$\{u_i\}=[N_i]\{q_i\} \tag{3.17}$$

Where $\{u_i\}$ is the vector of displacement components, and $\{q_i\}$ the vector of nodal displacements.

Matrix $[N_i]$ contains the interpolation functions of the element and is given by

$$[Ni]=\begin{bmatrix} n1 & 0 & 0 & n2 & 0 & 0 & n3 & 0 & 0 & n4 & 0 & 0 \\ 0 & n1 & 0 & 0 & n2 & 0 & 0 & n3 & 0 & 0 & n4 & 0 \\ 0 & 0 & n1 & 0 & 0 & n2 & 0 & 0 & n3 & 0 & 0 & n4 \end{bmatrix} \tag{3.18}$$

Where i=1, 2, 3 and 4

$$n_1=0.25(1-\xi-\eta+\xi\eta) \tag{3.19}$$

$$n_2=0.25(1+\xi-\eta-\xi\eta) \tag{3.20}$$

$$n_3=0.25(1+\xi+\eta+\xi\eta) \tag{3.21}$$

$$n_4=0.25(1-\xi+\eta-\xi\eta) \tag{3.22}$$

The relative displacements between the top and the bottom of the element can then be computed as

$$\{u\} = [[N_i]\{q_i\}_{top}-[N_i]\{q_i\}_{bottom}]=[B]\{q\} \tag{3.23}$$

Where

$$\{u\}=\{u\ v\ w\}^T \tag{3.24}$$

$$\{q\}=\{u_1\ v_1\ w_1\ u_2\ v_2\ w_2\ u_3\ v_3\ w_3\ u_4\ v_4\ w_4\ u_5\ v_5\ w_5\ u_6\ v_6\ w_6\ u_7\ v_7\ w_7\ u_8\ v_8\ w_8\ \} \quad (3.25)$$

From constitutive relation of stress and displacement, stress at plane $\{\sigma\}$ can be obtained from displacement at plane $\{u\}$ can be obtained from following equation

$$\{\sigma\}=[k]\{u\} \quad (3.26)$$

$$\{\sigma\}=\{\sigma_n\ \tau_1\ \tau_2\} \quad (3.27)$$

$$[k]=\begin{bmatrix} kn & 0 & 0 \\ 0 & ks1 & 0 \\ 0 & 0 & ks2 \end{bmatrix} \quad (3.28)$$

k_n is the normal stiffness and k_{s1} and k_{s2} are shear stiffness of rock joint, in this thesis k_{s1} and k_{s2} are taken similar. According to RocScience, for unfilled joints

$$kn=\frac{Ei\ Em}{L(Ei-Em)} \quad (3.29)$$

$$ks=\frac{GiGm}{L(Gi-Gm)} \quad (3.30)$$

Where, E_i and E_m are elastic young's moduli of intact rock and rock mass as explained in equation3.29 and 3.30, and G_i and G_m are shear moduli of intact rock and rock mass. L is the spacing of joint.

Similarly for filled joints

$$k_n=\frac{Eo}{h} \quad (3.31)$$

$$k_s=\frac{Go}{h} \quad (3.32)$$

Where E_o and G_o are young's and shear moduli of infilling material and h is thickness of infilling.

For derivation of relationship between force and displacement at each node of interface element. Let {F} be the force vector containing three directional forces in global coordinate system which can be expressed as

$$\{F\}=\{f_{x1},\ f_{y1},\ f_{z1},f_{x2},f_{y2},\ f_{z2},\ f_{x3},\ f_{y3},\ f_{z3},\ f_{x4},\ f_{y4},\ f_{z4},\ f_{x5},\ f_{y5},\ f_{z5},\ f_{x6},\ f_{y6},\ f_{z6},\ f_{x7},\ f_{y7},\ f_{z7},\ f_{x8},\ f_{y8},\ f_{z8}\} \quad (3.33)$$

Displacement vector {q} can be transformed to global deformation vector $\{q_g\}$ as below

$$\{q_g\}=[A]^{-1}\{q\} \quad (3.34)$$

$\{q_g\}=\{u_{x1}\ u_{y1}\ u_{z1}\ u_{x2}\ u_{y2}\ u_{z2}\ u_{x3}\ u_{y3}\ u_{z3}\ u_{x4}\ u_{y4}\ u_{z4}\ u_{x5}\ u_{y5}\ u_{z5}\ u_{x6}\ u_{y6}\ u_{z6}\ u_{x7}\ u_{y7}\ u_{z7}\ u_{x8}\ u_{y8}\ u_{z8}\ \}$ (3.35)

$$[A]=\begin{bmatrix}[a] & 0 & 0 & 0\\ 0 & [a] & 0 & 0\\ 0 & 0 & [a] & 0\\ 0 & 0 & 0 & [a]\end{bmatrix} \quad (3.36)$$

$$[a]=\begin{bmatrix}\cos(x',x) & \cos(x',y) & \cos(x',z)\\ \cos(y',x) & \cos(y',y) & \cos(y',z)\\ \cos(z',x) & \cos(z',y) & \cos(z',z)\end{bmatrix} \quad (3.37)$$

Where (x',y',z') is the coordinate system have one of plane as interface element and coordinate system (x,y,z) is the global coordinate system

Stiffness matrix in global coordinate system can be obtained by following equation

$[K_g]= [A]'[K][A]$ (3.38)

$[K]=\int_{area}[B]'[k][B]dA$ (3.39)

$\{q_g\} = [K_g]^{-1}\{F\}$ (3.40)

For small amount of force increment $\{\Delta F\}$, increment in stress $\{\Delta\sigma\}$ and increment in displacement vector $\{\Delta q\}$ can be obtained using equations 3.40,3.34,3.17and3.25, using Barton's criteria as in equation 2.8 failure criteria for discontinuities can be represented as in equation 3.41 for total stress $\{\sigma\}$.

$$f(\sigma n,\tau)= \sigma n.\tan[JRC\ \log10(\frac{JCS}{\sigma n})+\phi r\ ]- \tau \quad (3.41)$$

For small increment of stress vector $\{\Delta\sigma\}$ failure criteria can be expressed as below

$$f'(\Delta\sigma n,\Delta\tau)=\Delta\sigma n\tan([JRC\ \log10(\frac{JCS}{\sigma n})+\phi r\ ]-\Delta\tau \quad (3.42)$$

Where, $\tau=\sqrt{\tau_1^2+\tau_2^2}$ and (3.43)

$$\Delta\tau=\sqrt{\Delta\tau_1^2+\Delta\tau_2^2} \quad (3.44)$$

In this thesis it is considered that if $f(\sigma_n,\tau)$ or $f'(\Delta\sigma_n,\Delta\tau)$ is greater than zero then failure is considered to be occurred along discontinuity.

The behaviour of the joint material is both complex and non-linear. Figure 3.4 shows the idealized constitutive relations of the joint element in the normal and tangential direction to the joint that can be adopted for the sake of simplicity. The joint behaviour can be characterized as elastic-perfectly plastic, and incapable of withstanding any tensile stress in the direction normal to the bed joint. In relating stress to deformation in the direction normal to the joint, two distinct stages are defined:

- Separation, which occurs when the normal strain is less than or equal to zero; the joint cannot now sustain any tensile stress in the normal direction. During separation, both normal and shear stiffness of the interface element are set equal to zero; consequently shear and direct stress cannot be transmitted across the joint.
- Contact, which is restored when the normal strain returns to the value at which separation occurred.

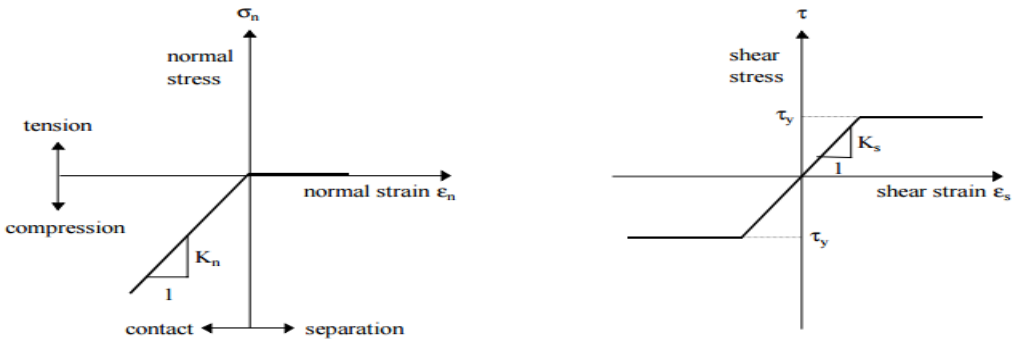

Figure 3-3 Idealized constitutive relationship of discontinuity

3.4 Design data acquisition

During modelling of arch dam and it's foundation through three dimensional finite element method different data are required such as geometrical, material and loading of whole system. Data's which are used during this thesis are as following:

3.4.1Material properties

Materials used for modelling are concrete for arch dam component and rock along with discontinuities. Methods of obtaining properties of those materials are as below:

3.4.1.1 Concrete properties

The material properties of the concrete for use in static analysis are influenced by mix proportions, cement, aggregate, admixtures, and age. M20 grade of concrete in accordance to Indian standard is used, which has following properties used in this thesis.

- Modulus of elasticity (E_c):
- Poisson's ratio (ν_c):
- Unit weight (γ_c):
- Compressive strength (σ_{cc}):
- Tensile strength (σ_{tc}):

3.4.1.2 Rock mass properties

There are different geotechnical properties of rock mass that can be useful for the analysis of strength of rock mass, according to International Society of Rock Mechanics (ISRM) some properties are:

i) Rock Mass Rating, RMR (Bieniawski, 1989);
ii) Dam Mass Rating, DMR (Romana, 2003);
iii) Problem Recognition Index, PRI (Price et al. 1996);
iv)Geological Strength Index, GSI (Hoek & Brown, 1997).

Out of which Geological strength Index is used as strength parameter for Hoek-Brown criterion in this thesis. The Geological Strength Index (GSI) developed by Hoek & Brown (1997) is a system of rock-mass characterization that provides reliable input data for numerical analyses or closed form solutions for designing tunnels, slopes or foundations in rocks. Its direct application is to estimate the parameters of the Hoek-Brown strength criterion for rock masses. Together with a visual assessment, the geological character of the rock mass can be used as a direct input to the selection of parameter, which is relevant for the geo-mechanical evaluation of the rock-mass. Key element of this approach and at the same time main reason for its application in this study is that it enables a rock mass to be considered as a mechanical continuum without losing the influence geology on its mechanical properties. Furthermore it provides a field method for characterizing difficult-to-describe rock masses. The obtained number of the GSI, which can be read of a table 3.1.

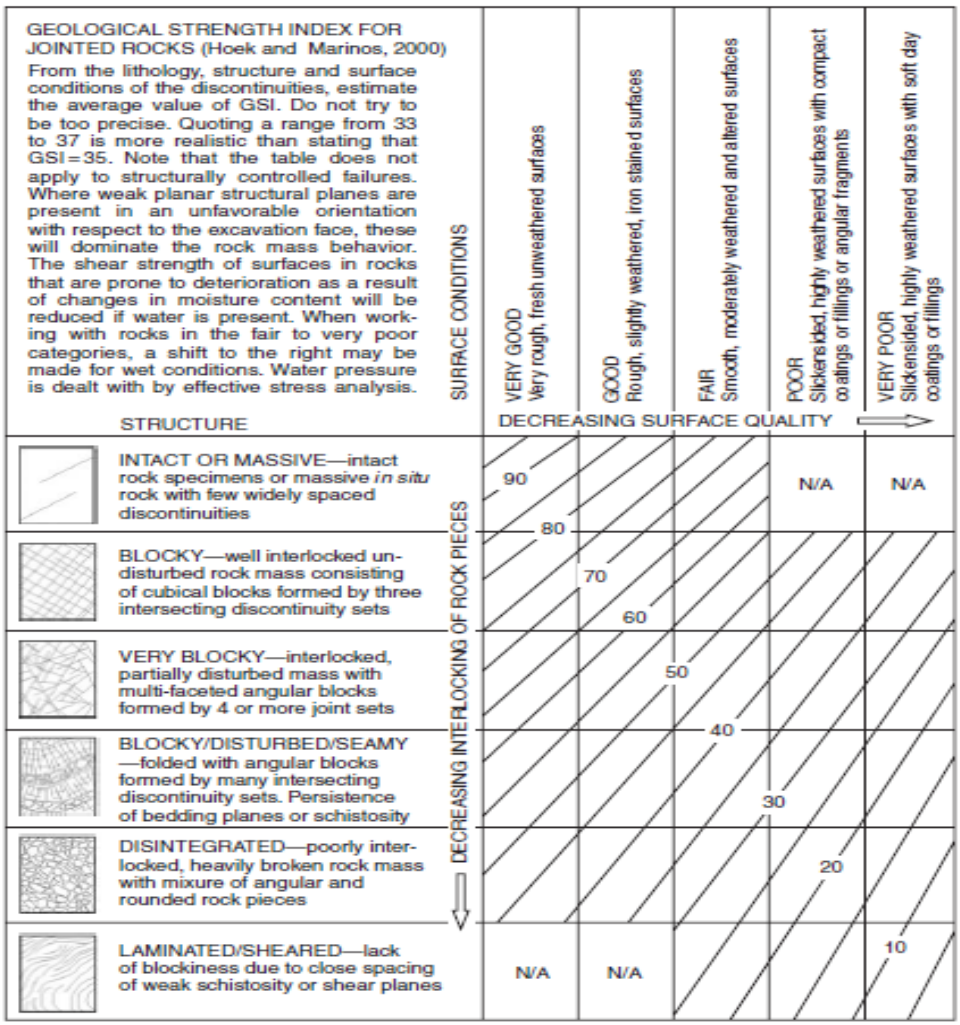

Table 3-1 Chart for estimating the Geological Strength Index, GSI. Taken from (Marinos, Marinos and Hoek 2005)

In Hoek –Brown criterion distribution coefficient 'D' is a factor that depends upon the degree of disturbance to which the rock mass has been subjected by blast damage and stress relaxation. It varies from 0 for undisturbed in situ rock masses to 1 for very disturbed rock masses Experience in the design of slopes in very large open pit mines has shown that the Hoek–Brown criterion for undisturbed in situ rock masses (D =0) results in rock mass properties that are too optimistic (Pierce et al., 2001; Sjöberg et al., 2001). The effects of heavy blast damage as well as stress relief due to removal of the overburden result in disturbance of the rock mass (Hoek and Brown, 1988). The value of D can be obtained from table 3.2.

Appearance of rock mass	Description of rock mass	Suggested value of D
	Excellent quality controlled blasting or excavation by Tunnel Boring Machine results in minimal disturbance to the confined rock mass surrounding a tunnel.	$D = 0$
	Mechanical or hand excavation in poor quality rock masses (no blasting) results in minimal disturbance to the surrounding rock mass. Where squeezing problems result in significant floor heave, disturbance can be severe unless a temporary invert, as shown in the photograph, is placed.	$D = 0$ $D = 0.5$ No invert
	Very poor quality blasting in a hard rock tunnel results in severe local damage, extending 2 or 3 m, in the surrounding rock mass.	$D = 0.8$
	Small scale blasting in civil engineering slopes results in modest rock mass damage, particularly if controlled blasting is used as shown on the left hand side of the photograph. However, stress relief results in some disturbance.	$D = 0.7$ Good blasting $D = 1.0$ Poor blasting
	Very large open pit mine slopes suffer significant disturbance due to heavy production blasting and also due to stress relief from overburden removal. In some softer rocks excavation can be carried out by ripping and dozing and the degree of damage to the slopes is less.	$D = 1.0$ Production blasting $D = 0.7$ Mechanical excavation

Table 3-2 Guidelines for estimating disturbance factor *D* (from Hoek et al, 2002)

In Hoek-Brown criterion also uses material constant (m_i) for the intact rock and uniaxial compressive strength (σ_{ci}), which are obtained through the whenever possible these values should be determined by statistical analysis of the results of a set of tri-axial tests on carefully prepared core samples, but if not possible for laboratory tests then m_i can be obtained from table 3.4 and σ_{ci} can be obtained from table 3.3(E. Hoek and E.T. Brown)

Grade*	Term	Uniaxial Comp. Strength (MPa)	Point Load Index (MPa)	Field estimate of strength	Examples
R6	Extremely Strong	> 250	>10	Specimen can only be chipped with a geological hammer	Fresh basalt, chert, diabase, gneiss, granite, quartzite
R5	Very strong	100 - 250	4 - 10	Specimen requires many blows of a geological hammer to fracture it	Amphibolite, sandstone, basalt, gabbro, gneiss, granodiorite, limestone, marble, rhyolite, tuff
R4	Strong	50 - 100	2 - 4	Specimen requires more than one blow of a geological hammer to fracture it	Limestone, marble, phyllite, sandstone, schist, shale
R3	Medium strong	25 - 50	1 - 2	Cannot be scraped or peeled with a pocket knife, specimen can be fractured with a single blow from a geological hammer	Claystone, coal, concrete, schist, shale, siltstone
R2	Weak	5 - 25	**	Can be peeled with a pocket knife with difficulty, shallow indentation made by firm blow with point of a geological hammer	Chalk, rocksalt, potash
R1	Very weak	1 - 5	**	Crumbles under firm blows with point of a geological hammer, can be peeled by a pocket knife	Highly weathered or altered rock
R0	Extremely weak	0.25 - 1	**	Indented by thumbnail	Stiff fault gouge

* Grade according to Brown [2]

** Point load tests on rocks with a uniaxial compressive strength below 25 MPa are likely to yield ambiguous results.

Table 3-3 Field estimates of uniaxial compressive strength (E. Hoek and E.T. Brown)

Rock type	Class	Group	Texture			
			Coarse	Medium	Fine	Very fine
SEDIMENTARY	Clastic		Conglomerate (22)	Sandstone 19	Siltstone 9	Claystone 4
				Greywacke (18)		
	Non-Clastic	Organic		Chalk 7		
				Coal (8-21)		
		Carbonate	Breccia (20)	Sparitic Limestone (10)	Micritic Limestone 8	
		Chemical		Gypstone 16	Anhydrite 13	
METAMORPHIC	Non Foliated		Marble 9	Hornfels (19)	Quartzite 24	
	Slightly foliated		Migmatite (30)	Amphibolite 25 - 31	Mylonites (6)	
	Foliated*		Gneiss 33	Schists 4 - 8	Phyllites (10)	Slate 9
IGNEOUS	Light		Granite 33		Rhyolite (16)	Obsidian (19)
			Granodiorite (30)		Dacite (17)	
	Dark		Diorite (28)		Andesite 19	
			Gabbro 27	Dolerite (19)	Basalt (17)	
			Norite 22			
	Extrusive pyroclastic type		Agglomerate (20)	Breccia (18)	Tuff (15)	

* These values are for intact rock specimens tested normal to bedding or foliation. The value of m_i will be significantly different if failure occurs along a weakness plane.

Table 3-4 Values of the constant mi for intact rock, by rock group. (E. Hoek and E.T. Brown)

For finite element modelling of rock mass and perform its stress-strain analysis modulus of elasticity of intact rock (E_i), modulus of elasticity of rock mass (E_{rm}) and Poisson's ratio (ν) are required which can be obtained from different empirical relations provided by different authors, used relations for this thesis are , modulus of rock mass when modulus of intact rock is unknown.

$$E_{rm}=\frac{1-D/2}{1+e^{(75+25D-GSI)/11}} \ .10^5 \ \text{Mpa} \tag{3.45}$$

When modulus of intact rock (E_i) is known

$$E_{rm}=E_i\left(0.02+\frac{1-D/2}{1+e^{(60+15D-GSI)/11}}\right) \tag{3.46}$$

Above relation are obtained from E. Hoek, M. S. Diederichs, (2006).

Poisson's ratio for rock mass can be estimated from Tokashiki and Aydan(2010), according to which,

$$\nu_m = 0.5 - \frac{0.2RMR}{RMR + 0.2(100 - RMR)} \quad (3.47)$$

As certain parameters are dependent up on RMR value rather than GSI, so relation between these according to Hoek and Brown(1997) if RMR>23 as below,

$$GSI = RMR - 5 \quad (3.48)$$

3.4.1.3 Rock joint properties

There are many criterions developed for the shear strength of rock discontinuity such as Mohr-Coulomb shear strength, Patton's shear strength (1966), Barton shear strength(1973, 1976), Barton and Choubey shear strength (1977), and Barton-Bandis criterion for rock joint strength and deformability (Barton and Bandis, 1990). In this thesis Barton-Bandis criterion for shear strength and deformability is considered for discontinuities, for that criterion as shown in equation 2.8 following parameters should be obtained.

3.4.1.3.1 Joint wall compressive strength (JCS)

Suggested methods for estimating the joint wall compressive strength were published by the ISRM (1978). The use of the Schmidt rebound hammer for estimating joint wall compressive strength was proposed by Deere and Miller (1966), as illustrated in Figure 3.5.

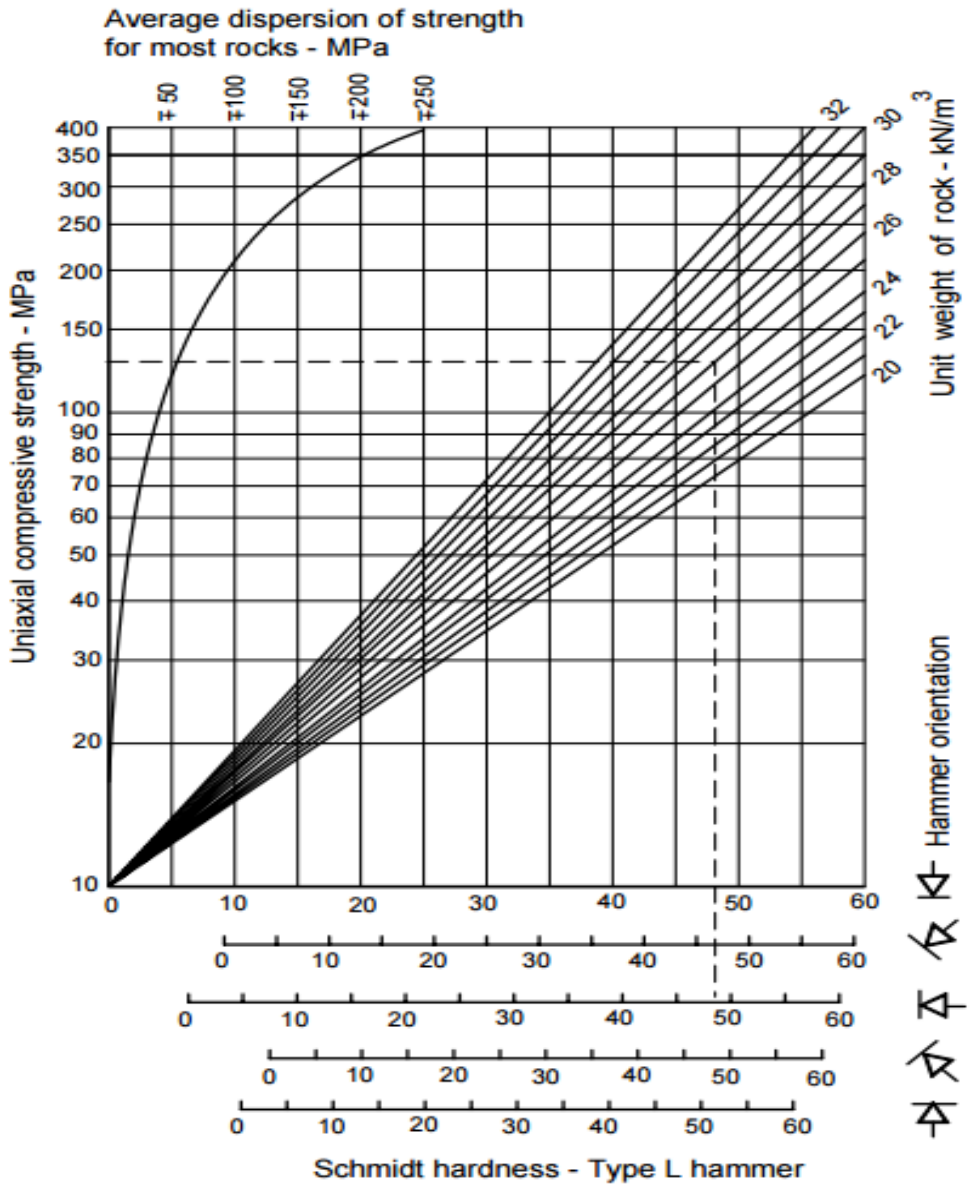

Figure 3-4 Estimate of joint wall compressive strength from Schmidt hardness.

3.4.1.3.2 Joint roughness coefficient (JRC)

The joint roughness coefficient JRC is a number that can be estimated by comparing the appearance of a discontinuity surface with standard profiles published by Barton and others. One of the most useful of these profile sets was published by Barton (1982) and is reproduced in Figure 3.6.The appearance of the discontinuity surface is compared visually with the profiles shown and the JRC value corresponding to the profile which most closely matches that of the discontinuity surface is chosen. In the case of small scale laboratory specimens, the scale of the surface roughness will be approximately the same as that of the profiles illustrated. However, in the field the length of the surface

of interest may be several metres or even tens of metres and the JRC value must be estimated for the full scale surface.

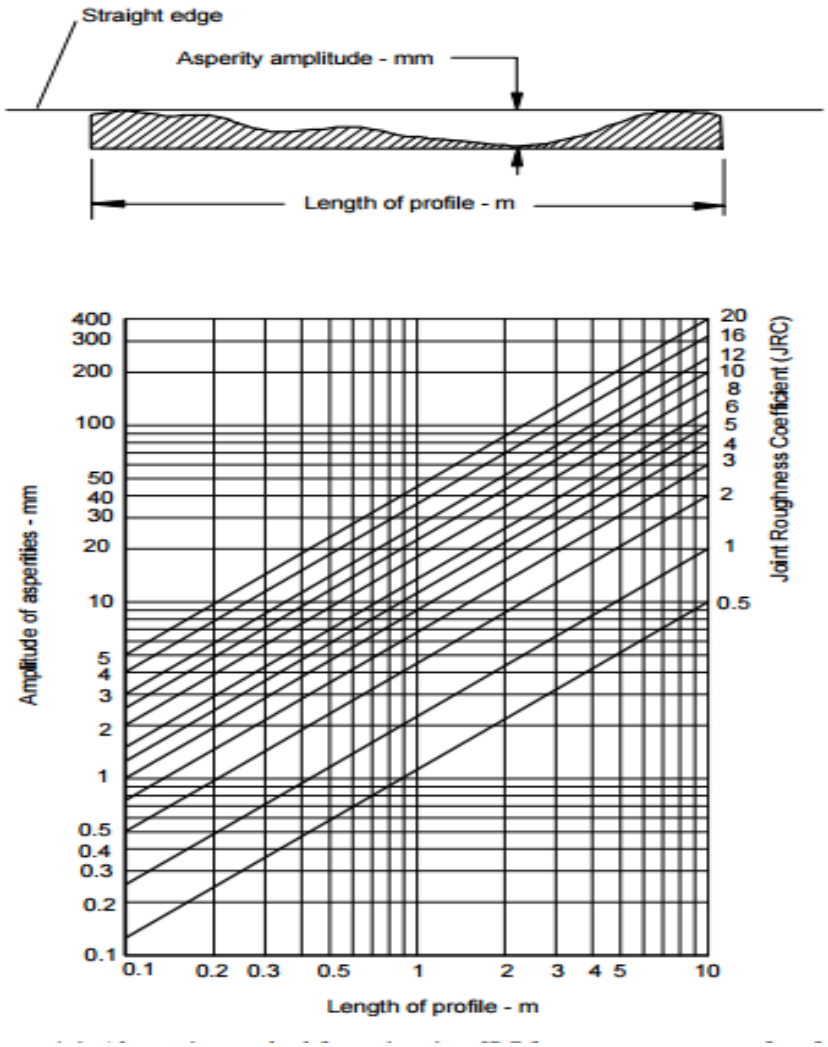

Figure 3-5 Alternative method for estimating JRC from measurements of surface roughness amplitude from a straight edge (Barton 1982).

3.4.1.3.3Basic frictional angle (ϕ_b)

Conceptually, ϕ_b refers to smooth, planar surface in fresh rock and can be considered as a material constant. Methods for ϕ_b characterization include direct shear test or tilt tests on saw cut surface. The values of ϕ_b depend on the rock type and the moisture conditions (Horn and Deere, 1962; Coulson, 1972). Indicative ranges for ϕ_b (dry) = 26-38^o and ϕ_b (wet) = 21-35^o, the majority of rocks falling in the 25-35^o range.

3.5 Static loads

The basic loads contributing to the design or safety analysis of arch dams are gravity, reservoir water, temperature changes, and silt, ice, uplift, and earthquake loads. In this thesis for safety

- Gravity Loads: Gravity loads due to weight of the material are computed from the unit weight and geometry of the finite elements.

- Reservoir Water: In finite element program is developed to handle hydrostatic loads as distributed surface loads. The surface loads are then applied to the structure as concentrated nodal loads. Therefore, hydrostatically varying surface pressure can be specified by using a reference fluid surface and a fluid weight density as input.

- Silt. Arch dams often are subjected to silt pressures due to sedimentary materials deposited in the reservoir. The saturated silt loads are treated as hydrostatically varying pressures acting on the upstream face of the dam and on the valley floor. A silt reference level and the weight density of the equivalent fluid are needed to specify the silt pressures.

- Pore pressure. Pore pressure at level surface of discontinuities is considered according to the permeability of the discontinuities and rock.

3.1.1 Geometrical data of dam

The necessary data for constructing a finite element mesh of an arch dam is obtained from drawings containing information defining the geometry of the dam shape. These include the plan view and section along the reference plane. In practice, arch dams are geometrically described as multicentre arches with their centres varied by elevation in addition to the arch opening angles and radii varying for each side with elevation. Elliptical arch shapes may be approximated for the various elevations by three-centred arches including central segments with shorter radii and two outer segments with equal but longer radii. The basic geometric data of a multi centred dam at each elevation for the upstream and downstream faces are as follows:

- Radius of central arcs
- Radius of outer arcs
- Angles to point of compounding curvatures
- Angles to abutments
- Location of centres of central arcs

3.1.2 Orientations of discontinuities

Orientation of discontinuity is generally represented by it's tend and plunge which is defined by (Ragan 1973, Phillips 1971, Hicst 1985, Hoek & Bray 1974, Hoek & Brown 1980). During the geological survey of the Budhigandaki dam site numbers of joints set were observed and for each joint set numbers of orientation data were observed. For the numerical simulation of those joint sets statically reduction of data should be performed, there are numbers of statically reduction methods as (CANMET 1977, priest 1985, Markland 1974, Fisher 1953), for this thesis Priest (1985) method is adopted.

For the convenient implementation in numerical analysis and modelling of discontinuities their trend and plunge (α and β) can be represented in direction cosines (λ_x , λ_y and λ_z) as recommended by Priest(1985) :

$$\lambda_x = \cos\alpha \,.\, \cos\beta \tag{3.45}$$

$$\lambda_y = \sin\alpha \,.\, \cos\beta \tag{3.46}$$

$$\lambda_z = \sin\beta \tag{3.47}$$

Above direction cosines are represented in Cartesian coordinate system where x-axis represents horizontal north, y-axis represents horizontal east and z-axis represents vertical downward axis.

For statistical reduction of 'N' number of (α,β) in a resultant trend and plunge following procedure is followed.

i) For discontinuity i, calculate the angle δ_i between its normal and the sampling line:

$$\text{Cos } \delta i = |\lambda xi.\lambda xs + \lambda yi\lambda ys + \lambda zi\lambda zs| \quad (3.48)$$

Where (λ_{xi}, λyi, λzi) and (λ_{xs}, λ_{ys}, λ_{zs}) are the direction cosines respectively of the normal to discontinuity i and the sampling line.

ii) For discontinuity i, calculate the weighting factor w_i based on the angle δ_i

$$w_i = \frac{1}{cos\delta i} \quad (3.49)$$

iii) After the weighting factor for each discontinuity is obtained, calculate the total weighted sample size N_w for a sample of size N by

$$Nw = \sum_{i=1}^{N} wi \quad (3.50)$$

iv) Calculate the normalized weighting factor w_{ni} for each discontinuity by

$$w_{ni} = \frac{wiN}{Nw} \quad (3.51)$$

v) Calculate the corrected direction cosines for normal to each discontinuity

$$(\lambda'_{xi}, \lambda'_{yi}, \lambda'_{zi}) = w_{ni}.(\lambda_{xi}, \lambda yi, \lambda zi) \quad (3.52)$$

vi) Calculate resultant vector ($\lambda_x, \lambda_y, \lambda_z$) by

$$\lambda_x = \sum_{i=1}^{N} \lambda' xi \qquad \lambda_y = \sum_{i=1}^{N} \lambda' yi \qquad \lambda_z = \sum_{i=1}^{N} \lambda' zi \quad (3.53)$$

4. MODEL FORMULATION, ANALYSIS, RESULTS and DISSCUSSION

4.1 Geometry for the finite element model preparation

In finite element modelling dam over Budhigandaki River for Budhigandaki hydroelectric project and its rock foundation as abutment in both left and right side of dam, rock foundation below, upstream and downstream portion of river valley is considered. Their geometric properties are obtained as following.

4.1.1 Geometry of the dam

Double curvature arch dam is considered with maximum height 263m, crest length at top 760m, width at base 80m and top width 15m. Reduced level of crest is considered 542m. Total volume of dam (concrete) is evaluated as 5.75 million m^3, from feasibility study and detailed design of BudhiGandaki HEP.

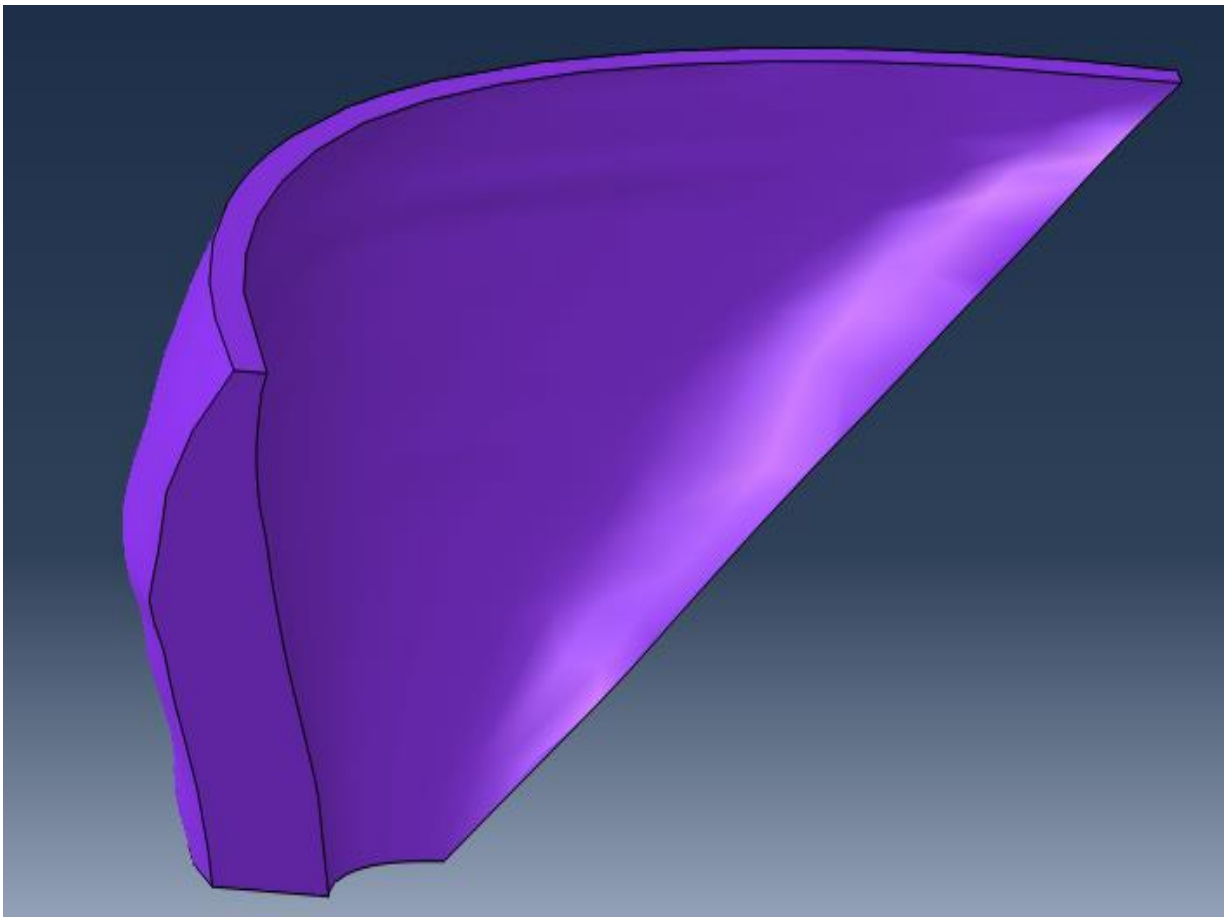

Figure 4-1 Model of dam (Prepared from Autocad Civil 3D 2015)

4.1.2 Geometry of foundation

Foundation of thickness 1000m from top of dam, width 2000m and length 1600m is taken for consideration of foundation as infinite medium. Slopes of river valley and its orientation is obtained from available topographic map of dam site. It was found from bore hole log data provided in feasibility study and detailed design report, bed rock generally started after 3m to 15 m thick layer of colluvium deposit, which is considered during formation of foundation model. Rock above R.L. of dam is not considered but its equivalent weight is applied on top model. Slopes of river valley are considered as plane with equivalent slope to ease the modelling and finite element generation process. Main feature of foundation is found at left abutment where ridge is present narrowing the river channel.

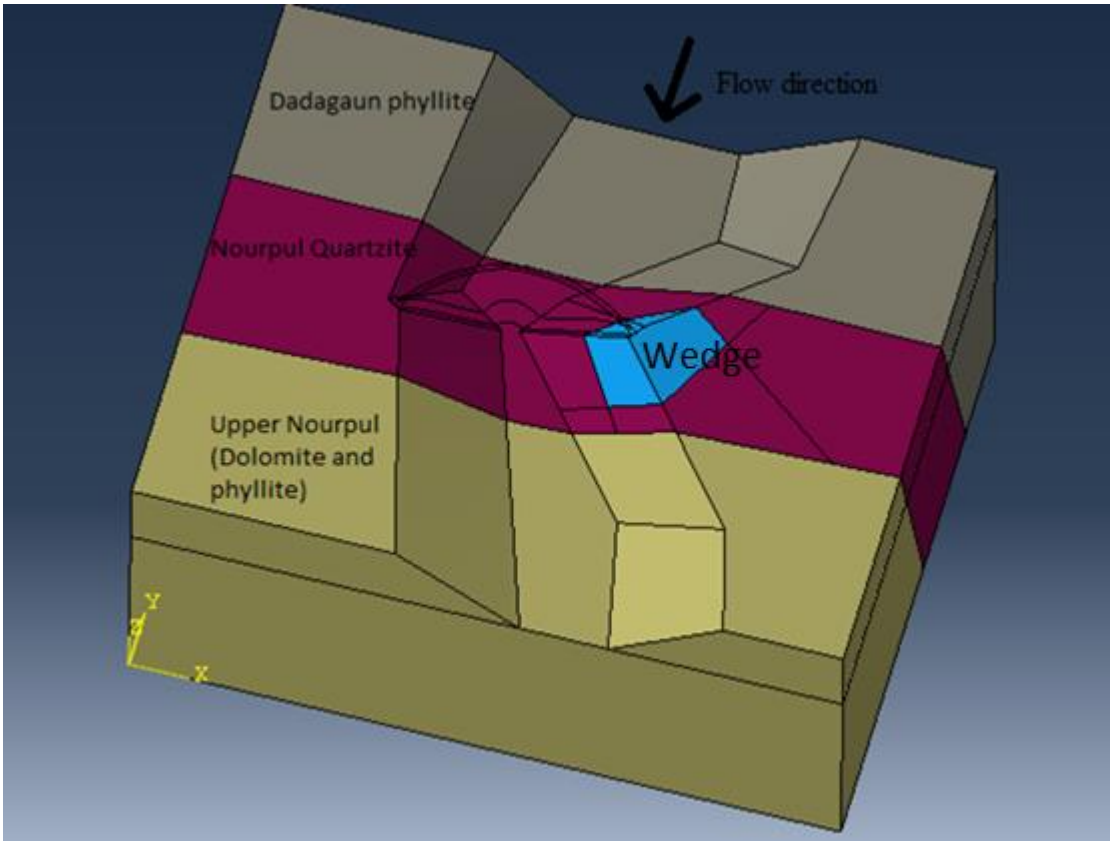

Figure 4-2 Geometric model of dam foundation and abutments

4.2 Material properties for analysis

4.2.1 Material property of dam

Concrete of M20 grade is considered having modulus of elasticity 20000 MPa, Poisson's ratio 0.2 and unit weight 24 kN/m^3.

4.2.2 Material property of foundation

Material properties of rock mass and discontinuity is obtained from geotechnical study report of Budhigandaki HEP, and following main features are considered for modelling.

I. Rock type and Rock mass properties

In region of dam site different type of rocks from different formation where found such as Fagfog formation, Dandagaun formation , Lower Nourpul formation, Upper Nourpul formation and Dhading Dolomite formation sequentially from north to south. Some of them are only considered during modelling for thesis which are,

a. Dandagaun Formation:

It consists of thinly foliated grey Phyllite having bedding plane oriented in East West and having steep dip amount in North (upstream). It was found dip amount is about 70-80^0 near river and decreases to 50-65^0 with increase in elevation. Rocks of Dandagaon formation appears in immediate upstream of dam area. Northern contact of this formation was found with Fagfog formation which consists white Quartzite, and southern contact is with Nourpul formation, which is dominant rock type at dam site. According to feasibility study conducted for Budhgandaki HEP and report of Jaya laxmi Singh and Naresh Tamrakar (2013) following geotechnical data were acquired,

- Geological Strength Index (GSI)= 40
- Uniaxial compressive strength(intact rock) σ_{ci}= 35 MPa
- Young's modulus of elasticity(intact rock)E_i=40 GPa
- Young's modulus of elasticity (rock mass)E_{rm}=8.0 GPa (from S wave)
- Disturbance factor(D)=0.2 (Blasting was rarely done)
- Young's modulus of elasticity(rock mass) E_{rm} =4.76 GPa (from equation 3.46)

- Young's modulus of elasticity(rock mass)E_{rm} =2.31GPa (from equation 3.45)
- Hoek and Brown material constant for intact rock(m_i)=10
- Hoek and Brown reduced material constant (m_b)=0.92 (from equation 2.3)
- Hoek and Brown criterion constant (s)= 0.0079 (from equation 2.4)
- Hoek and Brown criterion constant (a)= 0.511 (from equation 2.5)
- Poisson's ratio of rock mass (ν)= 0.32
- Unit weight of rock(γ_m)=22 kN/m^3

b. Nourpul Formation :

Nourpul Formation involves lithological rock consisting of quartzite, dolomite and phyllite. The upper part of the Nourpul Formation consists of mainly pink and light grey quartzite is found at dam site, this rock type is also known as Purebesi quartzite which are fractured to blocky at dam site. Strike and dip of this quartzite is also similar to the Dandagaun phyllite, steeply dipping towards north. Southern portion of Purebesi quartzite consists Upper Nourpul Formation which consists alternating dolomite and phyllite. Southern contact of Nourpul formation is Dhading dolomite. According to feasibility study conducted for Budhgandaki HEP and report of Jaya laxmi Singh and Naresh Tamrakar (2013) following geotechnical data for Purebesi quartzite were acquired.

- Geological Strength Index (GSI)= 60
- Uniaxial compressive strength(intact rock) σ_{ci}= 62 MPa
- Young's modulus of elasticity(intact rock)E_i=52 GPa
- Young's modulus of elasticity (rock mass)E_{rm}=27 GPa (from S wave)
- Disturbance factor(D)=0.2 (Blasting was rarely done)
- Young's modulus of elasticity(rock mass)E_{rm} =21.27GPa(from equation 3.46)
- Young's modulus of elasticity(rock mass) E_{rm}=12.57GPa(from equation 3.45)
- Hoek and Brown material constant for intact rock(m_i)=24
- Hoek and Brown reduced material constant (m_b)=4.907 (from equation 2.3)
- Hoek and Brown criterion constant (s)= 0.00855 (from equation 2.4)
- Hoek and Brown criterion constant (a)= 0.503 (from equation 2.5)

- Poisson's ratio of rock mass (ν)= 0.27
- Unit weight of rock(γ_m)=25 kN/m^3

According to feasibility study conducted for Budhgandaki HEP and report of Jaya laxmi Singh and Naresh Tamrakar (2013) following geotechnical data for Upper Nourpul Formation were acquired,

- Geological Strength Index (GSI)= 50
- Uniaxial compressive strength(intact rock) σ_{ci}= 40 MPa
- Young's modulus of elasticity(intact rock)E_i=46 GPa
- Young's modulus of elasticity (rock mass)E_{rm}=15.4 GPa (from S wave)
- Disturbance factor(D)=0.2 (Blasting was rarely done)
- Young's modulus of elasticity(rock mass)E_{rm} =10.6GPa(from equation 3.46)
- Young's modulus of elasticity(rock mass) E_{rm}=5.52GPa(from equation 3.45)
- Hoek and Brown material constant for intact rock(m_i)=10
- Hoek and Brown reduced material constant (m_b)=1.37 (from equation 2.3)
- Hoek and Brown criterion constant (s)= 0.0026 (from equation 2.4)
- Hoek and Brown criterion constant (a)= 0.506 (from equation 2.5)
- Poisson's ratio of rock mass (ν)= 0.3
- Unit weight of rock(γ_m)=25 kN/m^3

In finite element model for this thesis three types of rock are considered as discussed above, all with similar E-W oriented strike and dip amount 75^0 to north. Apparent thickness of rock layers are considered as, Dandagaun phyllite 580m, Lower Nourpul Formation or Purebesi quartzite 225m, and Upper Nourpul Formation 595m. Geotechnical study has suggested that at contact of Dandagaun Formation and Fagfog Formation deformation zone occurs, similarly at contact of Upper Nourpul Formation and Dhading dolomite Formation deformation zone occurs, which are beyond the scale of selected so are not considered in this thesis.

To perform the variation of deformation and stresses in dam and foundation according to variation of modulus of elasticity of foundation rock. For this purpose different value of modulus of elasticity of Purebesi Quartzite is varied through variation of its GSI value. GSI value is increased to obtain greater values of modulus of elasticity than as of site condition, similarly GSI value is decreased to obtain smaller value of modulus of elasticity.

S.N.	Rock Properties	Case I (Actual condition of project area)			Case II			Case III			Case IV		
		Dandagaun Phyllite(D.P.)	Purebesi Quarzite (P.Q.)	Nourpul phyllite (N.P.)	D.P.	P.Q.	N.P.	D.P.	P.Q.	N.P.	D.P.	P.Q.	N.P.
1	GSI	40	60	50	30	50	40	30	35	40	40	80	50
2	σ_{ci}(Mpa)	35	62	40	30	62	30	35	62	40	35	62	40
3	E_i (Gpa)	40	52	46	40	52	46	40	52	46	40	52	46
4	E_{rm}(Gpa)	4.76	15	8	1	12	5.47	1	4.5	5.47	4.76	40	8
5	D	0.2	0.2	0.2	0.2	0.2	0.2	0.2	0.2	0.2	0.2	0.2	0.2
6	m_b	0.92	4.907	1.37	0.62	3.3	0.63	0.62	1.82	0.63	0.92	10.85	1.37
7	s	0.0079	0.00855	0.0026	0.0024	0.0026	0.0079	0.0024	0.00436	0.0079	0.0079	0.092	0.0026
8	a	0.511	0.503	0.506	0.522	0.5057	0.511	0.522	0.516	0.511	0.511	0.5	0.506
9	v	0.32	0.27	0.3	0.35	0.3	0.32	0.35	0.32	0.32	0.32	0.25	0.3
10	γ_{mb}(kN/m3)	22	25	25	22	25	25	22	25	25	22	25	25

Table 4-1 Different cases of rock mass properties in foundation

S.N.	Rock Properties	Case V			Case VI			Case VII			Case VIII		
		D.P.	P.Q.	N.P.	D.P.	P.Q.	N.P.	D.P.	P.Q.	N.P.	D.P.	P.Q.	N.P.
1	GSI	40	40	50	40	70	50	40	60	50	40	25	50
2	σ_{ci}(Mpa)	35	62	40	35	62	40	35	62	40	35	62	40
3	E_i (Gpa)	40	52	46	40	52	46	40	52	46	40	52	46
4	E_{rm}(Gpa)	4.76	6.187	8	4.76	31.5	8	4.76	20	8	4.76	2.47	8
5	D	0.2	0.2	0.2	0.2	0.2	0.2	0.2	0.2	0.2	0.2	0.2	0.2
6	m_b	0.92	2.22	1.37	0.92	7.3	1.37	0.92	10.85	1.37	0.92	0.62	1.37
7	s	0.0079	0.0079	0.0026	0.0079	0.028	0.0026	0.0079	0.00924	0.0026	0.0079	0.002	0.0026
8	a	0.511	0.51136	0.506	0.511	0.5013	0.506	0.511	0.5	0.506	0.511	0.62	0.506
9	v	0.32	0.27	0.3	0.32	0.26	0.3	0.32	0.25	0.3	0.32	0.35	0.3
10	γ_{mb}(kN/m3)	22	25	25	22	25	25	22	25	25	22	25	25

Table 4-2 Different cases of rock mass properties in foundation

II. Discontinuities

Generally three sets of joints were found at both abutment, which were planar and smooth to planar and rough, tight to open (0.1mm to 5mm). Major discontinuities after surface measurement are shown in figure 4.3. According to which a potential wedge formed due to two set joint having dip direction and dip amount $107^0/23^0$ and $288^0/42^0$

respectively. Potential wedge in right bank was not taken in account as its intersection line is plunging inside the slope.

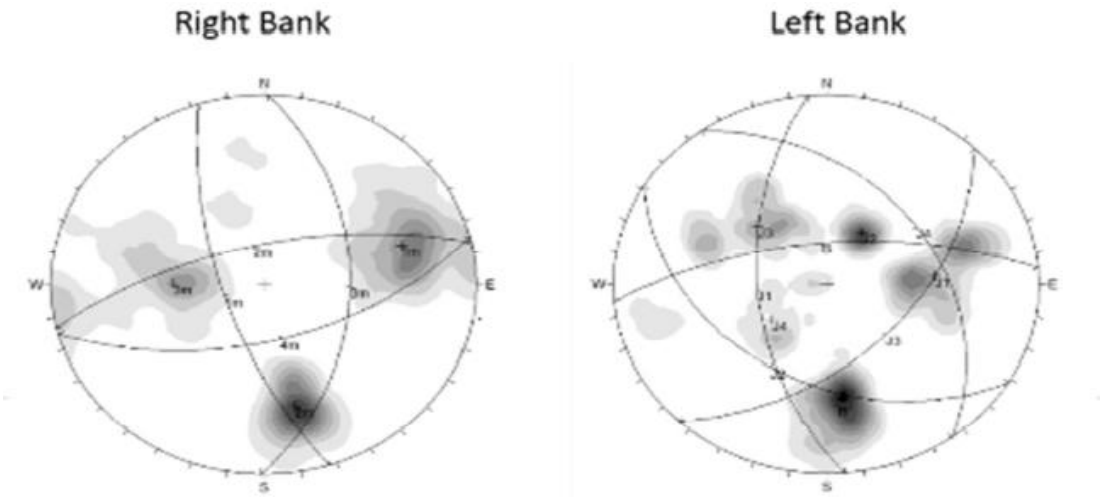

Figure 4-3 Major joint sets at dam site after surface measurements (feasibility study and detailed design of Budhigandaki HEP)

Properties of discontinuity required for analysis of its failure criteria as discussed in chapter 2 and 3 are obtained from feasibility study and detailed design of Budhigandaki HEP , report of Jaya laxmi Singh and Naresh Tamrakar (2013),from empirical relationships and some assumed are as following.

First joint of wedge having dip direction and dip amount $107^0/23^0$,

- Joint wall compressive strength (JCS)= 60 MPa
- Joint roughness coefficient (JRC)=2
- Frictional angle (residual)(ϕ_r)=20^0
- Normal stiffness (k_n)=22.5 GPa/m
- Shear stiffness (k_s)=1.2 GPa/m

Second joint of wedge having dip direction and dip amount $288^0/42^0$,

- Joint wall compressive strength (JCS)= 60 MPa
- Joint roughness coefficient (JRC)=2
- Frictional angle (residual)(ϕ_r)=18^0
- Normal stiffness (k_n)=22.5 GPa/m
- Shear stiffness (k_s)=1.2 GPa/m

4.3 Mesh generation

Hexahedral element with eight nodes is used and as mesh generation for complex geometry is tough so to do this job software package for finite element analysis Abaqus CAE 6.14 is used for mesh generation with locally controlled edge seeds by user but mesh generated is not slightly as preferred according to geometry and problem focus area, although it is adopted for analysis considering it would not affect the results. Total 6807 number of nodes and 5409 number of hexahedral element were developed. For simulation of contact of wedge joints 72 numbers of eight node zero thickness interface element were developed.

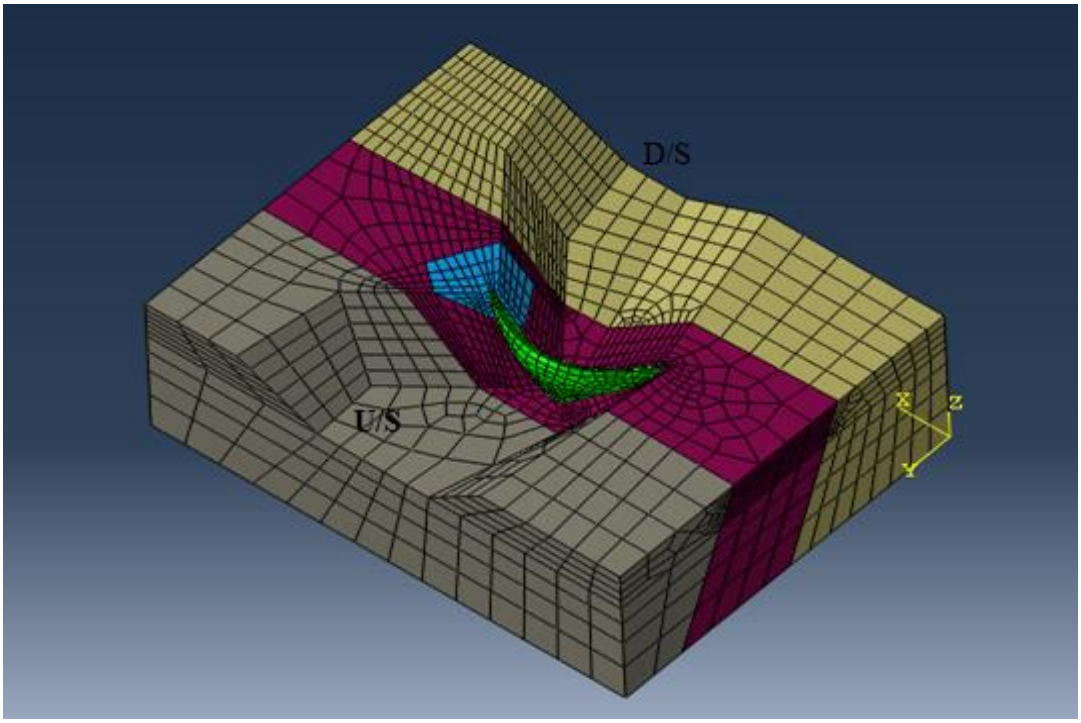

Figure 4-4 Meshed model

4.4 Boundary condition

Bottom nodes of model having z-ordinate zero are considered fixed, i.e. degree of freedom zeros of every node or zero displacement in x, y and z directions. Upstream and downstream end nodes of model are considered free in x and z direction and fixed in y direction i.e. with two degree of freedom. Left and right end nodes of model are considered free in y and z direction and fixed in x direction i.e. with two degrees of freedom. Rest nodes are considered with three degrees of freedom. Total 1219 nodes are completely restrained out of 6807 number of nodes, rest of nodes were assigned 3 degree of freedom which resulted total 17070 degree of freedom in model.

4.5 Loads

Static loading is only considered to contribute for safety stability analysis of wedge in left abutment and Hoek and Brown criterion analysis of arch dam foundation, which are gravity, reservoir water, temperature changes, and silt, ice, uplift, and earthquake loads.

- Gravity Loads: Gravity loads due to weight of the material are computed from the unit weight and geometry of the finite elements. In this thesis gravity loads acting on dam and wedge is only considered and unit weight of concrete and Purebesi phyllite (rock type of wedge) is discussed in section 4.2.2.
- Hydrostatic pressure: In finite element program is developed to handle hydrostatic loads as distributed surface loads. The surface loads are then applied to the structure as concentrated nodal loads. Therefore, hydrostatically varying surface pressure can be specified by using a reference fluid surface and a fluid weight density as input. Hydrostatic load is applied to upstream face of dam, upstream portion of wedge that faces to reservoir and to the walls of reservoir basin. Hydrostatic load is applied for incremental reservoir level as
    - Empty reservoir
    - Water level RL 392m (reservoir depth 112m)
    - Water level RL 442m(reservoir depth 162m)
    - Water level RL 467m (MOL)(reservoir depth 187m)
    - Water level RL 492m (reservoir depth 212m)
    - Water level RL 540m (FSL)(reservoir depth 260m)
- Silt. Arch dams often are subjected to silt pressures due to sedimentary materials deposited in the reservoir. The saturated silt loads are treated as hydrostatically varying pressures acting on the upstream face of the dam and on the valley floor. According to IS 6512-1984 silt load can be estimated by increasing unit weight of water in silt zone for horizontal pressure by 360 kg/m^3 and vertical pressure by 925 kg/m^3.
- Pore pressure. Pore pressure acting on discontinuities that is forming wedge is computed using $\gamma * h$, where 'γ' is unit weight of water and 'h' is the height of free water surface from point where pore pressure is to be computed. Downstream end edge of wedge is considered with zero pore pressure.

4.5 Analysis and result of wedge stability

Wedge stability is analyzed by obtaining factor of safety (F.O.S) against sliding through contact planes of wedge, here wedge has two contact planes. It is obtained by finite element model and compared with the vector method of analysis. Calculation of vector method is given in Appendix C, summary of which is in table4.1.

Reseviour level(m)		280	392	442	467	500	540
Reseviour depth(m)		0	112	162	187	220	260
Pore water pressure on surface1(kN)	Fx	0	0	-40067.14452	-113129	-221911	-454737
	Fy	0	0	-51227.77371	-144692	-283842	-581670
	Fz	0	0	156565.5138	442339.7	867795.7	1778386
Pore water pressure on surface2(kN)	Fx	0	0	-2058200.956	-3373996	-4689790	-7321379
	Fy	0	0	1095547.128	1795923	2496300	3897052
	Fz	0	0	2543018.969	4168755	5794490	9045961
Thrust from dam (kN)	Fx	-1061761.3	-134390.2	1851094	3477679	5381191	10123689
	Fy	509064.9	-194603.1	-1650791	-3001350	-4693890	-9471828
	Fz	-797597.1	-864185	-945068	-910928	-869397	-929369
Water pressure on US face of	Fx	0	0	0	0	109593.7	1627789
	Fy	0	0	0	0	-97013.2	-1734425
	Fz	0	0	0	0	-170751	-2717504
Weight of Wedge(kN)	Fx	0	0	0	0	0	0
	Fy	0	0	0	0	0	0
	Fz	-76168567.8	-76168567.8	-76168567.8	-7.6E+07	-7.6E+07	-7.6E+07
Total Force on wedge(kN)	Fx	-1061761.3	-134390.2	-247174.1008	-9445.98	579083.9	3975362
	Fy	509064.9	-194603.1	-606471.6461	-1350118	-2578445	-7890871
	Fz	-76966164.9	-77032752.8	-74414051.32	-7.2E+07	-7.1E+07	-6.9E+07
F.O.S		1.673584451	1.660808706	1.630741981	1.590476	1.529467	1.298942
From FEM		1.819750626	2.170252388	2.051356652	1.78387	1.481341	1.145

Table 4-3 Factor of safety calculation of wedge from Vector method (Londe method) and finite element analysis at left abutment

From above obtained results for factor of safety for wedge, it can be observed that as intersection line of planes forming wedge is directed towards downstream and one face of wedge lies with in reservoir that caused the decrease in factor of safety with increase of water level in reservoir. In case of finite element analysis factor of safety increased initially with increase in reservoir level as thrust from dam increased but there is no pore pressure and hydrostatic force on face of wedge but with further increase in water level these two forces developed in wedge which resulted to decrease in factor of safety.

4.6 Analysis results of continuum model

4.6.1 Deformation at top of dam

Horizontal deformation at top downstream nodes of dam at different reservoir level for Case I foundation properties (actual properties of site) is obtained as in figure 4.5. It is found that deformation at top downstream deformation of dam due to gravitational load occurs towards upstream due to curved shape of dam and is maximum of 5.8 cm at mid of dam to arc, with increase in water level in reservoir deformation gradually shifts towards downstream and maximum deformation is observed 19.4 cm at full supply level. According to 'Feasibility study and detailed design of Budhigandaki HPP' published by Budhigandaki Hydroelectric Project Development Committee, maximum downstream deformation at crest of dam is found 17cm when COBEF a finite element code is used for modelling, and in this analysis maximum deformation at crest is 19.4cm.

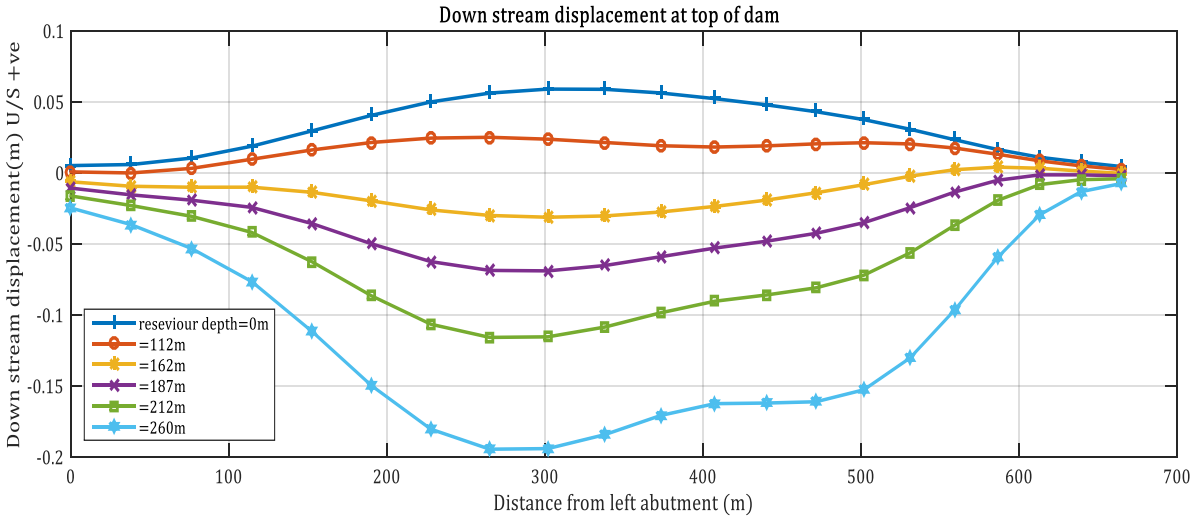

Figure 4-5 Downstream deformation at top nodes of dam for different reservoir level (Case I properties of foundation)

Vertical displacement at top of dam as obtained in figure 4.6 due to gravitational load only is downward and with increase of water level in reservoir, due to curved shape of dam in vertical axis upward hydrostatic force also acts which reduces the vertical displacement due to gravitational load and with further increase in reservoir level upward displacement has occurred at top of dam, but at bottom of dam there is very less amount of upward displacement which may produce tensile opening at contact of foundation and dam that should be minimized by increasing base width of dam.

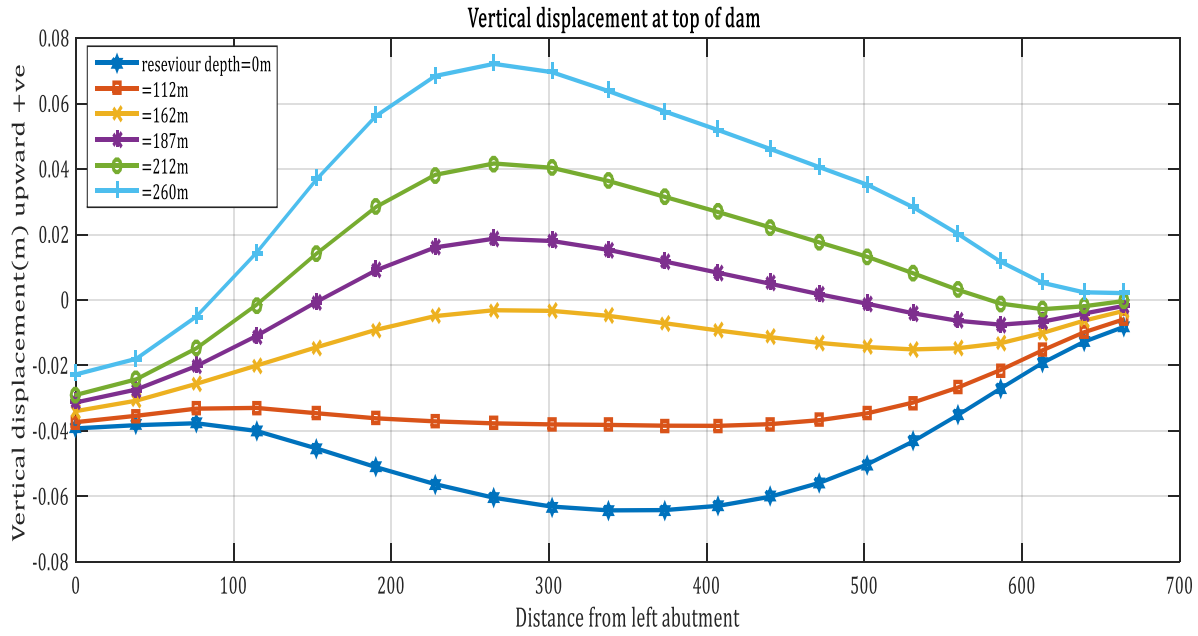

Figure 4-6 Vertical displacement at top nodes of dam for different reservoir level (Case I properties of foundation)

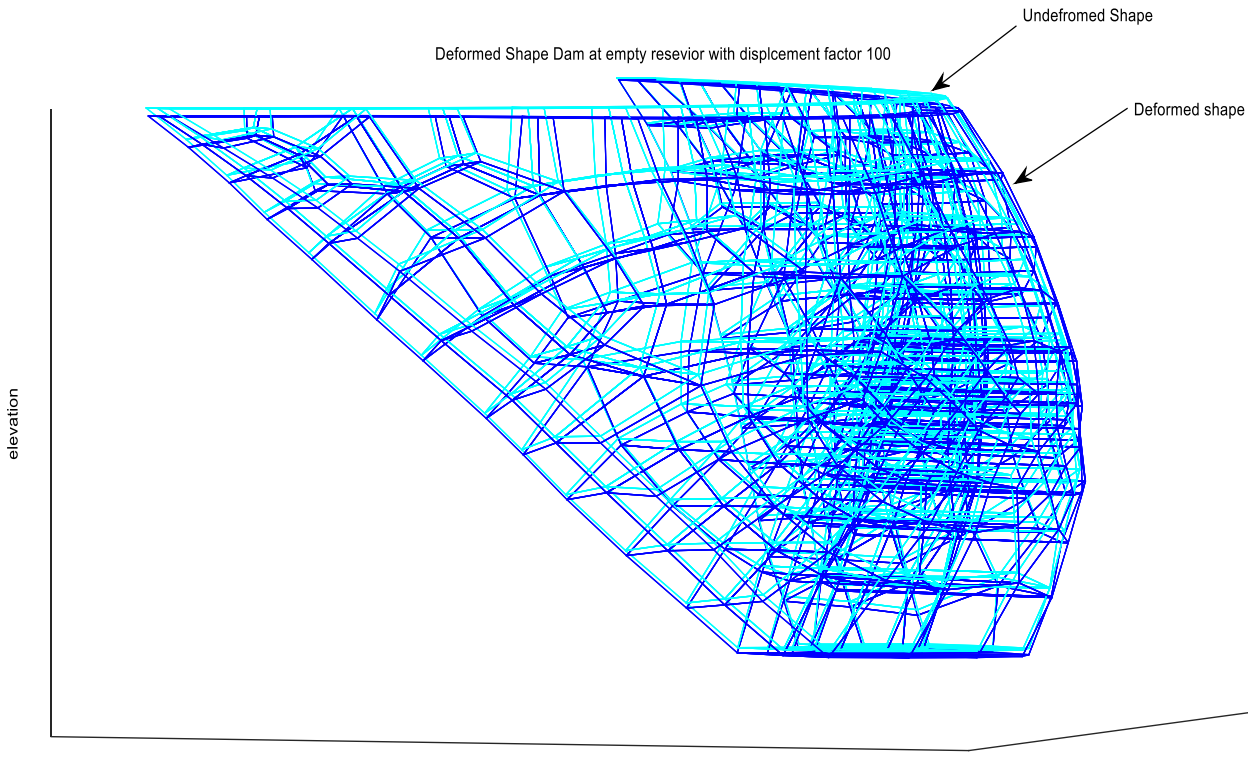

Figure 4-7 Deformed shape of dam at empty reservoir level (Case I properties of foundation) due to self weight

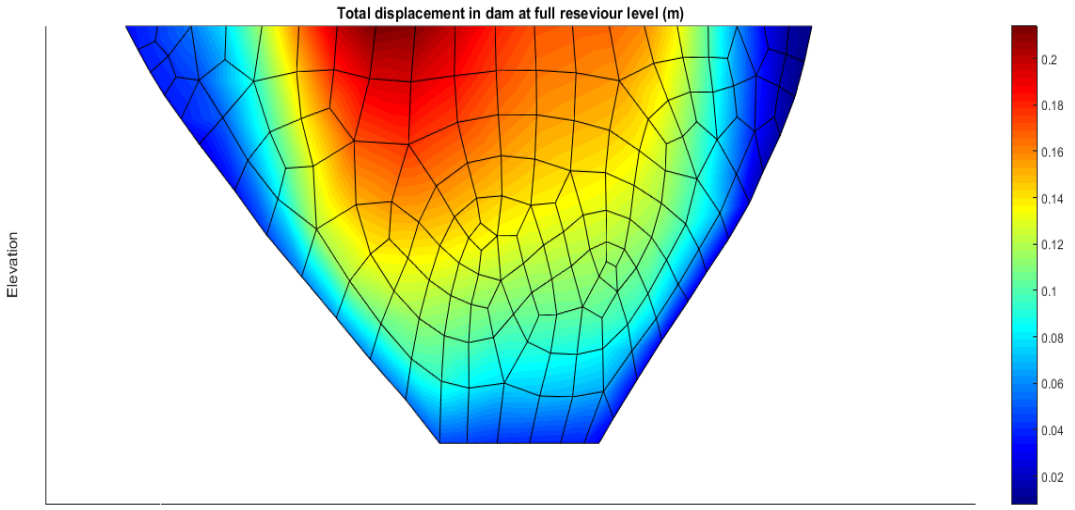

Figure 4-8 Total displacement (m) contour on D/S face dam at FSL for Case I foundation property

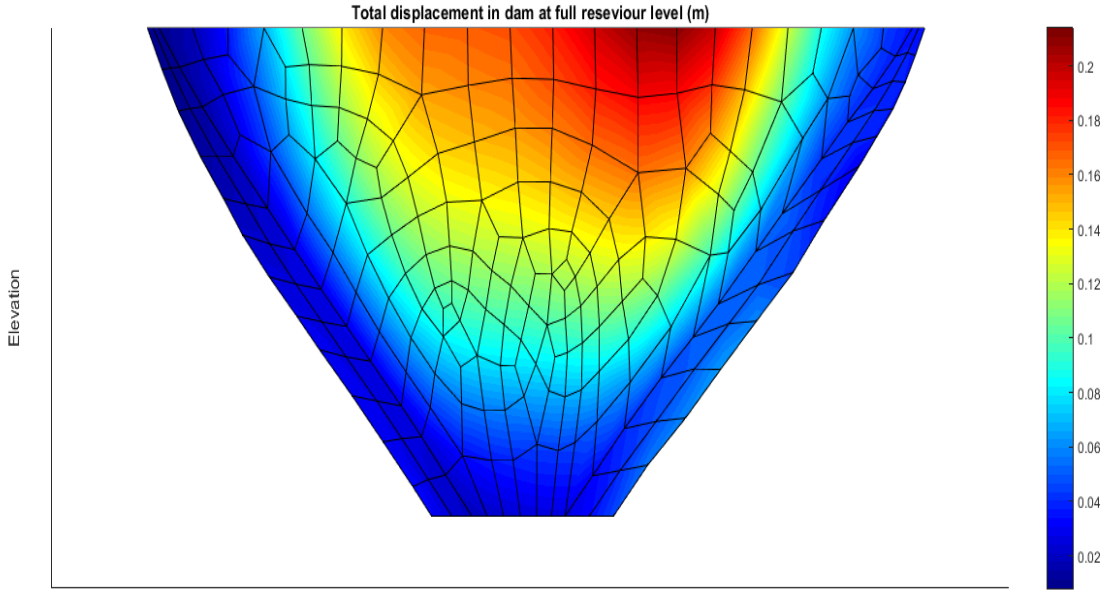

Figure 4-9 Total displacement (m) contour on U/S face of dam at FSL for Case I foundation property

Plot of total deformation with in dam at full supply level and case I foundation condition is presented in figure 4.8 and 4.9, from which it can be observed that maximum deformation of magnitude of 21cm occurs at top of dam. Maximum total deformation occurred near to left abutment from the center of dam which might has occurred due to difference in the shape of abutments, left abutment consists ridge. Deformed shape to

visualize deformation with in dam at empty reservoir condition and full supply level are presented in figure 4.7 and 4.10. During empty reservoir level U/S displacement at top of dam occurred due to shape of dam, curvature in elevation, provided C.G. of dam in U/S direction.

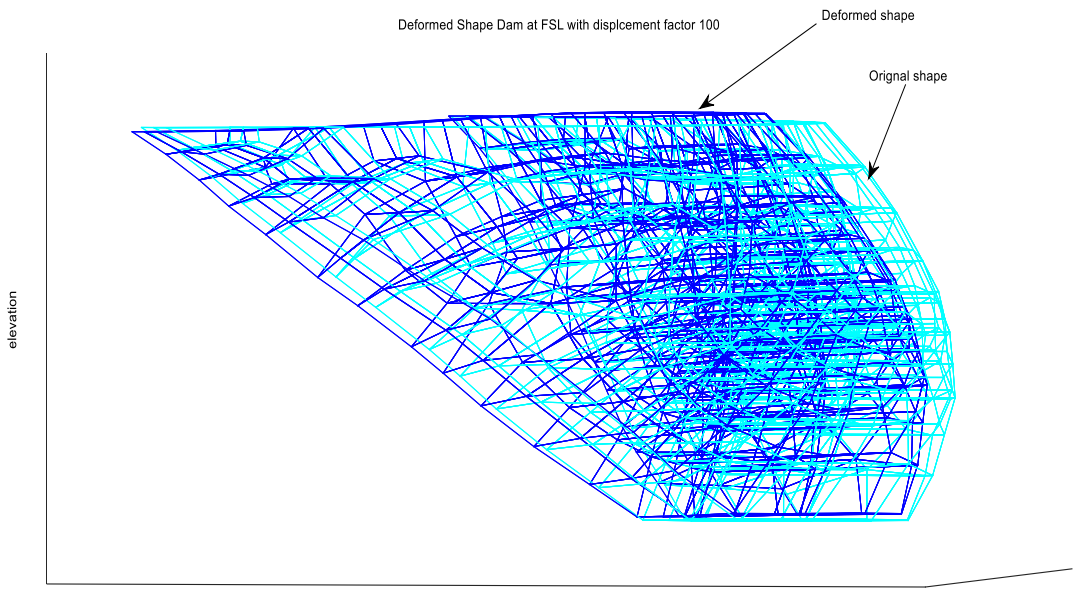

Figure 4-10 Deformed plot of dam at FSL (Case I properties of foundation)

Crest downstream (horizontal) deformation of dam for different cases (I-IV) of foundation properties at increasing reservoir depth is observed as in fig 4.11, which indicates that with decrease in GSI value of rock mainly modulus of elasticity of rock mass there is increase in deformation at crest of dam. When modulus of elasticity of rock is taken 40 GPa maximum deformation at crest is observed 16cm and for modulus of elasticity 4.5 GPa maximum deformation is observed 33cm. Similar effect is observed for the vertical displacement at the crest of the dam, increase in deformation with decrease in modulus of elasticity of foundation rock. Variation of total deformation at top of dam with changes in variation of rock mass properties of foundation is presented in figure 4.13, which also results similar as in figure 4.11 and 4.12. It is observed that total maximum deformation in dam decreases slightly from empty reservoir level (due to self-weight) to reservoir depth 110m, which occurred because total vertical load in model decreased due to uplift force from reservoir water on U/S curved face of dam.

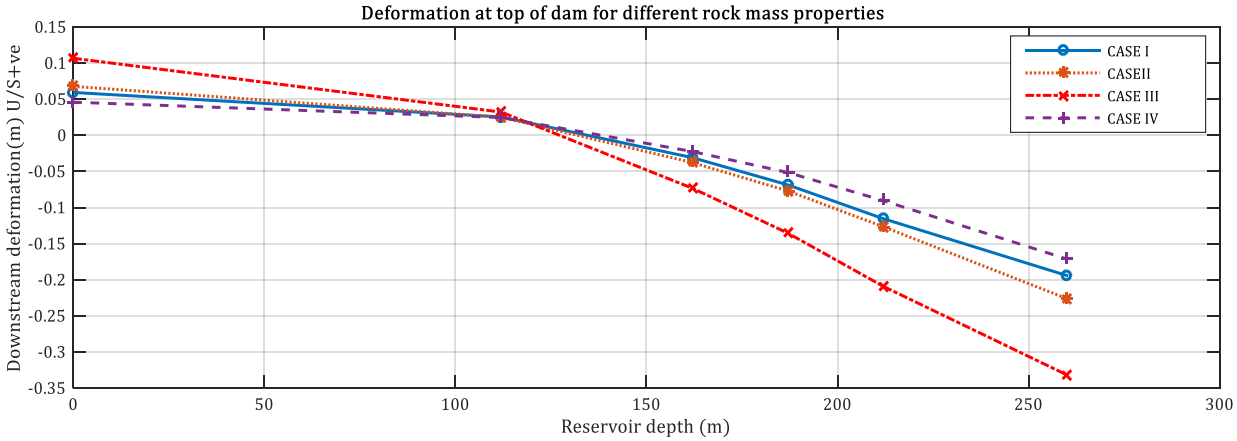

Figure 4-11 Comparison of maximum downstream deformation at crest of dam for different foundation properties and reservoir depth

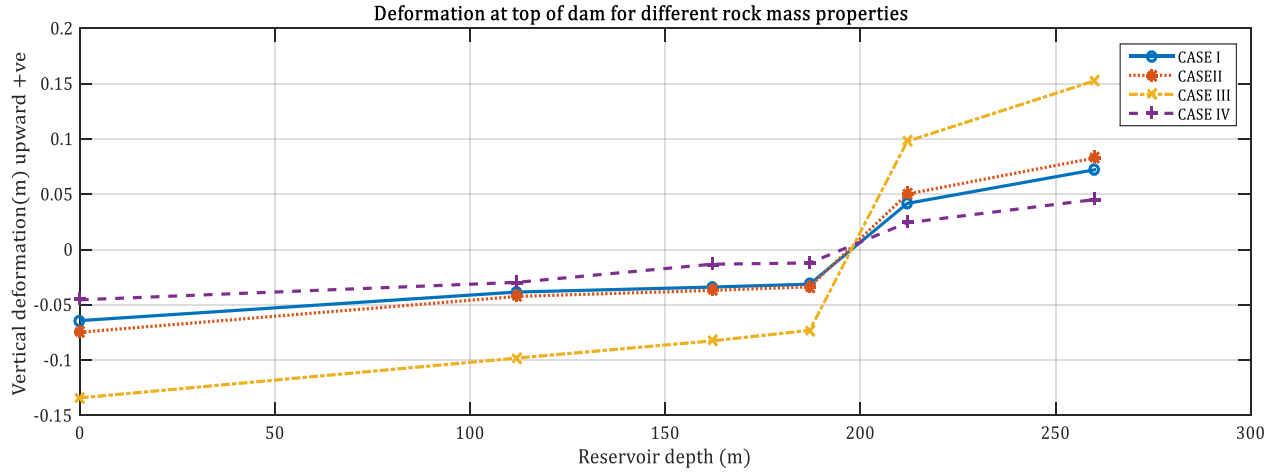

Figure 4-12Comparison of vertical deformation at crest of dam for different foundation properties and reservoir depth

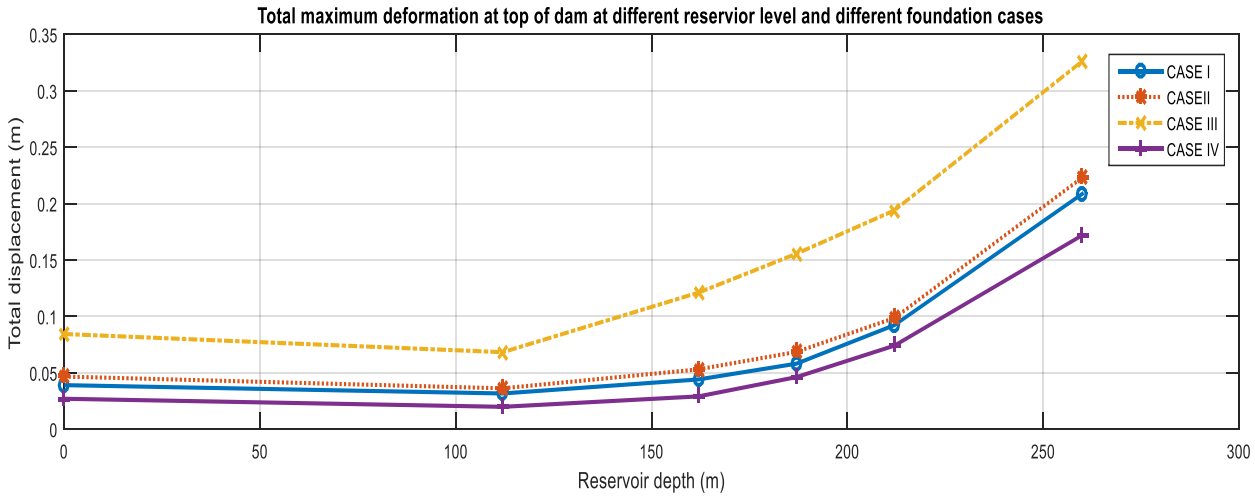

Figure 4-13 Comparison of total maximum deformation at crest of dam for different reservoir depth and foundation properties

4.6.2 Maximum compressive and tensile stress in dam

Principle stress contour for full supply level (maximum static loading condition) are given in figures 4.14, 4.15 and 4.16 which are obtained for case I foundation properties i.e. for actual foundation properties of site. It can be observed that maximum compressive stress developed in dam at full supply level is 11.5 MPa and, tensile stress is developed at contact with abutments (in US face). Which is developed due to bending action in dam due to hydrostatic load.

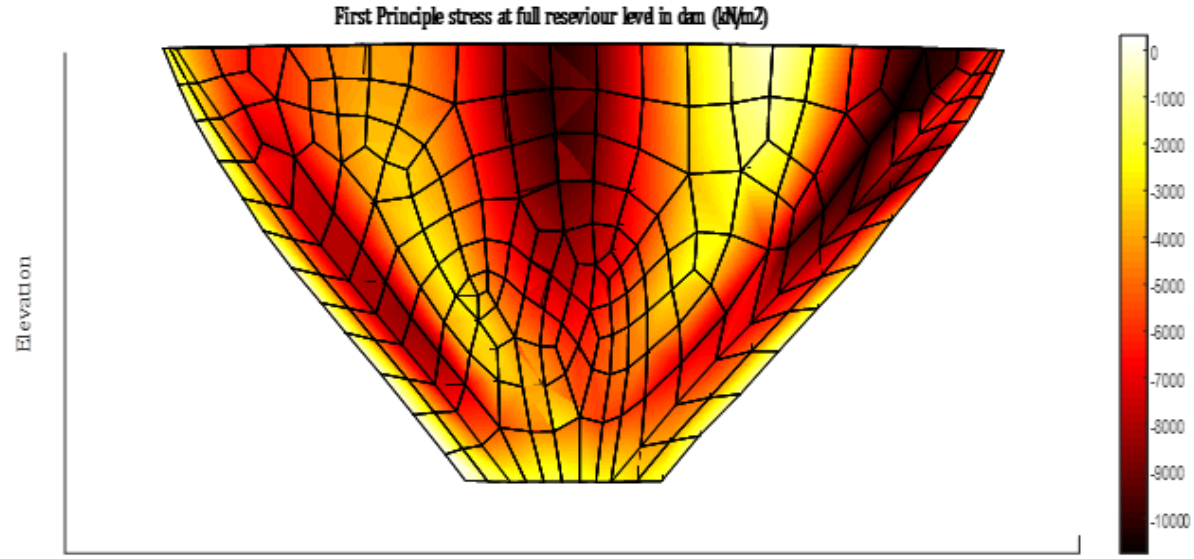

Figure 4-14Major principle stress contour on downstream face of dam at FSL

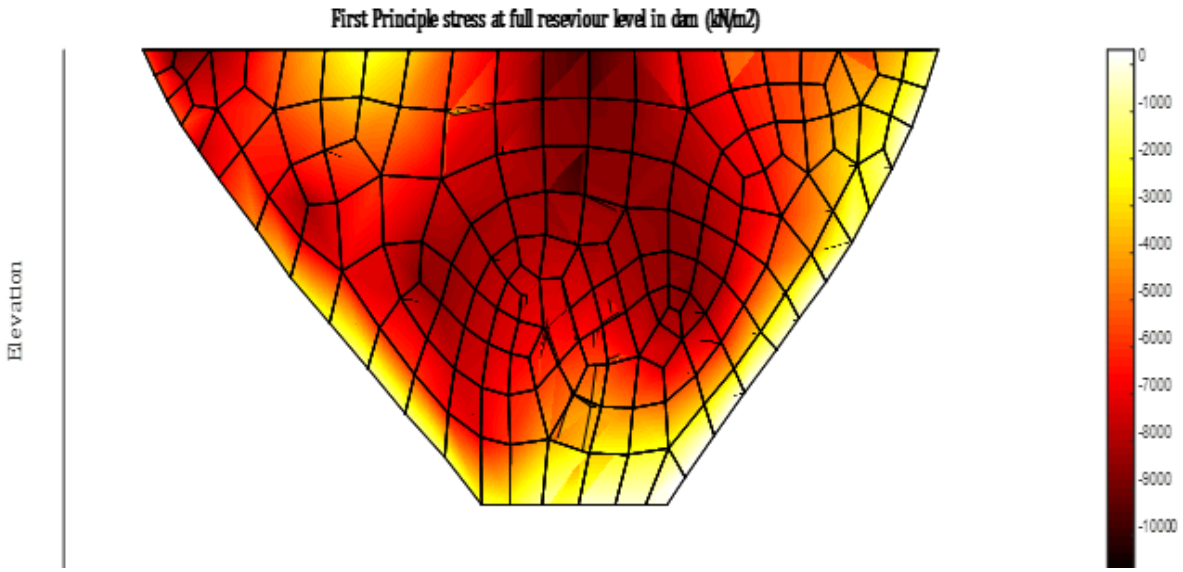

Figure 4-15Major principle stress contour on upstream face of dam at FSL

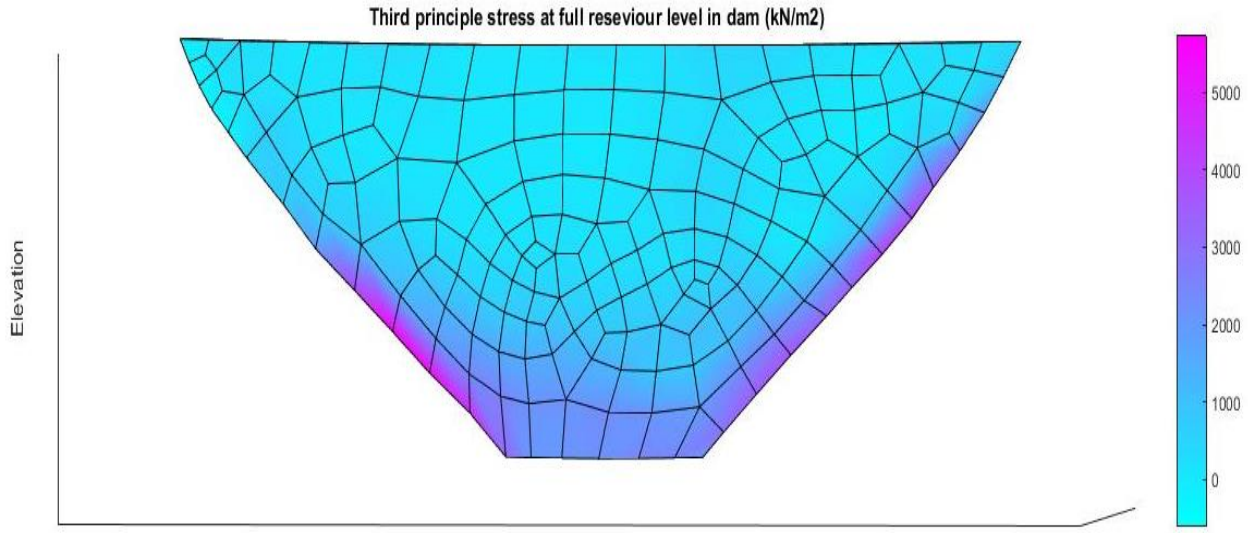

Figure 4-16 Minor principle stress contour on upstream face of dam at FSL

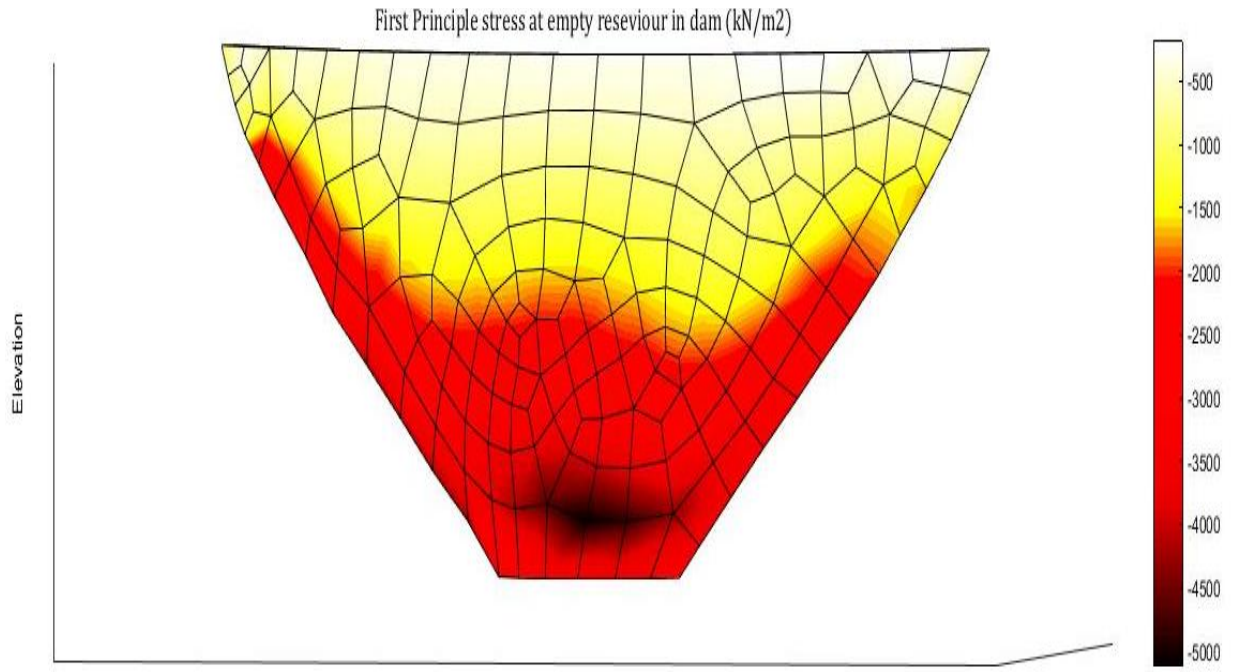

Figure 4-17 Major principle stress contour on upstream face at empty reservoir

Maximum tensile stress developed is 5 MPa at upstream edge contact of dam with abutments, this may cause the opening of the contact between dam and abutment that is unfavorable condition for the dam stability to avoid this base width of dam may be increased. Federal Energy Regulatory Commission Division of Dam Safety and Inspection (1999) has recommended that during finite element analysis there is

possibility of tensile stress developed at upstream edges of dam due to hydrostatic load, and if these tensile cracks are capable of developing cracks then uplift pressure should also be considered at interface. According to guidelines provided by Federal Energy Regulatory Commission Division of Dam Safety and Inspection (1999) during finite element analysis the tensile stressed element's stiffness can be reduced to consider redistribution of stress in dam.

According to 'Feasibility study and detailed design of Budhigandaki HPP' published by Budhigandaki Hydroelectric Project Development Committee, maximum compressive stress in dam is found 12MPa when COBEF a finite element code is used for modelling.

Variation in maximum compressive stress developed in dam for different case (I-IV) of foundation properties at increasing water depth in reservoir is shown in figure 4.18, according to these graphs it can be observed that with increase in the modulus of elasticity of foundation rock there is slight decrease in maximum stress in dam but has not much impact as with deformation in dam.

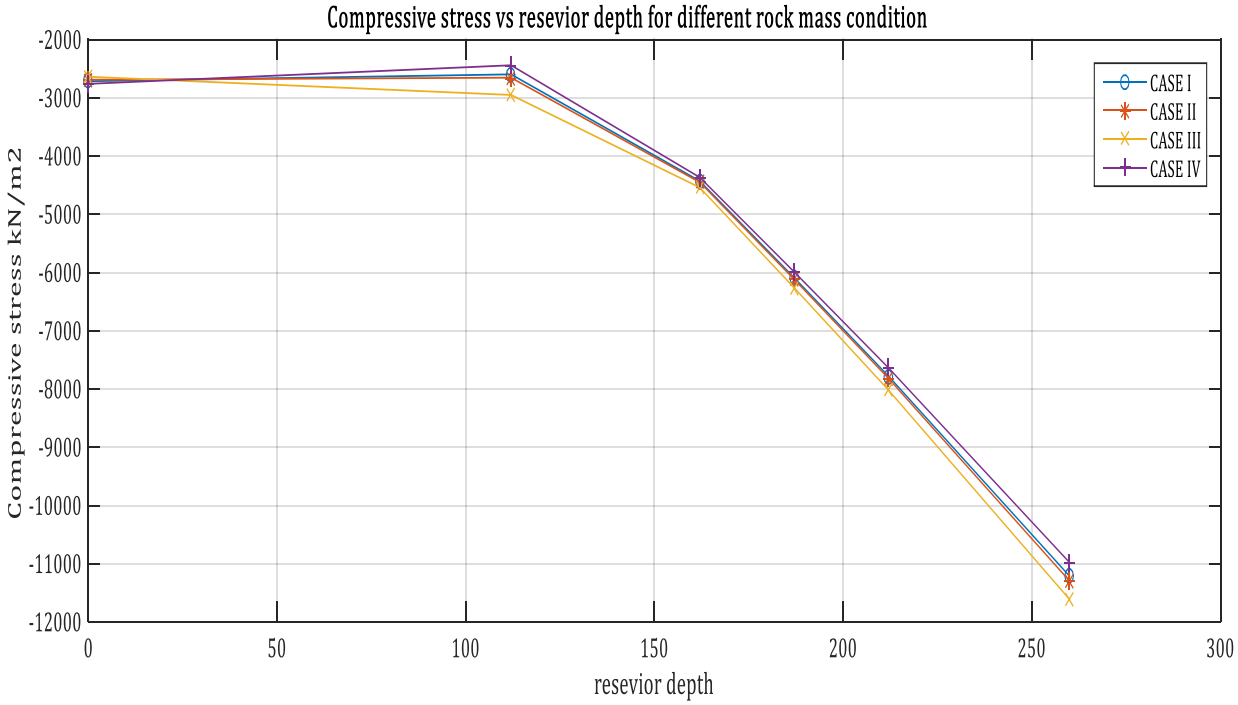

Figure 4-18Maximum compressive stress vs reservoir depth

4.6.3 Deformation in foundation rock

Contours of downstream deformation of abutments at full supply level is obtained as in figure 4.19 according to which maximum downstream deformation is observed 6cm at left abutment , deformation at left abutment is higher than of right which has occurred due to the ridge shape of abutment.

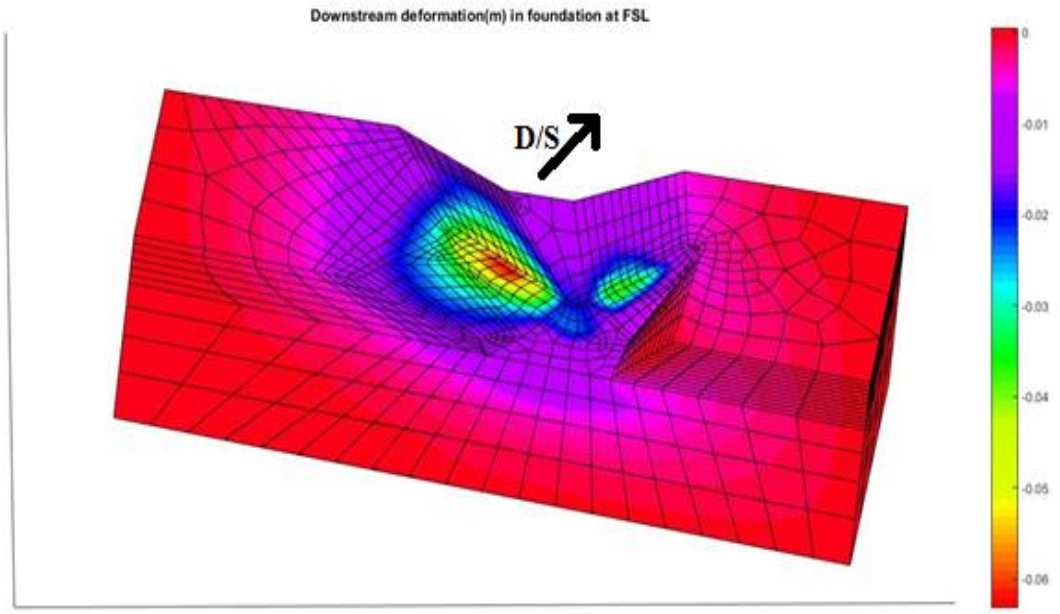

Figure 4-19 Downstream deformation (m) in foundation at FSL

Significant variation in the total maximum deformation in the foundation is observed with change in the modulus and GSI value of rock mass as presented in figure 4.20, maximum total deformation in foundation observed at modulus of elasticity 40 GPa is 2.8cm, 15 GPa is 6.3cm, 12 GPa is 8.3cm and 4.5 GPa is 19cm.

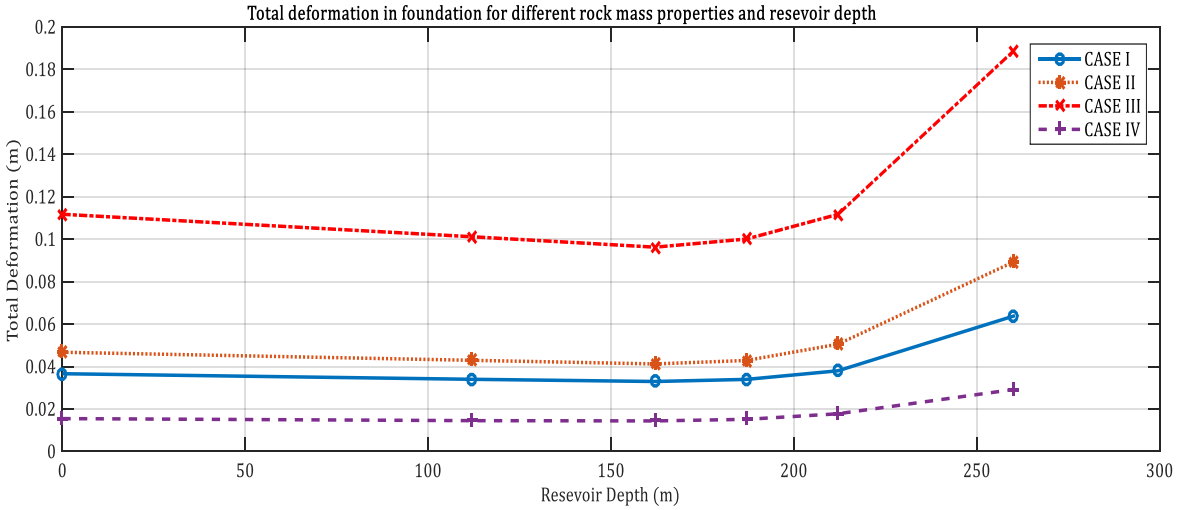

Figure 4-20 Total maximum deformation in foundation at different rock mass properties and reservoir level.

During plastic analysis with Hoek and Brown criterion, few rock in both abutment yielded resulting plastic deformation, amount of plastic strain developed also depended upon the properties foundation, variation of plastic strain with rock properties and reservoir level is presented in figure 4.21. According to which it can be observed that plastic strain increased rapidly when modulus of elasticity is decreased from 12 GPa to 4.5 GPa, whereas there is slight increment in plastic strain for decrease in modulus of elasticity above 12GPa.

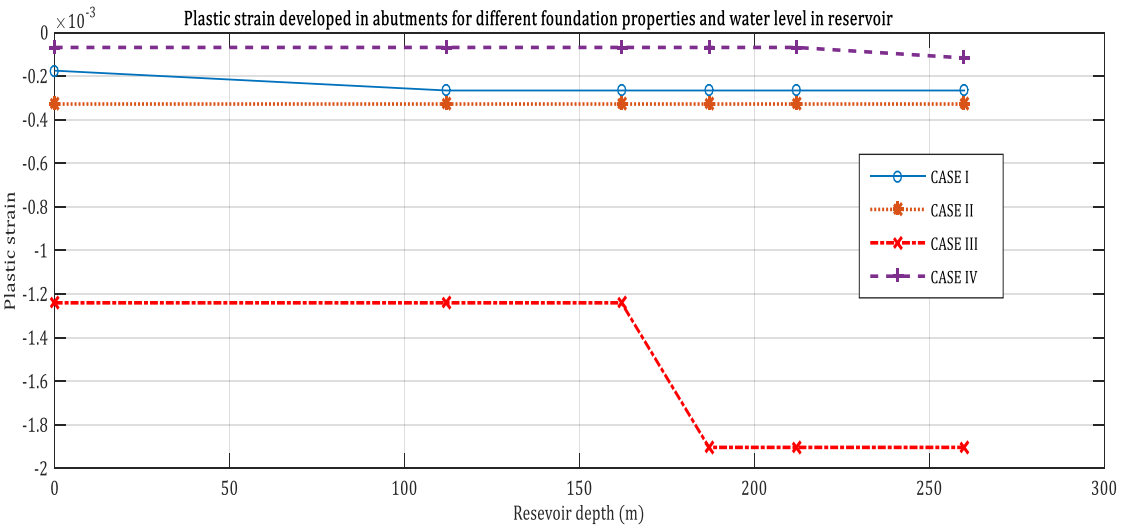

Figure 4-21 Maximum plastic strain developed in foundation for different rock mass properties and reservoir level

4.6.4 Stresses developed in foundation rock

Principle stress developed in rock foundation is represented in figure 4.22 and 4.23, in these figure stress contour on surface of model is only represented, variation of stress with in depth of rock mass is not represented here. Maximum of 4.2 MPa compressive stress is developed and maximum tensile stress of 5MPa is observed. Similar as in the stress in dam there is no significant variation in the stress in foundation with variation of rock mass properties.

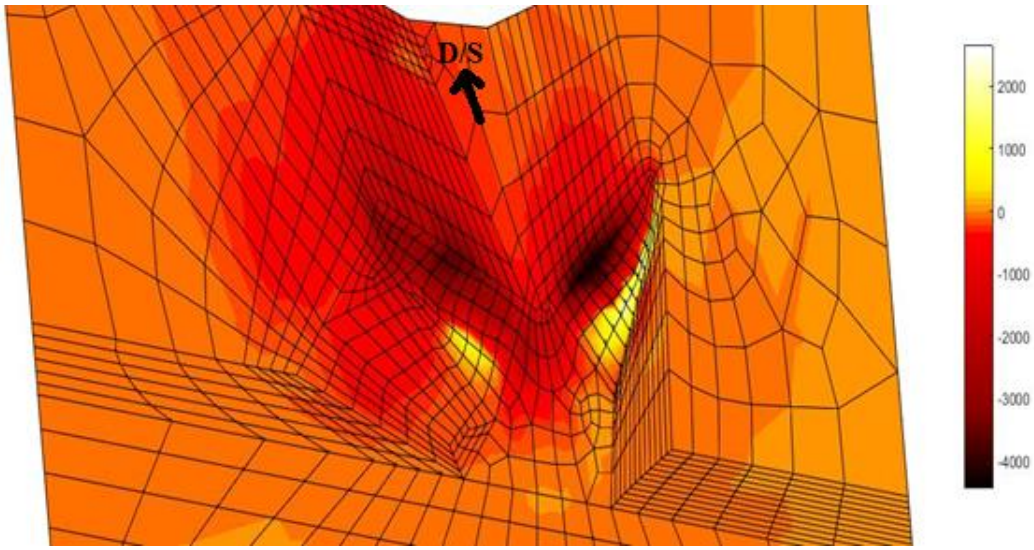

Figure 4-22 First principle stress (kN/m^2) developed in foundation at FSL

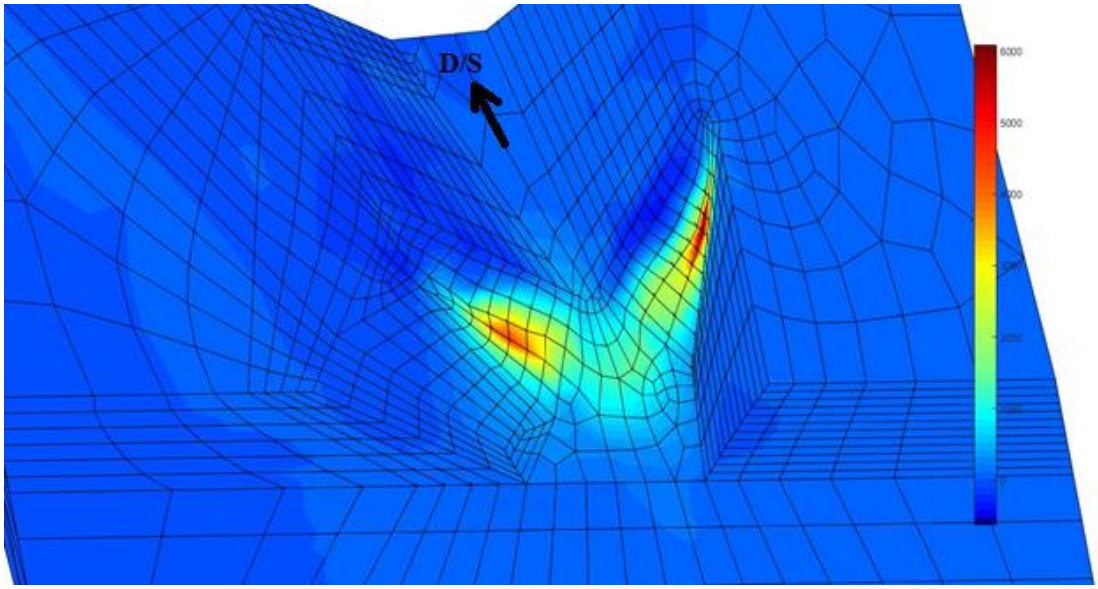

Figure 4-23 Third principle stress (kN/m^2) developed in foundation at FSL

4.7 Verification of work

For the verification of the works done in this thesis are compared with the results of the analysis of the Budhigandaki hydropower dam presented in 'Feasibility Study and Detailed design of Budhi Gandaki HPP' published by Budhigandaki Hydroelectric Project Development Committee, in this report static analysis of arch dam with consideration of similar properties of concrete for and modulus of elasticity of rock as 12 GPa using a finite element computation code COBEF, which resulted maximum downstream deformation at full supply load (similar as defined in this thesis) 17cm and maximum compressive stress in concrete at full supply load 12 MPa. Similar result is obtained with slight higher value in deformation 19.5cm, this difference might have occurred to difference in the consideration of left abutment shape, and maximum compressive stress developed in dam is 12MPa.

For the stability analysis of wedge verification is done by comparing the results from two methods vector method of wedge stability analysis and FEM analysis. From table 4.2, it can be absorbed that difference between factors of safety from two methods is higher at intermediate reservoir level but except those values there is not significant difference.

Variation of the deformation and stress are identical to the variation of these value with respect to the modulus of elasticity of rock mass to the modulus of elasticity of concrete presented in the 'Engineering guidelines for the evaluation of hydropower projects, chapter 11' by Federal Energy Regulatory Commission Division of Dam Safety and Inspection (1999), in which also it is presented in figure 11-5.11, deformation in dam increases with decrease in foundation modulus of elasticity and the increase rate of deformation increases for lesser value of foundation modulus of elasticity, which is also observed from the results of this thesis. Similar results is also provided for the arc stress developed in figure 11-5.13 of above cited guideline but lesser rate of increment in stress with decrease in modulus of elasticity of foundation than rate of increase in deformation, from this thesis work also it was observed that rate of increase in stress is less.

5. CONCLUSION

The overall objective with this thesis is to perform three dimensional finite element analysis of the double curvature arc dam and its abutments (considering nonlinear behavior of rock mass) through numerical modelling using MATLAB R2013a that will give realistic experience of the three dimensional finite element analysis of geotechnical and structural problems. During three dimensional modelling of foundation and arc dam irregularities in surface of model is considered as plane of similar slope and area (mostly in case of foundation) so that mesh generation for hexahedral elements would be done without complexities, although some difficulties occurred during mesh generation due to which compromising has to done with mesh quality. Mesh distribution has important impact over the performance of model during analysis and results obtained, so it is tried to develop finer mesh at the contact area of dam and foundation and within dam, but finer mesh results higher number of elements and nodes which results very large global stiffness matrix that requires larger amount of memory in RAM and decreases processing speed. So considering these factors compromises were done during mesh generation. Total 6807 number of nodes were generated that resulted global stiffness matrix of size 17070 *17070, which required about 4 GB of space in RAM.

After finite element numerical model analysis results were obtained in terms of nodal displacement, nodal reaction forces, elemental stress, principle stress, strain and plastic strain. Some of these results are presented in previous chapter. Analysis is done for five different loading condition with respect to water level in reservoir, maximum static loading condition is during full supply level in reservoir, during this loading, maximum compressive stress in dam and foundation is 12 MPa and 4.2 MPa respectively. Also during full supply level maximum deformation obtained in dam and foundation is 12cm and 6.3cm respectively. These values can be considered with in permissible limit.

From both displacement and stress contours in figure 4-8,4-9 and 4-14,4-15, it is observed that both stress and deformation at left abutment is higher than compression to right, which might has been occurred due to shape of abutment at left (occurrence of ridge) or presence of wedge.

Comparative analysis to study effect on the stresses and deformation in dam and foundation for different GSI value foundation rock mass is performed, four different GSI values are considered from which different rock mass properties such as modulus

of elasticity, poison's ratio and Hoek and Brown parameters are obtained and used for analysis. From analysis it is observed that with decrease in the GSI value there is significant increase in the deformation in both dam and rock foundation, but there is only slight increment in the stress developed in them. It is also observed that plastic strain increased rapidly when modulus of elasticity is decreased from 12 GPa to 4.5 GPa, whereas there is slight increment in plastic strain for decrease in modulus of elasticity above 12GPa.

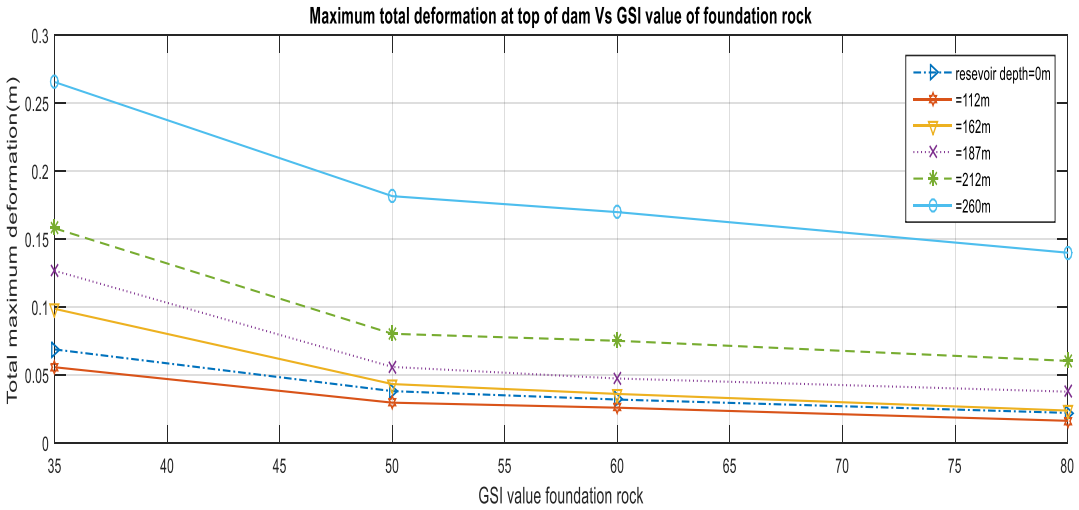

Figure 5-1 Maximum deformation in dam vs GSI value of foundation rock

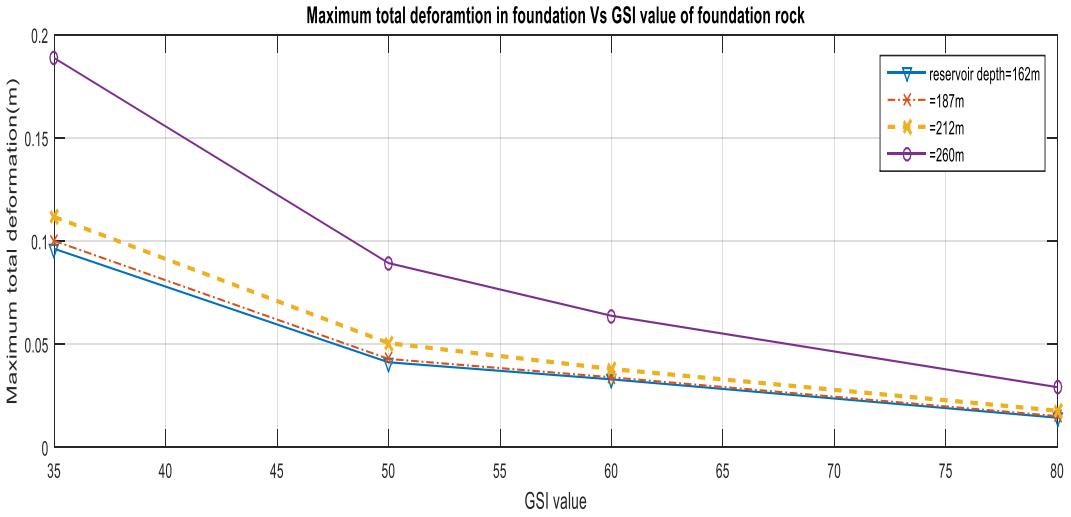

Figure 5-2 Maximum deformation in foundation vs GSI value of foundation rock

Rate of variation in deformation in both dam body and foundation with respect to GSI value is presented in figure 5-1 and 5-2, which reflects that rate of variation is not uniform, rate of increment in deformation is lesser for higher value of GSI and rate increases with decrease in the GSI value. Both these figure shows bilinear curve which

is result of fewer number of data, only four, and if smooth curve fit is drawn then an explicit relationship can be concluded.

As figure 5-1 and 5-2 does not reflect clear picture of relationship between GSI value and deformation. So more cases of different GSI value or modulus of elasticity of foundation rock, total eight cases were considered. From which following results are observed for GSI value vs total deformation in dam and foundation in figure 5-3 and 5-4.

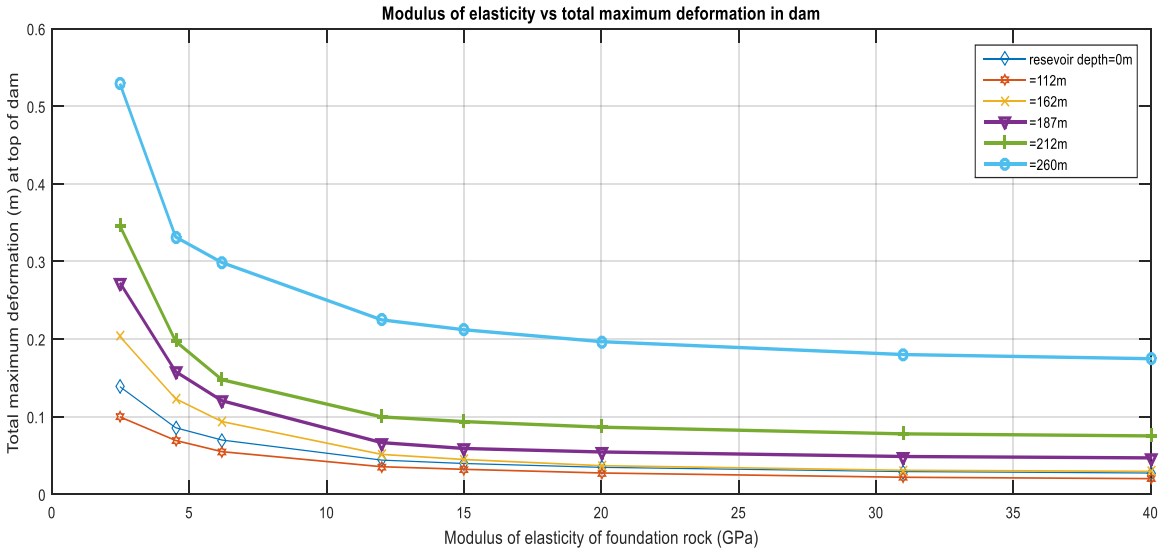

Figure 5-3 Modulus of elasticity of foundation rock vs Total deformation in foundation

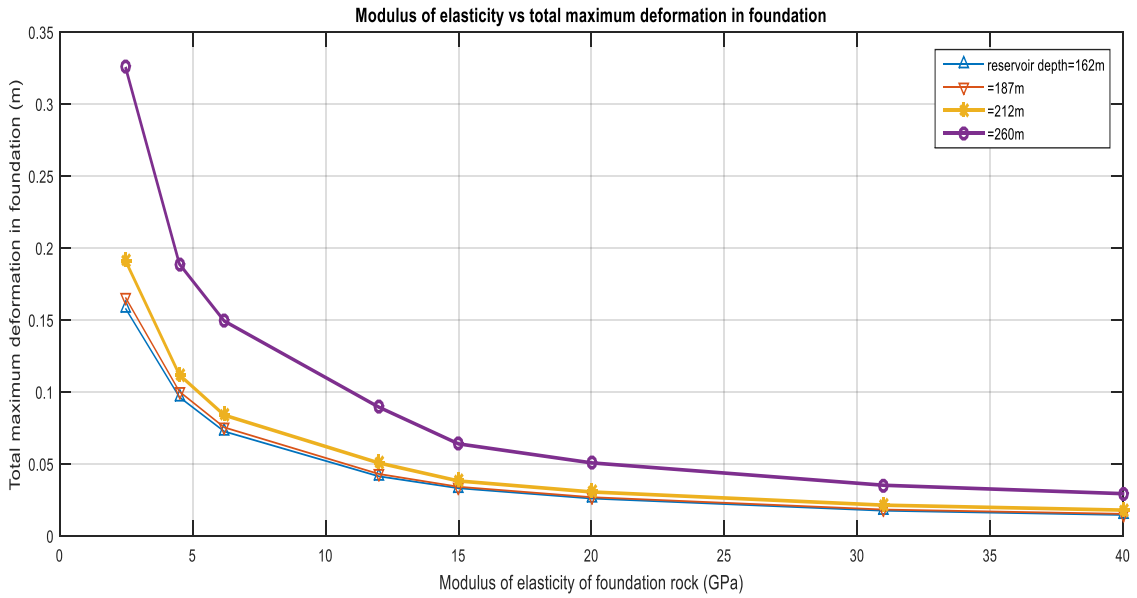

Figure 5-4 Modulus of elasticity of foundation rock vs Total deformation in

When regression analysis is performed on MS-Excel for relationship between total maximum deformations against GSI value of foundation rock, it was observed that four degree of polynomial equation is obtained, which can be observed from figure 5-5 and figure 5-6.

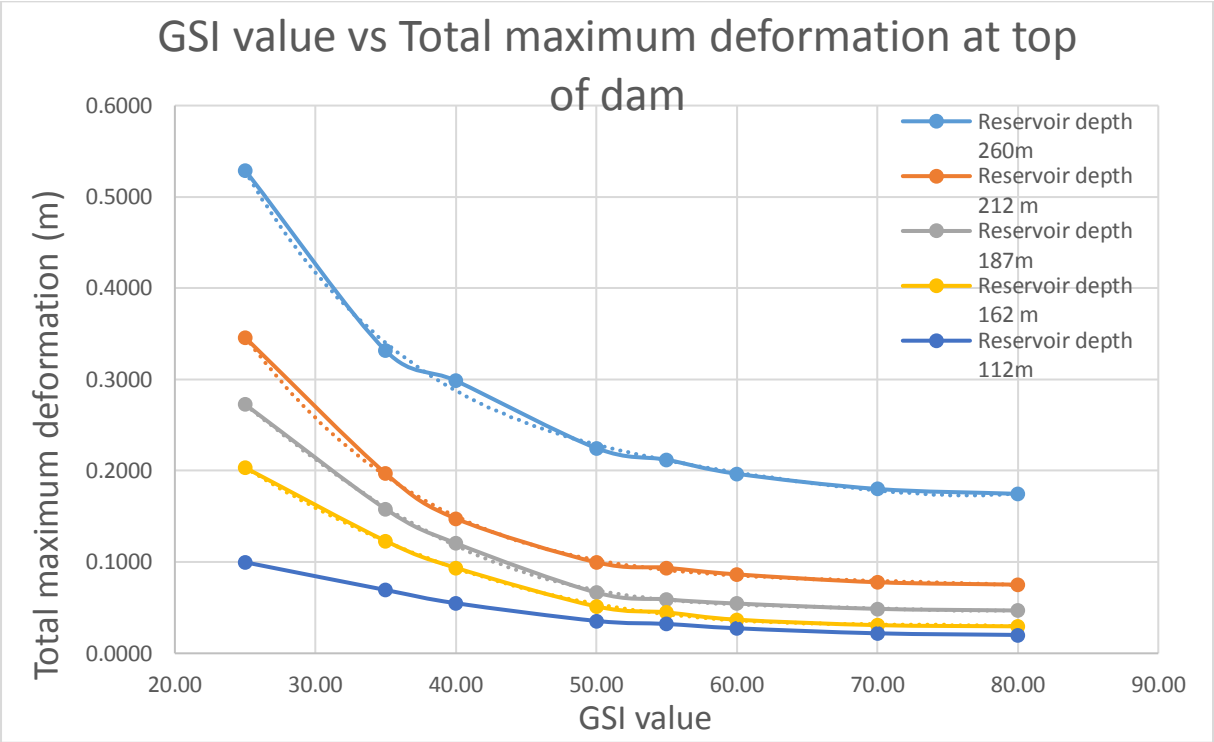

Figure 5-5 Total maximum deformation in dam vs GSI value of foundation rock

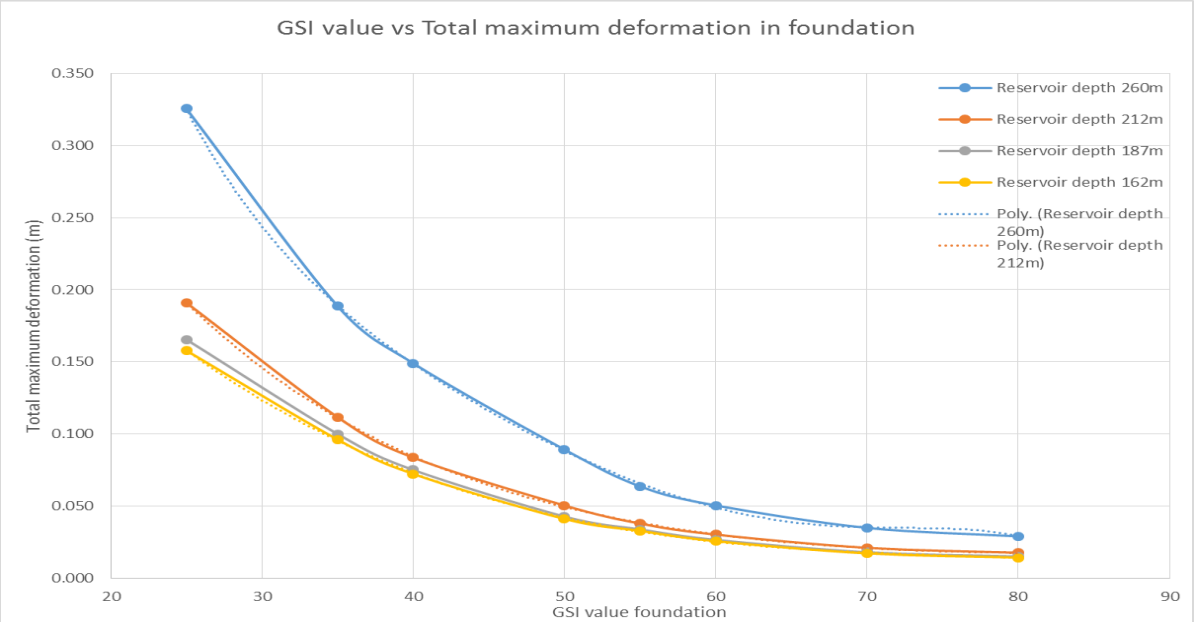

Figure 5-6 Total maximum deformation in foundation vs GSI value of foundation rock

As modulus of elasticity is more specific parameter than GSI value so empirical equation for variation of total maximum deformation in both dam and foundation with variation in modulus of elasticity of foundation is obtained for different reservoir level, regression analysis is performed using MATLAB application, according to which exponential relation is observed for both dam and foundation with highest R-squared value. Equations and graphs for full supply level are presented as below. Equation 5.1 and figure 5-7 are obtained for total maximum deformation in dam at FSL.

$$d = 2.569 * e^{-1.29 * E_r^{0.5}} + 0.1851 \qquad 5.1$$

Where, d is displacement in meter

E_r is modulus of elasticity in (GPa) of foundation rock

During regression analysis the R-squared value obtained for equation 5.1 is 0.9909.

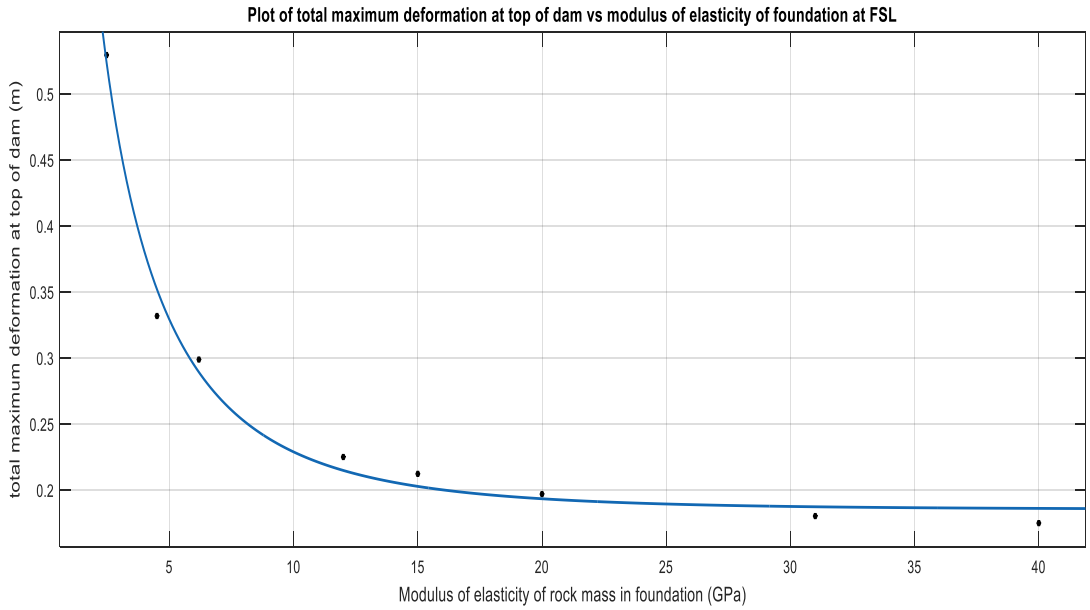

Figure 5-7 Relation between total maximum deformation in dam vs modulus of elasticity of foundation rock

Equation 5.2 and figure 5-8 are obtained for total maximum deformation in foundation at FSL.

$$d = 1.355 * e^{-0.9841 * E_r^{0.5}} + 0.03218 \qquad 5.2$$

Where, d is displacement in meter

E_r is modulus of elasticity in (GPa) of foundation rock

During regression analysis the R-squared value obtained for equation 5.2 is 0.9951.

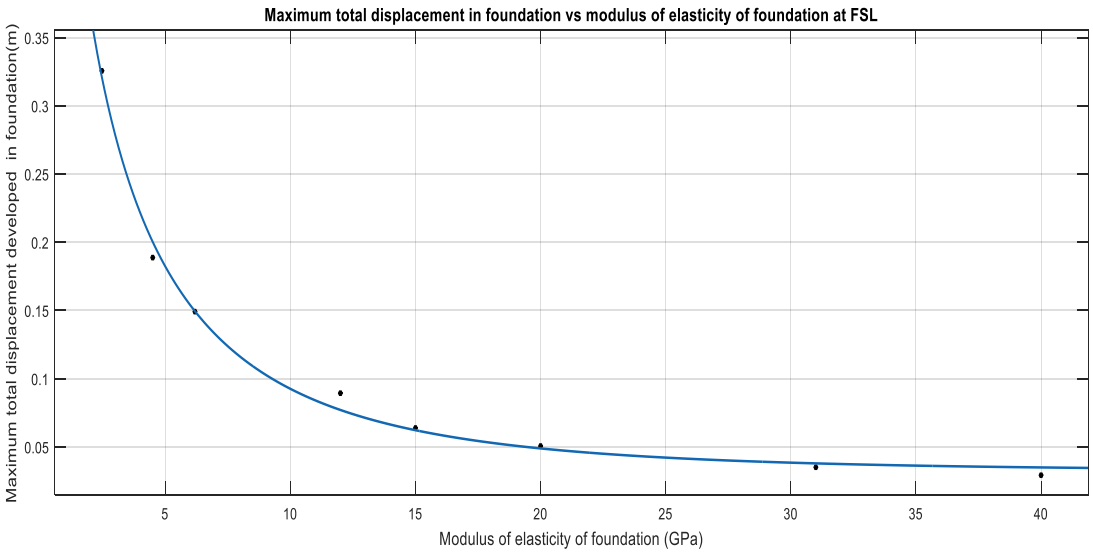

Figure 5-8 Relation between total maximum deformation in foundation vs modulus of elasticity of foundation rock

Similarly, when regression analysis is performed for maximum plastic strain developed in foundation rock, relation between maximum plastic strain (compression taken positive) and modulus of elasticity of foundation rock empirical equation obtained is exponential equation similar as for deformations. Equation 5.3 and figure 5-9 are obtained for maximum plastic strain in foundation at FSL.

$$ps = 0.01568 * e^{-1.132 * E_r^{0.5}} + 6.852 * 10^{-5} \quad 5.3$$

Where, ps is displacement in meter

E_r is modulus of elasticity in (GPa) of foundation rock

During regression analysis the R-squared value obtained for equation 5.3 is 0.9582

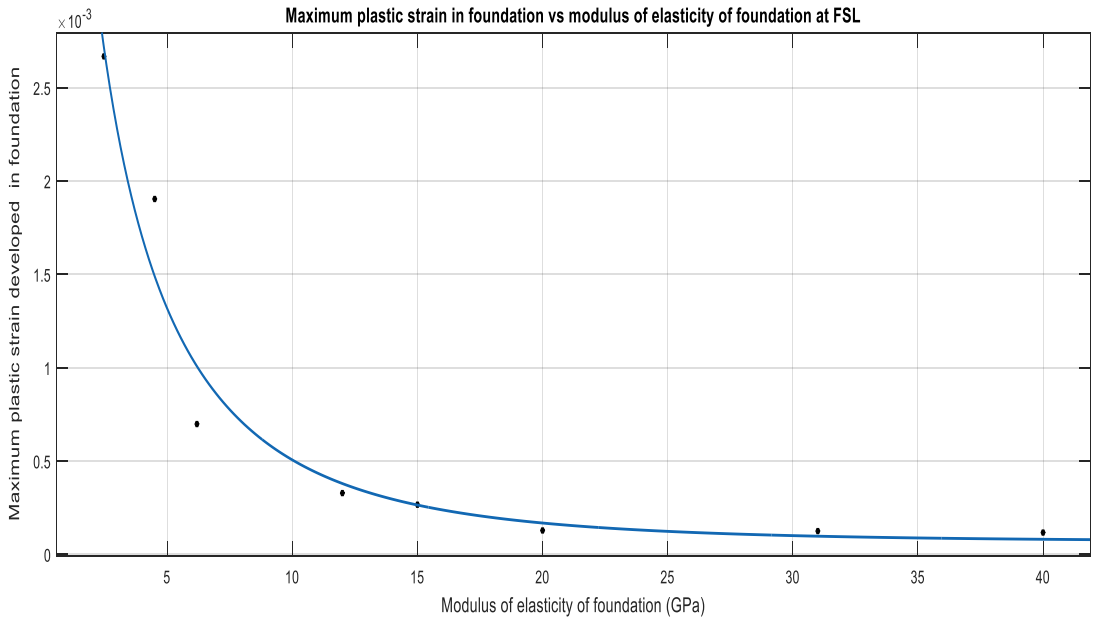

Figure 5-9 Relation between maximum plastic strain in foundation vs modulus of elasticity of foundation rock

Equations and graphs for relation between total maximum deformation of dam, foundation and plastic strain in foundation at different reservoir level is provided in appendix B.

In case of Budhigandaki HPP failure of foundation or abutment through bedding strata or other discontinuities were very less probable due to their orientation, except a potential wedge is identified at left abutment formed through two joints set having intersection directed downstream into river valley. After analysis of wedge stability through two different methods, minimum factor of safety obtained is 1.145, which is very less than acceptable limit (generally recommended minimum 2.0), so wedge should be stabilized using slope stabilization technique such as rock bolt anchoring or constructing thrust block.

6. SUGGESTION FOR FURTHER WORKS

As dynamic analysis considering for both seismic and hydrodynamics of reservoir water is not performed in this thesis, which are essential analysis to be performed for major projects like this so, dynamic analysis can be further considered. In river valleys wind load is also an important load to be considered so further analysis and flooding cases should also be considered.During this thesis bedding plane of rock is not considered as weak plane and one potential failure mechanism through is only considered, so other potential failure mechanisms can be identified and analyzed.

Another limitation of this work is that interface element is used at contact of dam and abutment so check for sliding through dam abutment contact is not analyzed. Which can be considered for further analysis.

7. REFERENCES

Nepal Hydropower Overview, November 2015, URL: www.didcl.org.np/nepal-hydropower.php

Status of Power Generation and Transmission in Nepal, November 2015, www.ippan.org.np/hpinNeapl.html

Feasibility Study and Detailed Design of BudhiGandaki HPP Phase 2: Final Detailed Design Report Volume 1. Main Report BG-FFR-vol.1-Rev.0.

Feasibility Study and Detailed Design of BudhiGandaki HPP Phase 3: Final Detailed Design Report Volume 1. Main Report BG-DDR-vol.1-Rev.0.

Feasibility Study and Detailed Design of BudhiGandaki HPP Phase 2: Field Investigation Report Volume 1. Main Report BG-INV-P2-C-Rev.0.

A Gens, I. Carol and E. Alonso, 1995, "Rock joints: FEM implementation and applications," Mechanics of Geo material Interfaces, vol. 42, pp. 395-420.

Bandis, S.C., Lumsden, A.C., Barton, N.R., 1983, "Fundamentals of Rock Joint Deformation. Int. J. Rock Mech. Min. Sci.", Vol. 20, No. 6, pp. 249-268.

Barton, N., 1973, "Review of a new shear-strength criterion for rock joints. Engineering geology", Vol. 7, No. 4, pp. 287-332.

Barton, N., 1974, "A review of the shear strength of filled discontinuities in rock, Norwegian Geotechnical Institute", Publication No. 105, p. 38.

Barton, N., Choubey, V., 1977, "The shear strength of rock joints in theory and practice. Rock Mechanics", Vol. 10, pp. 1-54.

Beer, G., 1985, "An isoparametric joint/interface element for finite element analysis. International Journal for Numerical methods in Engineering", 12:585-600.

Sheorey, P.R., 1997, "Empirical Rock Failure Criteria. Central Mining Research Institute", India, p. 176.

Bellier, J., 1976, “The Malpasset dam. Engineering foundation conference on ‘The evaluation of dam safety’ ”, Pacific Grove, CA, pp. 72-136. (First published in TRAVAUX, Paris, July 1967 in French).

CANMET, 1977, Pit Slope Manual, Ch. 2: Structural Geology. CANMET Report Tl4l. Olawa: Dept. of Energy Mines & Resources Canada.1-23 pages

Cundall, P.A., 1980, “UDEC – a generalized distinct element program for modelling jointed rock”. Report PCAR-1-80, Peter Cundall Associates, European Research Office, U.S. Army Corps of Engineers.

Desai, C.S. and Siriwardane, H.J., 1984, “Constitutive Laws for Engineering Materials”, Prentice Hall, Englewood Cliffs, NJ.

Edelbro, C., 2003, Rock mass strength – A review. Technical report Lulea University of Technology, 2003:16. Department of Civil and Mining Engineering, Division of Rock Mechanics.

Foster, J.; Jones, H.W., 1994, “Procedure for Static Analysis of Gravity Dams Including Foundation Effects Using the Finite Element Method – Phase 1B”, Technical Report ITL-94-5, U.S. Army Corps of Engineers, Water ways Experiment Station.

Ghaboussi, J., Wilson, E. L., and Isenberg, J., 1973, “Finite Element for Rock Joints and Interfaces”, Journal of the Soil Mechanics and Foundations Division, ASCE, Vol. 99, No M10, pp. 833-848.

Goodman, R.E., Taylor, R.L. and Brekke, T.L., 1968, “A Model for the Mechanics of Jointed Rock,” J. Soil Mech. Found. Div., ASCE, Vol. 94, SM3, pp. 637-659.

Goodman, R.E. and St. John., 1977, “Finite element analysis for discontinuous rocks”. Numerical Methods in Geotechnical Engineering, ch. 4, pages 149-175. McGraw-Hill, New York,

Goodman, R. E., and Dubois, J. J., 1972, “Duplication of Dilatancy in Analysis of Jointed Rocks”, Journal of Soil Mechanics and Foundations Div., ASCE, Vol. 98, No SM4, pp. 399- 422

HOEK E and J.W. BRAY, 1974, “Rock Slope Engineering”, 3rd. Edition. London: Institute of Mining and Metallurgy. 358 pages.

Hoek, E.; Wood, D.; Shah, S., 1992, "A modified Hoek-Brown criterion for jointed rock masses", Proc. Rock Characterization, Symp. Int. Soc. Rock. Mech.: Eurock 92, pp. 209-214.

Hoek, E., 1994, "Strength of rock and rock masses". ISRM News Journal, Vol. 2, No. 2, pp. 4-16.

Hoek, E.; Brown E.T., 1997, "Practical Estimates of Rock Mass Strength". Int. J. Rock Mech. Min. Sci., Vol. 34, No. 8, pp. 1165-1186.

David M. Potts and Lidija Zdravkovic, 2001, " Finite element analysis in geotechnical engineering: Application", Thomas Telford Ltd, London.

ISRM ,1978, "Suggested Methods for the Quantitative Description of Discontinuities in Rock Masses" Int. J. Rock Mech. Min. Sci. & Geo-mechanical. Vol. 15, Pergamon Press Ltd 1978, pp. 319-360.

Jing, L., 2003, "A review of techniques advances and outstanding issues in numerical modelling for rock mechanics and rock engineering", Int. J. Rock Mech. Min. Sci., Vol. 40, pp. 283-353.

Mahtab, M. A., and Goodman, R. E., 1970, "Three-Dimensional Finite Element Analysis of Jointed Rock Slopes", Proc., Second Congress of the International Society of Rock Mechanics, Belgrade, Vol. 3, pp. 353-360.

MARKIAND, 1974, "The analysis of principal components of orientation data." International Jour. Rock Mech. Min. Sci. & Geo mechanical Abstract. v. 11, pp 157-163.

Marinos, P. and E. Hoek, 2000, "GSI: a geologically friendly tool for rock mass strength estimation." In Proceedings of the GeoEng2000 at the international conference on geotechnical and geological engineering, Melbourne, Lancaster, pp. 1422–1446. Techonomic publishers.

Marinos, V., P. Marinos, and E. Hoek, 2005, "The geological strength index: applications and limitations" Bulletin of Engineering Geology and the Environment 64, 55–65.

Patton, F.D., 1966, "Multiple modes of shear failure in rock and related material", Ph.D. thesis, Univ. of Illinois.

PRIEST, S.D., 1985, “Hemispherical Projection Methods in Rock Mechanics”. London: George Allen & Unwin. 124 pages.

RAGAN, D.M., 1973, “Structural Geology. An Introduction to Geometrical Techniques”. 2nd. Edition. New York: Wiley. 208 pages.

Shi, G.H. and Goodman, R.E. ,1988, “Discontinuous deformation analysis - A new method for computing stress, strain and sliding of block systems” Key Questions in Rock Mechanics, Cundall et al. (eds) © Balkema, Rotterdam, pp. 381 – 393.

Tzamtzis, A.D., 1994, “Dynamic finite element analysis of complex discontinuous and jointed structural systems using interface elements”, PhD Thesis, Department of Civil Engineering, QMWC, University of London.

Tzamtzis, A.D, and Nath, B., 1992, “Application of a three-dimensional interface element to nonlinear static and dynamic finite element analysis of discontinuous systems”, Engineering Systems Design and Analysis Conference, ASME, Vol. 1, pp. 219-222.

Van Dillen, D. E., and Ewing, R. D., 1981, “BMINES: A Finite Element Code for Rock Mechanics Applications”, Proc. of the 22nd Symposium on Rock Mechanics, MIT Publishing, Cambridge, Mass., pp. 353-358.

Zienkiewicz, O. C., 1970, “Analysis of Nonlinear Problems in Rock Mechanics with Particular Reference to Jointed Rock Systems”, Proc. 2nd Congress Int. Soc. for Rock Mechanics, Belgrade, Yugoslavia.

E. Alonso et.al. , 1996, “Evaluation of safety factors in Discontinuous Rocks”.

Douglas D. Boyer and Keith A. Ferguson, 1999, “Important factors to be considered in evaluating sliding stability of rock foundation”.

Engineering Guidelines for the Evaluation of Hydropower Projects, Federal Energy Regulatory Commission Division of Dam Safety and Inspection-1999

APPENDIX A: CODES WRITTEN IN MATLAB

I. Main programme for analysis

```
%Total load vector before increament of load, which is written in
%Totalload.txt
FT=dlmread('FTTotalload4.txt');
%Total stress in elements before this increament step which is written in
%Totalstress.txt
STRESS=dlmread('FTTotalstress4.txt');
%Total strain in elements before this increament step which is written in
%Totalstrain.txt
STRAIN=dlmread('FTTotalstrain4.txt');
%Total displacement at nodes before this increament step which is written in
%Totaldisp.txt
DISPLACEMENT=dlmread('FTTotaldisp4.txt');
%Total reaction at nodes before this increament step which is written in
%Totaldisp.txt
TNF=dlmread('FTTotalnodalreactionforce4.txt');
%Total stress at  contact between wedge and rock
BSTRESS1=dlmread('FTTotalcontact1stress4.txt');
%Total stress at contact between wedge and rock
BSTRESS2=dlmread('FTTotalcontact2stress4.txt');
%Total reaction load at nodes of contact between wedge and dam
TNFC3=dlmread('FTTotalcontactload34.txt');
%Total plastic strain at elements
PSTRAIN=dlmread('FTTotalplasticstrain4.txt');
%previousaly yielded elemets
yieldfunelemental=dlmread('FTyieldvalue4.txt');
global Rockpara
nel=5481; % number of elements
nnd=6895; % number of nodes
nndc3=18;
nndc2=48;
nndc1=50;
nelc1=36;
nelc2=36;
%FT=zeros(nnd,3);
%TNFC3=zeros(nndc3,3);
%DISPLACEMENT=zeros(nnd,3);
%STRESS=zeros(5409,6);
%STRAIN=zeros(5409,6);
%TNF=zeros(nnd,3);
%PSTRAIN=zeros(5409,6);
%BSTRESS1=zeros(nelc1,3);
%BSTRESS2=zeros(nelc2,3);
%yieldfunelemental=zeros(5409,1);

% Material properties
% Dam Concrete grade M25
Ec=20000000; %N/m2
roc=24; %kN/m3
vuc=0.2; %poissions ratio
%Dandagaun phyllite  rock parameters for Hoek-Brown criterion
Ed=4760000;
rod=22;
vud=0.32;
sigcid=35*1000; % sigmaci kN/m^2
ydsd=0.0079; %
```

```
ydmbd=0.92;
ydad=0.511;
ydsgd=0.0079;
ydmgd=0.92;
ydagd=0.511;
%Nourpul quartzite
Eq=15000000;
roq=25;
vuq=0.27;
sigciq=62*1000; % sigmaci
ydsq=0.00855; %
ydmbq=4.907;
ydaq=0.503;
ydsgq=0.008855;
ydmgq=4.907;
ydagq=0.503;
%Nourpul phyliite and quartzite
Ep=8000000;
rop=25;
vup=0.3;
sigcip=40*1000; % sigmaci
ydsp=0.0026; %
ydmbp=1.37;
ydap=0.506;
ydsgp=0.00206;
ydmgp=1.37;
ydagp=0.506;
%
%
ro=9.81; %unit weight of water
rosv=0.925*9.81;% vertical pressure indensity of sediment
rosh=0.36*9.81;% horizontal pressure intensity of sediment
h=1000;%level of water
hs=800;%level of sdiment
ht=1000;% top level of rock
nne=8; %nodes per element
nodof=3; %nodal degree of freedom
eldof=nne*nodof; % elemental degree of freedom
nf=ones(nnd,3);
nndLS=209;
nndRS=207;
nndBottom=459;
nndUS=127;
nndDS=217;
neldadaphy=658;
nelNourphy=1518;
nelNourquartz=2767;
neldam=322;
nelwedge=144;
for i=1:nndLS
   node=nodesLS(i);
   nf(node,:)=[0 0 0];
end
for i=1:nndRS
   node=nodesRS(i);
   nf(node,:)=[0 0 0];
end
for i=1:nndUS
   node=nodesUS(i);
```

```
    nf(node,:)=[0 0 0];
end
for i=1:nndDS
    node=nodesDS(i);
    nf(node,:)=[0 0 0];
end
for i=1:nndBottom
    node=nodesBottom(i);
    nf(node,:)=[0 0 0];
end
n=0;
for i=1:nnd
    for j=1:nodof
        if nf(i,j)~=0
            n=n+1;
            nf(i,j)=n;
        end
    end
end

%%% calculation of dead load
ngp=5.;
samp=gauss(ngp);
fg=zeros(nnd,3); %gravity load
g=zeros(nne*nodof,1);
%assigment of density and rock properties in each element
rog=zeros(nel,1);
Rockpara=zeros(nel,9);
for k=1:nelNourquartz
    elem=elemNourquartz(k);
    rog(elem,1)=0;
    Rockpara(elem,1)=sigciq;
    Rockpara(elem,2)=ydsq;
    Rockpara(elem,3)=ydmbq;
    Rockpara(elem,4)=ydaq;
    Rockpara(elem,5)=ydsgq;
    Rockpara(elem,6)=ydmgq;
    Rockpara(elem,7)=ydagq;
    Rockpara(elem,8)=vuq;
    Rockpara(elem,9)=Eq;

end
 for k=1:neldam
     elem=elemDam(k);
     rog(elem,1)=roc;
 end
 for k=1:nelwedge
        elem=elemWedge(k);
        rog(elem,1)=roq;
    Rockpara(elem,1)=sigciq;
    Rockpara(elem,2)=ydsq;
    Rockpara(elem,3)=ydmbq;
    Rockpara(elem,4)=ydaq;
    Rockpara(elem,5)=ydsgq;
    Rockpara(elem,6)=ydmgq;
    Rockpara(elem,7)=ydagq;
    Rockpara(elem,8)=vuq;
    Rockpara(elem,9)=Eq;
 end
```

```
for k=1:nelNourphy
      elem=elemNourphy(k);
      rog(elem,1)=0;
   Rockpara(elem,1)=sigcip;
   Rockpara(elem,2)=ydsp;
   Rockpara(elem,3)=ydmbp;
   Rockpara(elem,4)=ydap;
   Rockpara(elem,5)=ydsgp;
   Rockpara(elem,6)=ydmgp;
   Rockpara(elem,7)=ydagp;
   Rockpara(elem,8)=vup;
   Rockpara(elem,9)=Ep;
end
for k=1:neldadaphy
      elem=elemdadaphy(k);
      rog(elem,1)=0;
      Rockpara(elem,1)=sigciq;
   Rockpara(elem,2)=ydsd;
   Rockpara(elem,3)=ydmbd;
   Rockpara(elem,4)=ydad;
   Rockpara(elem,5)=ydsgd;
   Rockpara(elem,6)=ydmgd;
   Rockpara(elem,7)=ydagd;
   Rockpara(elem,8)=vud;
   Rockpara(elem,9)=Ed;
end

for i=1:nel
   conec=Nodeelembound(i);
   l=0;
   coord=zeros(nne,nodof);
 for k=1:nne
     cord=Nodecordbound(conec(k+1));  %% change function name
   for j=1:nodof
      coord(k,j)=cord(j+1);
      l=l+1;
      g(l)=nf(conec(k+1),j);

   end
 end

   fg1=zeros(eldof,1);
   N=zeros(nodof,(nne*nodof));
   for ig=1:ngp
      wi=samp(ig,2);
   for jg=1:ngp
      wj=samp(jg,2);
   for kg=1:ngp
      wk=samp(kg,2);
         [der,fun] = fmlin3d(samp,ig,jg,kg);
         jac=der*coord; %% der(3,8) coord(8,3)
          d=det(jac);
        for j= 1:nne
           N(1,(3*j-2))=fun(j);
           N(2,(3*j-1))=fun(j);
           N(3,(3*j))=fun(j);
        end

         fg1=fg1+d*wi*wj*wk*N'*[0;0;-rog(i,1)];
```

```
    end
    end
    end

    l=0;
    for j=1:nne
        for k=1:nodof
            l=l+1;
            fg(conec(j+1),k)=fg(conec(j+1),k)+fg1(l);
        end
    end
end

frr=zeros(nnd,3); %hydrostatic force on right face of reseviour
flr=zeros(nnd,3); %hydrostatic force on left face of reseviour
ftr=zeros(nnd,3); %hydrostatic force on top of reseviour
ftrock=zeros(nnd,3);%load on top of rock
fw=zeros(nnd,3);%hydrosatic force on dam
fs=zeros(nnd,3);%sediment pressure on dam
for i=1:161   %243 number of element at Us face
    coords=zeros(4,3);
    USelem=USfacedam(i);
    for j=1:4
        cord=Nodecordbound(USelem(j));
        coords(j,1)=cord(2);
        coords(j,2)=cord(3);
        coords(j,3)=cord(4);
    end
    Ax=0;
    Ay=0;
    Az=0;
    for ig=1:ngp
        wi=samp(ig,2);
        for jg=1:ngp
            wj=samp(jg,2);
            [der,fun]=fmlin(samp,ig,jg);
            jac=der*coords(:,2:3);
            d=det(jac);
            Ax=Ax+wi*wj*d;
        end
    end
    for ig=1:ngp
        wi=samp(ig,2);
        for jg=1:ngp
            wj=samp(jg,2);
            [der,fun]=fmlin(samp,ig,jg);
            jac=der*coords(:,1:2:3);
            d=det(jac);
            Ay=Ay+wi*wj*d;
        end
    end
    for ig=1:ngp
        wi=samp(ig,2);
        for jg=1:ngp
            wj=samp(jg,2);
            [der,fun]=fmlin(samp,ig,jg);
            jac=der*coords(:,1:2);
            d=det(jac);
            Az=Az+wi*wj*d;
```

```
    end
  end
  Va=[coords(1,1)-coords(3,1) coords(1,2)-coords(3,2) coords(1,3)-coords(3,3)];
  Vb=[coords(2,1)-coords(4,1) coords(2,2)-coords(4,2) coords(2,3)-coords(4,3)];
  Norm=cross(Va,Vb);
  if Norm(2)>0
    Norm(1)=Norm(1)*-1.;
    Norm(2)=Norm(2)*-1;
    Norm(3)=Norm(3)*-1;
  end
  if Norm(1)<0
    aNorm(1)=-1*Norm(1);
  end
  if Norm(3)<0
    aNorm(3)=-1*Norm(3);
  end

  kx=Norm(1)/aNorm(1);
  kz=Norm(3)/aNorm(3);


  for j=1:4
    cord=Nodecordbound(USelem(j));

      if (h-cord(4))>=0
      if Ax<0
        Ax=-1*Ax;
      end
      if Az<0
        Az=-1*Az;
      end
      if Ay<0
        Ay=-1*Ay;
      end


  fw(USelem(j),3)=fw(USelem(j),3)+kz*(Az)/4*ro*(h-cord(4)); %
  fw(USelem(j),1)=fw(USelem(j),1)+kx*(Ax)/4*ro*(h-cord(4));
  fw(USelem(j),2)=fw(USelem(j),2)-((Ay)/4*ro*(h-cord(4)));
      end
      if (hs-cord(4))>=0
  fs(USelem(j),3)=fs(USelem(j),3)+kz*((Az)/4*rosv*(hs-cord(4))); %
  fs(USelem(j),1)=fs(USelem(j),1)+kx*((Ax)/4*rosh*(hs-cord(4)));
  fs(USelem(j),2)=fs(USelem(j),2)-((Ay)/4*rosh*(hs-cord(4)));
      end

  end

end

for i=1:130   %168 number of element at right side of reseviour
  coords=zeros(4,3);
  RRelem=RRfaceres(i);
  for j=1:4
    cord=Nodecordbound(RRelem(j));
    coords(j,1)=cord(2);
    coords(j,2)=cord(3);
    coords(j,3)=cord(4);
  end
```

```
    Ax=0;
    Ay=0;
    Az=0;
    for ig=1:ngp
       wi=samp(ig,2);
       for jg=1:ngp
          wj=samp(jg,2);
          [der,fun]=fmlin(samp,ig,jg);
          jac=der*coords(:,2:3);
          d=det(jac);
          Ax=Ax+wi*wj*d;
       end
    end
    for ig=1:ngp
       wi=samp(ig,2);
       for jg=1:ngp
          wj=samp(jg,2);
          [der,fun]=fmlin(samp,ig,jg);
          jac=der*coords(:,1:2:3);
          d=det(jac);
          Ay=Ay+wi*wj*d;
       end
    end
    for ig=1:ngp
       wi=samp(ig,2);
       for jg=1:ngp
          wj=samp(jg,2);
          [der,fun]=fmlin(samp,ig,jg);
          jac=der*coords(:,1:2);
          d=det(jac);
          Az=Az+wi*wj*d;
       end
    end


    for j=1:4
      cord=Nodecordbound(RRelem(j));

          if (h-cord(4))>=0
          if Ax<0
             Ax=-1*Ax;
          end
          if Az<0
             Az=-1*Az;
          end
          if Ay<0
             Ay=-1*Ay;
          end

    %frr(RRelem(j),3)=frr(RRelem(j),3)-((Az)/4*ro*(h-cord(4))); %
    %frr(RRelem(j),1)=frr(RRelem(j),1)-((Ax)/4*ro*(h-cord(4)));
    %frr(RRelem(j),2)=frr(RRelem(j),2)-((Ay)/4*ro*(h-cord(4)));
          end

    end
end
for i=1:160   %175 number of element at left side of reseviour
    coords=zeros(4,3);
    RLelem=RLfaceres(i);
```

```
for j=1:4
   cord=Nodecordbound(RLelem(j));
   coords(j,1)=cord(2);
   coords(j,2)=cord(3);
   coords(j,3)=cord(4);
end
Ax=0;
Ay=0;
Az=0;
for ig=1:ngp
   wi=samp(ig,2);
   for jg=1:ngp
      wj=samp(jg,2);
      [der,fun]=fmlin(samp,ig,jg);
      jac=der*coords(:,2:3);
      d=det(jac);
      Ax=Ax+wi*wj*d;
   end
end
for ig=1:ngp
   wi=samp(ig,2);
   for jg=1:ngp
      wj=samp(jg,2);
      [der,fun]=fmlin(samp,ig,jg);
      jac=der*coords(:,1:2:3);
      d=det(jac);
      Ay=Ay+wi*wj*d;
   end
end
for ig=1:ngp
   wi=samp(ig,2);
   for jg=1:ngp
      wj=samp(jg,2);
      [der,fun]=fmlin(samp,ig,jg);
      jac=der*coords(:,1:2);
      d=det(jac);
      Az=Az+wi*wj*d;
   end
end


for j=1:4
  cord=Nodecordbound(RLelem(j));

      if (h-cord(4))>=0
      if Ax<0
         Ax=-1*Ax;
      end
      if Az<0
         Az=-1*Az;
      end
      if Ay<0
         Ay=-1*Ay;
      end

%flr(RLelem(j),3)=flr(RLelem(j),3)-((Az)/4*ro*(h-cord(4))); %
%flr(RLelem(j),1)=flr(RLelem(j),1)+((Ax)/4*ro*(h-cord(4)));
%flr(RLelem(j),2)=flr(RLelem(j),2)-((Ay)/4*ro*(h-cord(4)));
      end
```

```
    end
end
fwedu=zeros(31,3); % hydrostatic pressure on wedge
for i=1:31
    node=Nodes_upstreamwedge(i);
    for j=1:nnd
        if node==j
         fwedu(i,:)=flr(j,:);
        end
    end
end
dlmwrite('forcewedgeus4.txt',fwedu);
for i=1:66   %69 number of element at top of reseviour
    coords=zeros(4,3);
    RTelem=RTfaceres(i);
    for j=1:4
        cord=Nodecordbound(RTelem(j));
        coords(j,1)=cord(2);
        coords(j,2)=cord(3);
        coords(j,3)=cord(4);
    end
    Az=0;

    for ig=1:ngp
        wi=samp(ig,2);
        for jg=1:ngp
            wj=samp(jg,2);
            [der,fun]=fmlin(samp,ig,jg);
            jac=der*coords(:,1:2);
            d=det(jac);
            Az=Az+wi*wj*d;
        end
    end

    for j=1:4
       cord=Nodecordbound(RTelem(j));
          if (h-cord(4))>=0
           if Az<0
               Az=-1*Az;
           end
    %ftr(RTelem(j),3)=ftr(RTelem(j),3)-((Az)/4*ro*(h-cord(4))); %
          end
    end
end

for i=1:368   %391 number of element at top of rock
    coords=zeros(4,3);
    RTrockelem=TRock(i);
    for j=1:4
        cord=Nodecordbound(RTrockelem(j));
        coords(j,1)=cord(2);
        coords(j,2)=cord(3);
        coords(j,3)=cord(4);
    end
    Az=0;

    for ig=1:ngp
        wi=samp(ig,2);
```

```
        for jg=1:ngp
            wj=samp(jg,2);
            [der,fun]=fmlin(samp,ig,jg);
            jac=der*coords(:,1:2);
            d=det(jac);
            Az=Az+wi*wj*d;
        end
    end

    for j=1:4
      cord=Nodecordbound(RTrockelem(j));

          if Az<0
             Az=-1*Az;
          end

    ftrock(RTelem(j),3)=ftrock(RTelem(j),3)-((Az)/4*roq*(ht-cord(4))); %

    end
end
ft=zeros(nnd,3); %total load
for i=1:nnd
    for j=1:nodof
    ft(i,j)=frr(i,j)+flr(i,j)+ftr(i,j)+ftrock(i,j)+fw(i,j)+fs(i,j)+fg(i,j);
    end
end
%increament in load in this increament step
fti=ft-FT;
Tdelta=zeros(n,1); %total displacement at global degree of freedom
ftp=zeros(n,1);
fp=zeros(n,1);% increament in load per freedom point
for i=1:nnd
    for j=1:nodof
       if nf(i,j)~=0
          fp(nf(i,j))=fti(i,j);
          ftp(nf(i,j))=ft(i,j);
          Tdelta(nf(i,j))=DISPLACEMENT(i,j);
       end
    end
end
Dee1=dlmread('FDee4.txt');
Dee=zeros(6,6,nel);
for i=1:nel
  for j=1:6
    for k=1:6
     Dee(j,k,i)=Dee1(j,(i*6-(6-k)));
    end
  end
end

%formation of elemental stiffness matrix

kn=22500000;
ks=2000000;
K=[kn 0 0;
   0 ks 0;
   0 0 ks];
A1=[-0.3021 -0.2359 0.9236;
   0.5937 -0.8046 -0.0113;
```

```
   0.7458 0.5449 0.3831];
A2=[-0.5020 0.4524  0.7371;
   -0.2387 0.7467  -0.6209;
   -0.8313 -0.4876 -0.2668];
K1=A1'*K*A1;
K2=A2'*K*A2;
delta=zeros(n,1); % displacement at each load increament
 %loop for check and correction in residual force
 rm=20;    % assume initial value of error
 iteration=0;
 %kk=zeros(n,n);
 %dlmwrite('KK.txt',kk);

%Numerical integration and assembly of the global stiffness matrix
%kk=dlmread('KK.txt');
ngp=2;
samp=gauss(ngp);
while rm>10
    kk=zeros(n,n);
 iteration=iteration+1
 for i=1:nel
    conec=Nodeelembound(i);

   l=0;
   coord=zeros(nne,nodof);
   for k=1:nne
      cord=Nodecordbound(conec(k+1));
   for j=1:nodof
      coord(k,j)=cord(j+1);
      l=l+1;
      g(l)=nf(conec(k+1),j);
   end
   end
   tk=0;
    for j=5410:5445
       if i==j
          tk=1;
       end
    end
    for j=5446:5481
       if i==j
          tk=2;
       end
    end
    %stifffness matrix for continum model
    if tk==0
    % coordinates of the nodes of element i, % and its steering vector
  ke=zeros(eldof,eldof) ; % Initialize the element stiffness % matrix to zero
    for ig=1: ngp
       wi = samp(ig,2);
    for jg=1: ngp
       wj=samp(jg,2);
    for kg=1: ngp
       wk = samp(kg,2);
        [der,fun] = fmlin3d(samp,ig,jg,kg); % Derivative of shape functions
          jac=der*coord; % Compute Jacobian matrix
          d=det(jac); % Compute determinant of Jacobian %
          deriv=jac\der; % Derivative of shape functions in
          bee=formbee3d(deriv,nne,eldof); % Form matrix [B]
```

```
    ke=ke + d*wi*wj*wk*bee'*Dee(:,:,i)*bee; % Integrate stiffness matrix

 end
 end
 end
 end
 %stiffness matrix for contact1
 if tk==1
Tcoords=zeros(4,3);
ke=zeros(eldof,eldof) ;
for j=1:4
   tcord=A1*coord(j,:)';
   Tcoords(j,:)=tcord';
end

 for ig=1:ngp
   wi=samp(ig,2);
   for jg=1:ngp
      wj=samp(jg,2);
      [der,fun]=fmlin(samp,ig,jg);
      jac=der*Tcoords(1:4,2:3);
      d=det(jac);
      B=zeros(3,24);
      N=form_bee2d(samp,ig,jg);
    for j=1:4
       B(1,(1+(j-1)*3))=N(j);
       B(2,(2+(j-1)*3))=N(j);
       B(3,(3+(j-1)*3))=N(j);
    end
     for j=5:8
       B(1,(1+(j-1)*3))=-N(5-(j-4));
       B(2,(2+(j-1)*3))=-N(5-(j-4));
       B(3,(3+(j-1)*3))=-N(5-(j-4));
    end
    ke=ke+wi*wj*d*B'*K1*B;
   end
 end
 end
 %stiffness matrix for contact2
if tk==2
 Tcoords=zeros(4,3);
ke=zeros(eldof,eldof) ;
for j=1:4
   tcord=A2*coord(j,:)';
   Tcoords(j,:)=tcord';
end
  Area=0;
 for ig=1:ngp
   wi=samp(ig,2);
   for jg=1:ngp
      wj=samp(jg,2);
      [der,fun]=fmlin(samp,ig,jg);
      jac=der*Tcoords(1:4,2:3);
      d=det(jac);
      B=zeros(3,24);
      N=form_bee2d(samp,ig,jg);
    for j=1:4
       B(1,(1+(j-1)*3))=0.25;
       B(2,(2+(j-1)*3))=0.25;
```

```
            B(3,(3+(j-1)*3))=0.25;
        end
         for j=5:8
            B(1,(1+(j-1)*3))=-0.25;
            B(2,(2+(j-1)*3))=-0.25;
            B(3,(3+(j-1)*3))=-0.25;
        end
        ke=ke+wi*wj*d*B'*K1*B;
        Area=Area+wi*wj*d;
       end
     end
   end
   %Global stiffness matrix
  if i==5447
      ke
  end
   for k=1:eldof
    if g(k) ~= 0
       for j=1:eldof
          if g(j) ~= 0
             %kk(g(k),g(j))= kk(g(k),g(j)) + ke(k,j);
          end

       end
    end
    end

 end

%Calculation of residual force
r=ftp-kk*(Tdelta+delta);
rm=max(max(r),-1*min(r))/max(max(ftp),-1*min(ftp))*100;
deltai=kk\r; %displacement due to residual force
deltan=kk\r;
clearvars kk
for i=1:n
delta(i)=delta(i)+deltai(i);
end

principlestress=zeros(5409,3); % only for continum material
%Displacement at each element due to residual force
eld=zeros(nel,eldof);

 for i=1:nel
     connec=Nodeelembound(i);
    l=0;
    for k=1:nne
    for j=1:nodof
       l=l+1;
       g(l)=nf(connec(k+1),j);
    end
    end

     for k=1:eldof
        if g(k)==0
           eld(i,k)=0.;
        else
           eld(i,k)=deltai(g(k));
        end
```

```
    end
  end
  % stress and strain calculation at each continum element
stress=zeros(5409,6);
strain=zeros(5409,6);

 for i=1:5409
    connec=Nodeelembound(i);
    coord=zeros(nne,nodof);
  for k=1:nne
    cord=Nodecordbound(connec(k+1));
    for j=1:nodof
    coord(k,j)=cord(j+1);
    end
  end
         for ig=1: ngp
            wi = samp(ig,2);
         for jg=1: ngp
            wj=samp(jg,2);
         for kg=1:ngp
            wg=samp(kg,2);
[der,fun]=fmlin3d(samp,ig,jg,kg);%Derivative of shape functions in local coordinates
            jac=der*coord; % Compute Jacobian matrix
      deriv=jac\der; % Derivative of shape functions in % global coordinates
            bee=formbee3d(deriv,nne,eldof); % Form matrix [B]
            eps=bee*eld(i,:)'; % Compute strains due to total displacement
            sigma=Dee(:,:,i)*eps; % Compute stresses from total strain

         end
         end
         end
         for j=1:6
   stress(i,j)=sigma(j,1);
   strain(i,j)=eps(j,1);

         end
 % Calculating total stress and strain after this load increament
 STRESS(i,:)=STRESS(i,:)+stress(i,:);
 STRAIN(i,:)=STRAIN(i,:)+strain(i,:);
% calculation of principle stress and its direction cosines
 [p,dc]=pstress(STRESS(i,:));
  principlestress(i,:)=p(:);
  %calculation of Hoek-Brown yield function except dam
  po=0;
 for jj=1:neldam
      elem=elemDam(jj);
   if i == elem
       po=1;
   end
 end
if po==0
  [fy]=yieldfun(p,i);
  if fy>1
  yieldfunelemental(i)=real(fy);
  end
end

if po==0
     % if fy is grater than 1 than plastic deformation will occur, plastic
```

```
    % stress, strain and new constitutive matrix is obtained using return
    % field method
  if fy > 1
     if isreal(fy)==0
      else
          for j=1:3
           dc1(j)=dc(1,j)*dc(1,j);
          dc2(j)=dc(2,j)*dc(2,j);
           dc3(j)=dc(3,j)*dc(3,j);
           dc12(j)=dc(1,j)*dc(2,j);
           dc13(j)=dc(1,j)*dc(3,j);
           dc23(j)=dc(2,j)*dc(3,j);
           dc21(j)=2*dc(j,1)*dc(j,2);
           dc31(j)=2*dc(j,1)*dc(j,3);
           dc32(j)=2*dc(j,2)*dc(j,3);
          end
          dca1=dc(1,1)*dc(2,2)+dc(1,2)*dc(2,1);
          dcb1=dc(3,1)*dc(1,2)+dc(3,2)*dc(1,1);
          dcc1=dc(2,1)*dc(3,2)+dc(2,2)*dc(3,1);
          dca2=dc(1,3)*dc(2,1)+dc(1,1)*dc(2,3);
          dcb2=dc(3,3)*dc(1,1)+dc(3,1)*dc(1,3);
          dcc2=dc(2,3)*dc(3,1)+dc(2,1)*dc(3,3);
          dca3=dc(1,2)*dc(2,3)+dc(1,3)*dc(2,2);
          dcb3=dc(3,2)*dc(1,3)+dc(3,3)*dc(1,2);
          dcc3=dc(2,2)*dc(3,3)+dc(2,3)*dc(3,2);

           A=[dc1(1) dc2(1) dc3(1) dc12(1) dc13(1) dc23(1);
              dc1(2) dc2(2) dc3(2) dc12(2) dc13(2) dc23(2);
              dc1(3) dc2(3) dc3(3) dc12(3) dc13(3) dc23(3);
              dc21(1) dc21(2) dc21(3) dca1 dcb1 dcc1;
              dc31(1) dc31(2) dc31(3) dca2 dcb2 dcc2;
              dc32(1) dc32(2) dc32(3) dca3 dcb3 dcc3];

%
          [pc,delp,delep,Depc]=returnfield(p,i);
           Dep=A'*Depc*A;

           for j=1:6
           for k=1:6
              Dee(j,k,i)=real(Dep(j,k));
           end
          end

          STRESS(i,:)=A'*[pc(1);pc(2);pc(3);0;0;0];% total stress from return field
         delepl=A\[delep(1);delep(2);delep(3);0;0;0]; %change in plastic strain from return field
          STRAIN(i,:)=STRAIN(i,:)+delepl(:)'; %total strain from return field
          PSTRAIN(i,:)=PSTRAIN(i,:)+delepl(:)';
          i
     end
  end
end
  end
end
 eld=zeros(nel,eldof);
%Displacement at each nodes
displacement=zeros(nnd,3);
 for i=1:nel
    connec=Nodeelembound(i);
   l=0;
```

```
   for k=1:nne
   for j=1:nodof
      l=l+1;
      g(l)=nf(connec(k+1),j);
   end
   end

    for k=1:eldof
       if g(k)==0
          eld(i,k)=0.;
       else
          eld(i,k)=delta(g(k));
       end
    end
    l=0;
   for j=1:nne
      for k=1:nodof
         l=l+1;
         displacement(connec(j+1),k)=eld(i,l);
      end
   end
end
%Total displacement after increament of load
DISPLACEMENT=DISPLACEMENT+displacement;
% Calcualtion of stress in interface element 1
Bstress1=zeros(nelc1,3); % normal and shear stress to plane 1
leld=zeros(1,eldof); %local displacements for interface element
it=0;
for i=5410:5445
    it=it+1;
    connec=Nodeelembound(i);
   coord=zeros(nne,nodof);
 for k=1:nne
   cord=Nodecordbound(connec(k+1));
   for j=1:nodof
   coord(k,j)=cord(j+1);
   end
 end
 for j=1:4
  leld(1,(3*(j-1)+1):(3*(j-1)+3))=A1*eld(i,(3*(j-1)+1):(3*(j-1)+3))';
 end
 B=zeros(3,24);
  for j=1:4
          B(1,(1+(j-1)*3))=0.25;
          B(2,(2+(j-1)*3))=0.25;
          B(3,(3+(j-1)*3))=0.25;
  end
  for j=5:8
          B(1,(1+(j-1)*3))=-0.25;
          B(2,(2+(j-1)*3))=-0.25;
          B(3,(3+(j-1)*3))=-0.25;
  end
  Bstress1(it,:)=K*B*leld';
 end
%Calculating stress at interface 2
 Bstress2=zeros(nelc1,3); % normal and shear stress to plane 2
 leld=zeros(1,eldof); %local displacements for interface element
 it=0;
 for i=5446:5481
```

```
    it=it+1;
    connec=Nodeelembound(i);
   coord=zeros(nne,nodof);
  for k=1:nne
   cord=Nodecordbound(connec(k+1));
   for j=1:nodof
   coord(k,j)=cord(j+1);
   end
  end
  for j=1:4
   leld(1,(3*(j-1)+1):(3*(j-1)+3))=A2*eld(i,(3*(j-1)+1):(3*(j-1)+3))';
  end
  B=zeros(3,24);
   for j=1:4
           B(1,(1+(j-1)*3))=0.25;
           B(2,(2+(j-1)*3))=0.25;
           B(3,(3+(j-1)*3))=0.25;
   end
   for j=5:8
           B(1,(1+(j-1)*3))=-0.25;
           B(2,(2+(j-1)*3))=-0.25;
           B(3,(3+(j-1)*3))=-0.25;
   end
   Bstress2(it,:)=K*B*leld';
  end
 BSTRESS1=BSTRESS1+Bstress1;
 BSTRESS2=BSTRESS2+Bstress2;
eldfxy=zeros(nel*nne,4);
numb=0;
 for i=1:nel
    connec=Nodeelembound(i);
    coord=zeros(nne,nodof);
  for k=1:nne
    cord=Nodecordbound(connec(k+1));
    for j=1:nodof
    coord(k,j)=cord(j+1);
    end
  end
    tk=0;
     for j=5410:5445
        if i==j
           tk=1;
        end
     end
     for j=5446:5481
        if i==j
           tk=2;
        end
     end
     %stifffness matrix for continum model
     if tk==0
     % coordinates of the nodes of element i, % and its steering vector
     ke=zeros(eldof,eldof) ; % Initialize the element stiffness % matrix to zero
     for ig=1: ngp
        wi = samp(ig,2);
     for jg=1: ngp
        wj=samp(jg,2);
     for kg=1: ngp
        wk = samp(kg,2);
```

```
        [der,fun] = fmlin3d(samp,ig,jg,kg); % Derivative of shape functions
        jac=der*coord; % Compute Jacobian matrix
        d=det(jac); % Compute determinant of Jacobian %
        deriv=jac\der; % Derivative of shape functions in
        bee=formbee3d(deriv,nne,eldof); % Form matrix [B]
    ke=ke + d*wi*wj*wk*bee'*Dee(:,:,i)*bee; % Integrate stiffness matrix

 end
 end
 end
 end
 %stiffness matrix for contact1
 if tk==1
Tcoords=zeros(4,3);
ke=zeros(eldof,eldof) ;
for j=1:4
   tcord=A1*coord(j,:)';
   Tcoords(j,:)=tcord';
end
 for ig=1:ngp
   wi=samp(ig,2);
   for jg=1:ngp
      wj=samp(jg,2);
      [der,fun]=fmlin(samp,ig,jg);
      jac=der*Tcoords(1:4,2:3);
      d=det(jac);
      B=zeros(3,24);
      N=form_bee2d(samp,ig,jg);
    for j=1:4
      B(1,(1+(j-1)*3))=N(j);
      B(2,(2+(j-1)*3))=N(j);
      B(3,(3+(j-1)*3))=N(j);
    end
     for j=5:8
      B(1,(1+(j-1)*3))=-N(5-(j-4));
      B(2,(2+(j-1)*3))=-N(5-(j-4));
      B(3,(3+(j-1)*3))=-N(5-(j-4));
    end
    ke=ke+wi*wj*d*B'*K1*B;
   end
 end
 end
 %stiffness matrix for contact2
if tk==2
 Tcoords=zeros(4,3);
ke=zeros(eldof,eldof) ;
for j=1:4
   tcord=A2*coord(j,:)';
   Tcoords(j,:)=tcord';
end
   for ig=1:ngp
   wi=samp(ig,2);
   for jg=1:ngp
      wj=samp(jg,2);
      [der,fun]=fmlin(samp,ig,jg);
      jac=der*Tcoords(1:4,2:3);
      d=det(jac);
      B=zeros(3,24);
      N=form_bee2d(samp,ig,jg);
```

```
        for j=1:4
           B(1,(1+(j-1)*3))=N(j);
           B(2,(2+(j-1)*3))=N(j);
           B(3,(3+(j-1)*3))=N(j);
        end
         for j=5:8
           B(1,(1+(j-1)*3))=-N(5-(j-4));
           B(2,(2+(j-1)*3))=-N(5-(j-4));
           B(3,(3+(j-1)*3))=-N(5-(j-4));
        end
        ke=ke+wi*wj*d*B'*K1*B;
       end
    end
  end
        elf=ke*eld(i,:)';

        for j=1:nne
           numb=numb+1;
           eldfxy(numb,1)=elf(3*j-2);%% force anlong x axis at node
           eldfxy(numb,2)=elf(3*j-1);%% force anlong y axis at node
           eldfxy(numb,3)=elf(3*j);%% force anlong z axis at node
           eldfxy(numb,4)=connec(j+1);%%  node
        end
end
seldfxy=zeros(nnd,3); % sum of forces at a node
 for i=1:nnd
   for j=1:nel*nne
          if eldfxy(j,4)==i
                seldfxy(i,1)=seldfxy(i,1)+eldfxy(j,1);
                seldfxy(i,2)=seldfxy(i,2)+eldfxy(j,2);
                seldfxy(i,3)=seldfxy(i,3)+eldfxy(j,3);

          end
   end
 end
 %Total nodal reaction force
 TNF=TNF+seldfxy;
% calculation of Nodal reaction at of wedge and dam on wedge
 nelc3=10; % number of elements at contact2
 nndc3=18; % number of nodes at contact 2
 numb=0;
 eldfxy=zeros(nne*nelc3,4);
 for i=1:nelc3
  cnelem=Contactdelement(i);
  connec=Nodeelembound(cnelem);
  coord=zeros(nne,nodof);
 for k=1:nne
   cord=Nodecordbound(connec(k+1));
   for j=1:nodof
   coord(k,j)=cord(j+1);
   end
 end
 ke=zeros(eldof,eldof);
        for ig=1: ngp
           wi = samp(ig,2);
        for jg=1: ngp
           wj=samp(jg,2);
        for kg=1:ngp
           wg=samp(kg,2);
```

```
            [der,fun] = fmlin3d(samp,ig,jg,kg); % Derivative of shape functions in % local coordinates
            jac=der*coord; % Compute Jacobian matrix
            deriv=jac\der; % Derivative of shape functions in % global coordinates
            bee=formbee3d(deriv,nne,eldof); % Form matrix [B]
            d=det(jac);
            ke=ke + d*wi*wj*wk*bee'*Dee(:,:,cnelem)*bee;
        end
        end
        end
        elf=ke*eld(cnelem,:)';
        for j=1:nne
          numb=numb+1;
          eldfxy(numb,1)=elf(3*j-2);%% force anlong x axis at node
          eldfxy(numb,2)=elf(3*j-1);%% force anlong y axis at node
          eldfxy(numb,3)=elf(3*j);%% force anlong z axis at node
          eldfxy(numb,4)=connec(j+1);%%  node
        end

end
cseldfxy3=zeros(nndc3,3); % sum of forces at a node contact 1
for i=1:nndc3
   node=Nodescontactd(i);
  for j=1:nelc3*nne
        if eldfxy(j,4)==node
              cseldfxy3(i,1)=cseldfxy3(i,1)+eldfxy(j,1);
              cseldfxy3(i,2)=cseldfxy3(i,2)+eldfxy(j,2);
              cseldfxy3(i,3)=cseldfxy3(i,3)+eldfxy(j,3);

        end
  end
end
TNFC3=TNFC3+cseldfxy3;
fxy=zeros(n,1); %% forces at each freedom points
 for i=1:nnd
  for j=1:nodof
     if nf(i,j) ~= 0
        fxy(nf(i,j))=TNF(i,j);
     end
  end
 end
  res=zeros(n,1); % residual force
 for i=1:n
    res(i)=ftp(i)-fxy(i); %% fgt is applied total load
 end
dlmwrite('FDee5.txt',Dee)
dlmwrite('FTTotalstress5.txt',STRESS)
dlmwrite('FTTotalstrain5.txt',STRAIN)
dlmwrite('FTTotaldisp5.txt',DISPLACEMENT)
dlmwrite('FTTotalload5.txt',ft)
dlmwrite('FTTotalnodalreactionforce5.txt',TNF)
dlmwrite('FTTotalcontact1stress5.txt',BSTRESS1)
dlmwrite('FTTotalcontact2stress5.txt',BSTRESS2)
dlmwrite('FTPrinciplestress5.txt',principlestress)
dlmwrite('FTyieldvalue5.txt',yieldfunelemental)
dlmwrite('FTTotalplasticstrain5.txt',PSTRAIN)
dlmwrite('FTTotalcontactload35.txt',TNFC3)
```

II. Function for return field

```
function[pcf,delp,delep,Depc]=returnfield(ps,elem)
global Rockpara
parameter=Rockpara(elem,:);
 E = parameter(9); % Elastic modulus in MPa
vu = parameter(8); % Poisson's ratio
sigci=parameter(1);
yields=parameter(2);
yieldmb=parameter(3);
yielda=parameter(4);
yieldsg=parameter(5);
yieldmg=parameter(6);
yieldag=parameter(7);
 %%% Calculation of sig1>sig2>sig3
[p1b, nu1]=max(ps);
[p3b, nu3]=min(ps);
nu2=6-nu1-nu3;
p2b=ps(1)+ps(2)+ps(3)-p1b-p3b;
pb=[p1b;
    p2b;
    p3b];
%%% Computation of consutative matrix linear
[dee,Dbar] = formdeps(E,vu);
I=eye(3);
Gbar=(E/(2*(1+vu)))*I;

%%% Computation of peak stress
sigmat=yields*sigci/yieldmb;
if pb(1)>sigmat
     pc=[sigmat;
           sigmat;
           sigmat];
        Depc=[Dbar zeros(3);
              zeros(3) Gbar];
        delp=[pb(1)-sigmat;
              pb(2)-sigmat;
              pb(3)-sigmat];
else
%%% Computation of yield function
[fy]=yieldfun(pb,elem);
%%% check for yield function
if fy <=0
    %%%% no need for return field
    Depc=[Dbar zeros(3);
       zeros(3) Gbar];
   pc=[pb(1);
       pb(2);
       pb(3)];
   delp=[0;0;0];

  else
    %%% need for return field
    [k,kg,delkg]=form_kkg(sigmat,elem);

    if (1/kg) == 0
        bt=[1;
            0;
            0];
```

```
    else
    bt=[kg;
        0;
        -1];
    end
    b1=[1;
        1;
        -2/kg];
    b2=[-2;
        1/kg;
        1/kg];
    st=Dbar*bt;
    s1=Dbar*b1;
    s2=Dbar*b2;
    n1=cross(st,s1);
    n2=cross(s2,st);
    p1=n1'*[pb(1)-sigmat;pb(2)-sigmat;pb(3)-sigmat];
    p2=n2'*[pb(1)-sigmat;pb(2)-sigmat;pb(3)-sigmat];
if p1>=0 && p2>=0
        %return to apex
        pc=[sigmat;
            sigmat;
            sigmat];
        Depc=zeros(6,6);
        delp=[pb(1)-sigmat;
              pb(2)-sigmat;
              pb(3)-sigmat];
       else
   %%% return to yield surface
  if p1b >=0
      syms x
      p1c=vpasolve(p3b-x+sigci*(yields-yieldmb*x/sigci)^yielda==0,x,[(p1b-2*fy) p1b]);
  else
     p1c=1.1*p1b;
  end
  error=10;
if fy<=0.8
 [k,kg,delkg]=form_kkg(p1b,elem);
  a=[k;
     0;
     -1];
  b=[kg;
     0;
     -1];
  r=(Dbar*b)/(b'*Dbar*a);
  pc=pb-r;
  p2c=pc(2);
  p3c=pc(3);
  p1c=pc(1);
 else
while error > 5

[p2c,p3c]=form_sig23(p1c,p1b,p2b,elem);
[k,kg,delkg]=form_kkg(p1c,elem);
%p1cnew=((p3c-p3b)*((1-vu)*kg-vu)/(vu*kg-1+vu))+p1b
%((p3c-p3b)/(p1c-p1b));
hf=((p3c-p3b)/(p1c-p1b))-(vu*kg+1-vu)/((1-vu)*kg-vu);
dalphar=(k*(p1c-p1b)-(p3c-p3b))/(p1c-p1b)^2;
dalphas=(vu*delkg*((1-vu)*kg-vu)-(vu*kg+1-vu)*(1-vu)*delkg)/((1-vu)*kg-vu)^2;
```

```
dhf=dalphar-dalphas;
p1cnew=p1c-hf/dhf;
if p1c >= sigmat
       p1c=0.9*sigmat+(1-0.9)*p1c;
end
error=abs(p1cnew-p1c)/p1c*100;
p1c=p1cnew;
end
pc=[p1c;
   p2c;
   p3c];
 end
delp=pb-pc;

%calculation of T
t1=(delp(1)-delp(2))/(p1c-p2c);
t2=(delp(1)-delp(3))/(p1c-p3c);
t3=(delp(2)-delp(3))/(p2c-p3c);
Tbarg=I+[t1 0 0;
        0 t2 0;
        0 0 t3];
   Tbarginverse=inv(Tbarg);

bbar=[kg;
      0;
     -1];

  dellamda=norm(delp)/norm(Dbar*bbar);
  delg2=[delkg 0 0;
         0 0 0;
         0 0 0];
     Tbar=inv(I+dellamda*Dbar*delg2);
     T=[Tbar zeros(3);
        zeros(3) Tbarginverse];
      %calculation of Depc

D=[Dbar zeros(3);
   zeros(3) Gbar];
Dc=T*D;
a=[k 0 -1 0 0 0];
b=[kg 0 -1 0 0 0];
Depc=Dc-(Dc*b'*a*Dc)/(a*Dc*b');

%%%return to curve1
if p2c > p1c
    error=10;
    while error >=5
  [p2c,p3c]=form_sig23(p1c,p1b,p2b,elem);
 [k,kg,delkg]=form_kkg(p1c,elem);
 pc=[p1c;
    p2c;
    p3c];
delp=pb-pc; %plastic stress
    delep=(Dbar)\delp; %plastic strain
  h1=[1 1 kg]*delep;
  dh1=[0 0 delkg]*delep+[1 1 kg]*(-inv(Dbar)*[1 1 k]');
  p1cnew=p1c-h1/dh1;
  if p1c >= sigmat
       p1cnew=0.9*sigmat+(1-0.9)*p1c;
```

```
  end
  error=abs(p1cnew-p1c)/p1c*100;
  p1c=p1cnew;
    end
    %calculation of T
    dlamda=delep(1)/kg;
    dlamdan=delep(2)/kg;
    dgn=[0 0 0;
         0 delkg 0;
         0 0 0];
     dg=[delkg 0 0;
         0 0 0;
         0 0 0];
     Tbarl=inv(I+dlamda*Dbar*dg+dlamdan*Dbar*dgn);
     t1=(delp(1)-delp(2))/(p1c-p2c);
t2=(delp(1)-delp(3))/(p1c-p3c);
t3=(delp(2)-delp(3))/(p2c-p3c);
Tbarg=I+[t1 0 0;
         0 t2 0;
         0 0 t3];
    Tbarginverse=inv(Tbarg);
    T=[Tbarl zeros(3);
       zeros(3) Tbarginverse];
    %calculation of Depc
    Tbar=inv(I+dlamda*Dbar*dg);
    Dc=(I+dlamda*Dbar*dg)\Dbar;
    r=[1 1 k];
    rg=[1 1 kg];
    size(Dc);
    Depc1=r'*rg/(r*inv(Dc)*rg');
    Depc=[Depc1 zeros(3);
          zeros(3) Gbar];
end
  %%% return to curve2
if p2c <= p3c
          error=10;
    while error >=5
   [p2c,p3c]=form_sig23(p1c,p1b,p2b,elem);
 [k,kg,delkg]=form_kkg(p1c,elem);
 pc=[p1c;
    p2c;
    p3c];
delp=pb-pc; %plastic stress
    delep=(Dbar)\delp; %plastic strain
  h2=[1 kg kg]*delep;
  dh2=[0 delkg delkg]*delep+[1 kg kg]*(-inv(Dbar)*[1 k k]');
  p1cnew=p1c-h2/dh2;
  if p1c >= sigmat
        p1cnew=0.9*sigmat+(1-0.9)*p1c;
  end
  error=abs(p1cnew-p1c)/p1c*100;
  p1c=p1cnew;
    end
    %calculation of T
    dlamda=-delep(3);
    dlamdan=-delep(2);
    dgn=[0 0 0;
         0 delkg 0;
         0 0 0];
```

```
    dg=[delkg 0 0;
        0 0 0;
        0 0 0];
    Tbarl=inv(I+dlamda*Dbar*dg+dlamda*Dbar*dg);
    t1=(delp(1)-delp(2))/(p1c-p2c);
t2=(delp(1)-delp(3))/(p1c-p3c);
t3=(delp(2)-delp(3))/(p2c-p3c);
Tbarg=I+[t1 0 0;
       0 t2 0;
       0 0 t3];
   Tbarginverse=inv(Tbarg);
   T=[Tbarl zeros(3);
      zeros(3) Tbarginverse];
   %calculation of Depc
   Tbar=inv(I+dlamda*Dbar*dg);
   Dc=(I+dlamda*Dbar*dg)\Dbar;
   r=[1 k k];
   rg=[1 kg kg];
   Depc1=r'*rg/(r*inv(Dc)*rg');
   Depc=[Depc1 zeros(3);
        zeros(3) Gbar];
end
 end
end
end
pcf(nu1)=pc(1);
pcf(nu2)=pc(2);
pcf(nu3)=pc(3);
delep=Dbar\delp;
```

III . Function for yield value

```
  function[fy]=yieldfun(ps,elem)
global Rockpara
para=Rockpara(elem,:);
sigci=para(1);
yields=para(2);
yieldmb=para(3);
yielda=para(4);
yieldsg=para(5);
yieldmg=para(6);
yieldag=para(7);
 p1=max(ps);
p3=min(ps);
fy= p1-p3-sigci*abs((yields-yieldmb*p1/sigci)).^yielda;
end
```

IV . Function for slope of yield surface

```
function[k,kg,delkg]=form_kkg(p1,elem)
global Rockpara
para=Rockpara(elem,:);
sigci=para(1);
yields=para(2);
yieldmb=para(3);
yielda=para(4);
yieldsg=para(5);
yieldmg=para(6);
yieldag=para(7);
k=1+yielda*yieldmb*(yields-yieldmb*p1/sigci)^(yielda-1);
```

```
kg=1+yieldag*yieldmg*(yieldsg-yieldmg*p1/sigci)^(yieldag-1);
delkg=(1-yieldag)*yieldag*yieldmg^2/sigci*(yieldsg-yieldmg*p1/sigci)^(yieldag-2);
```

V . Sub function for return field

```
function[p2c,p3c]=form_sig23(p1c,p1b,p2b,elem)
%%global vu sigci yields yieldmb yielda
global Rockpara
para=Rockpara(elem,:);
sigci=para(1);
vu = para(8);
yields=para(2);
yieldmb=para(3);
yielda=para(4);
yieldsg=para(5);
yieldmg=para(6);
yieldag=para(7);
[k,kg,delkg]=form_kkg(p1c,elem);
s1=(1-vu)*kg-vu;
s2=vu*kg-vu;
tf=(p1c-p1b)/s1;
p3c=p1c-sigci*(yields-yieldmb*p1c/sigci)^yielda;
p2c=tf*s2+p2b;
end
```

VI. Function for Gauss Number and values

```
function[samp]=gauss(ngp)
% % This function returns the abscissas and weights of the Gauss
% points for ngp equal up to 4 % %
samp=zeros(ngp,2);
%
if ngp==1
   samp=[0. 2];
elseif ngp==2
   samp=[-1./sqrt(3) 1.;
        1./sqrt(3) 1.];
elseif ngp==3
   samp= [-.2*sqrt(15.) 5./9;
          0. 8./9.;
          2*sqrt(15.) 5./9];
elseif ngp==4
   samp= [-0.861136311594053 0.347854845137454;
         -0.339981043584856 0.652145154862546;
          0.339981043584856 0.652145154862546;
          0.861136311594053 0.347854845137454];
elseif ngp==5
   samp= [0.000000000000000 0.5688888888888889;
         -0.5384693101056831 0.4786286704993665;
         0.5384693101056831 0.4786286704993665;
         -0.9061798459386640 0.2369268850561891;
         0.9061798459386640 0.2369268850561891];
end
% % End function Gauss
```

VII. Function for strain transformation matrix

```
   function[bee] = formbee3d(deriv,nne,eldof)
% % This function assembles the matrix [bee] from the
% derivatives of the shape functions in global coordinates %
bee=zeros(6,eldof);
p=1;
for i=1:nne
   bee(1,p)=deriv(1,i);
   bee(2,(p+1))=deriv(2,i);
   bee(3,(p+2))=deriv(3,i);
   bee(4,p)=deriv(2,i);
   bee(4,(p+1))=deriv(1,i);
   bee(5,p)=deriv(3,i);
   bee(5,(p+2))=deriv(1,i);
   bee(6,(p+1))=deriv(3,i);
   bee(6,(p+2))=deriv(2,i);
   p=p+3;
end
```

VIII. Function for shape function and it's derivative

```
function[der,fun] = fmlin3d(samp,ig,jg,kg)
xi=samp(ig,1);
eta=samp(jg,1);
zeta=samp(kg,1);
fun = 1/8*[(1.- xi)*(1.- eta)*(1.-zeta);
         (1.+ xi)*(1.- eta)*(1.-zeta);
         (1.+ xi)*(1.+ eta)*(1.-zeta);
         (1.- xi)*(1.+ eta)*(1.-zeta);
         (1.- xi)*(1.- eta)*(1.+zeta);
         (1.+ xi)*(1.- eta)*(1.+zeta);
         (1.+ xi)*(1.+ eta)*(1.+zeta);
         (1.- xi)*(1.+ eta)*(1.+zeta)];

dert = 0.125*[-(1-eta)*(1-zeta) -(1-xi)*(1-zeta) -(1-xi)*(1-eta);
             (1-eta)*(1-zeta) -(1+xi)*(1-zeta) -(1+xi)*(1-eta);
             (1+eta)*(1-zeta) (1+xi)*(1-zeta) -(1+xi)*(1+eta);
            -(1+eta)*(1-zeta) (1-xi)*(1-zeta) -(1-xi)*(1+eta);
            -(1-eta)*(1+zeta) -(1-xi)*(1+zeta) (1-xi)*(1-eta);
             (1-eta)*(1+zeta) -(1+xi)*(1+zeta) (1+xi)*(1-eta);
             (1+eta)*(1+zeta) (1+xi)*(1+zeta) (1+xi)*(1+eta);
            -(1+eta)*(1+zeta) (1-xi)*(1+zeta) (1-xi)*(1+eta)];
 der=dert';
```

IX. Program for shear stress calculation

```
% Programme for calculation of factor of saftey against sliding of wedge
pstress=dlmread('FTTotalcontact1stress0.txt');
Pressure=dlmread('Porepressure10.txt');% pore pressure
nelc1=36;
JRC=2;
JCS=60*1000; %kN/m2
phir=20;
stress=zeros(nelc1,3);
Fos2=zeros(nelc1,1);
for i=1:nelc1
   stress(i,:)=[abs(pstress(i,1))-Pressure(i,1) abs(pstress(i,2)) abs(pstress(i,3))];
   Fos2(i)=stress(i,1)*tand(JRC*log10(JCS/stress(i,1))+phir)/(stress(i,2)^2+stress(i,3)^2)^0.5;
end
```

X. Program for displaying results of dam

```
% Plotting field on dam only
%plotting principle stress 1 and 3
displacement=dlmread('FcTprinciplestress5.txt');
field=Nodal_avg(displacement(:,3));
nnd=6807;
nel=5409;
neldam=322;
nne=8;
X=zeros(nne,neldam);
Y=zeros(nne,neldam);
Z=zeros(nne,neldam);
XYZ=cell(1,neldam);
profile=zeros(nne,neldam);
Profile=cell(1,neldam);
 fm = [1 2 6 5; 2 3 7 6; 3 4 8 7; 4 1 5 8; 1 2 3 4; 5 6 7 8];
 for i=1:neldam
    elem=elemDam(i);
    nd=Nodeelem(elem);
    for j=1:nne
        coord=Nodecord(nd(j+1));
        X(j,i)=coord(2);
        Y(j,i)=coord(3);
        Z(j,i)=coord(4);
        profile(j,i)=field(nd(j+1),1);
    end
    Profile{i}=[profile(:,i)];
    XYZ{i}=[X(:,i) Y(:,i) Z(:,i)];
end
figure
        set(gcf,'color','w')
cellfun(@patch,repmat({'Vertices'},1,neldam),XYZ,.....
            repmat({'Faces'},1,neldam),repmat({fm},1,neldam),.....
            repmat({'FaceVertexCdata'},1,neldam),Profile,.....
            repmat({'FaceColor'},1,neldam),repmat({'interp'},1,neldam));

        set(gca,'XTick',[]) ; set(gca,'YTick',[]); set(gca,'ZTick',[]) ;
colorbar

xlabel('West-East')
ylabel('North-South')
zlabel('Elevation')
title('First Principle stress at full reseviour level in dam (kN/m2)')
```

XI. Program for displaying results of foundation

```
%Plot of Foundation only with field
neldam=322;
nel=5409;
neldadaphy=658;
nelNourphy=1518;
%nel=5481;
%nnd=6895;
nnd=6807;
rnel=nel-neldam-neldadaphy-nelNourphy;
nne=8;
X=zeros(nne,rnel);
Y=zeros(nne,rnel);
Z=zeros(nne,rnel);
```

```
XYZ=cell(1,rnel);
deformation=dlmread('FcTPrinciplestress5.txt');
field=Nodal_avg(deformation(:,3));
%field=deformation(:,3);
profile=zeros(nne,rnel);
Profile=cell(1,rnel);
fm = [1 2 6 5; 2 3 7 6; 3 4 8 7; 4 1 5 8; 1 2 3 4; 5 6 7 8];
t=0;
 for i=1:nel
    po=0;
    for j=1:neldam
        elem=elemDam(j);
        if i==elem
            po=1;
        end
    end
    for k=1:nelNourphy
         elem=elemNourphy(k);
         if i==elem
             po=1;
         end
    end
     for k=1:neldadaphy
         elem=elemdadaphy(k);
         if i==elem
             po=1;
         end
     end
    if po==0
        t=t+1;
    nd=Nodeelem(i);
    for j=1:nne
        coord=Nodecord(nd(j+1));
        X(j,t)=coord(2);
        Y(j,t)=coord(3);
        Z(j,t)=coord(4);

        profile(j,t)=field(nd(j+1),1);
    end
    end
    Profile{t}=[profile(:,t)];
    XYZ{t}=[X(:,t) Y(:,t) Z(:,t)];
end
figure
        set(gcf,'color','w')

 cellfun(@patch,repmat({'Vertices'},1,rnel),XYZ,.......
            repmat({'Faces'},1,rnel),repmat({fm},1,rnel),.....
            repmat({'FaceVertexCdata'},1,rnel),Profile,......
            repmat({'FaceColor'},1,rnel),repmat({'interp'},1,rnel));
        view(3)
        set(gca,'XTick',[]) ; set(gca,'YTick',[]); set(gca,'ZTick',[]) ;
colorbar
title('Plastic strain in foundation at FSL')
 axis auto
```

XII Program for pore pressure calculation

```
Nodal pore pressure calculation
%calculation of pore pressure equation of upper surface
%cordinates of contact surface 1
pa=[1328.95 607.75 935.43];
pb=[1285.6  371.46 860.89];
pc=[1608.29 502.88 1000];
%equivalent pore pressure at above points
ppa=850-935.43;
ppb=850-860.89;
ppc=850-1000;
%direction cosines of normal to the plane 1
ab=[pa(1)-pb(1) pa(2)-pb(2) pa(3)-pb(3)];
ac=[pa(1)-pc(1) pa(2)-pc(2) pa(3)-pc(3)];
nd1=cross(ab,ac);
dnd1=(nd1(1)^2+nd1(2)^2+nd1(3)^2)^0.5;

%Cordinate of points on upper surface of pore pressure
usa=[(ppa*nd1(1)/dnd1)+pa(1) (ppa*nd1(2)/dnd1)+pa(2) (ppa*nd1(3)/dnd1)+pa(3)];
usb=[(ppb*nd1(1)/dnd1)+pb(1) (ppb*nd1(2)/dnd1)+pb(2) (ppb*nd1(3)/dnd1)+pb(3)];
usc=[(ppc*nd1(1)/dnd1)+pc(1) (ppc*nd1(2)/dnd1)+pc(2) (ppc*nd1(3)/dnd1)+pc(3)];
%Direction cosine of normal of upper pore pressure surface
abs=[usa(1)-usb(1) usa(2)-usb(2) usa(3)-usb(3)];
acs=[usa(1)-usc(1) usa(2)-usc(2) usa(3)-usc(3)];
nd1s=cross(acs,abs);
dd=-1*(usc(1)*nd1s(1)+usc(2)*nd1s(2)+usc(3)*nd1s(3));
%equivalent pore pressure at any point in contact surface 1
%Calculation of pore pressure
ro=9.81;% kN/m3
nodof=3;
cn1=50; % number of nodes at contact
nnd=6807;
cen1=36;%number of elements at contact1
fcn1=zeros(nnd,3);
fce1=zeros(cen1,12);
porepressure1=zeros(cen1,1);
f=zeros(cen1,4);
ngp=5;
samp=gauss(ngp);
Area=0;
for i=1:cen1   % number of element at contact
   coords=zeros(4,3);
   Cnelem=Contactelementa(i);
   for j=1:4
      cord=Nodecord(Cnelem(j));
      coords(j,1)=cord(2);
      coords(j,2)=cord(3);
      coords(j,3)=cord(4);
   end

   Ax=0;
   Ay=0;
   Az=0;
   for ig=1:ngp
      wi=samp(ig,2);
      for jg=1:ngp
         wj=samp(jg,2);
         [der,fun]=fmlin(samp,ig,jg);
```

```
        jac=der*coords(:,2:3);
        d=det(jac);
        Ax=Ax+wi*wj*d;
      end
    end
    for ig=1:ngp
      wi=samp(ig,2);
      for jg=1:ngp
        wj=samp(jg,2);
        [der,fun]=fmlin(samp,ig,jg);
        jac=der*coords(:,1:2:3);
        d=det(jac);
        Ay=Ay+wi*wj*d;
      end
    end
    for ig=1:ngp
      wi=samp(ig,2);
      for jg=1:ngp
        wj=samp(jg,2);
        [der,fun]=fmlin(samp,ig,jg);
        jac=der*coords(:,1:2);
        d=det(jac);
        Az=Az+wi*wj*d;
      end
    end
     if Ax <=0
       Ax=-1*Ax;
     end
     if Ay <=0
       Ay=-1*Ay;
     end
     if Az >=0
      Az=-1*Az;
     end
    m=0;
    for j=1:4
      cord=Nodecord(Cnelem(j));

     D=-
1*((cord(2)*nd1s(1)+cord(3)*nd1s(2)+cord(4)*nd1s(3))+dd)*dnd1/(nd1(1)*nd1s(1)+nd1(2)*nd1s(2)+
nd1(3)*nd1s(3));

        if D>=0

    fcn1(Cnelem(j),3)=fcn1(Cnelem(j),3)+((Az)*ro*D)/4.;
    fcn1(Cnelem(j),1)=fcn1(Cnelem(j),1)+((Ax)/4.*ro*D);
    fcn1(Cnelem(j),2)=fcn1(Cnelem(j),2)+((Ay)/4.*ro*D);



     fce1(i,(3*j-2))=(Ax)/4.*ro*D;

     fce1(i,(3*j-1))=(Ay)/4.*ro*D;

     fce1(i,(3*j))=(Az)/4.*ro*D;

        end
      f(i,j)=(fce1(i,(3*j-2))^2+ fce1(i,(3*j-1))^2+fce1(i,(3*j))^2)^0.5;
    end
```

```
    porepressure1(i,1)=(f(i,1)+f(i,2)+f(i,3)+f(i,4))/((Ax^2+Ay^2+Az^2)^0.5);
    Area=Area+((Ax^2+Ay^2+Az^2)^0.5);
end

fc1n=zeros(cn1,3);
for i=1:cn1
    nod=Contactnodesa(i);
    for j=1:nodof
    fc1n(i,j)=fcn1(nod,j);
    %fc1n(i,4)=nod;
    end
end
dlmwrite('Porepressure11.txt',porepressure1)
dlmwrite('Poreforce11.txt',fc1n)
```

APPENDIX B: RESULTS OF REGRESSION ANALYSIS FOR RELATION BETWEEN DEFORMATION RAIN WITH MODULUS OF ELASTICITY OF FOUNDATION ROCK

As discussed in chapter 5, regression analysis performed for the variation of total maximum deformation in dam and foundation with variation of modulus of elasticity of foundation is done at different reservoir level i.e. at empty reservoir, reservoir depth 112m, reservoir depth 162m, reservoir depth 187m, reservoir depth 212m, and reservoir depth 260m (FSL), out of which most critical state i.e. at FSL is already explained in main body chapter 5. Results of rest are as below. In following equations displacement (d) has unit meter, modulus of elasticity of foundation rock (Er) has unit GPa, and maximum plastic strain (ps).

Relation between total maximum deformations in dam vs modulus of elasticity of foundation rock.

- At empty reservoir level

  d= 0.5953*$e^{-1.082*E_r^{0.5}}$+0.02878

  R-squared value =0.9978

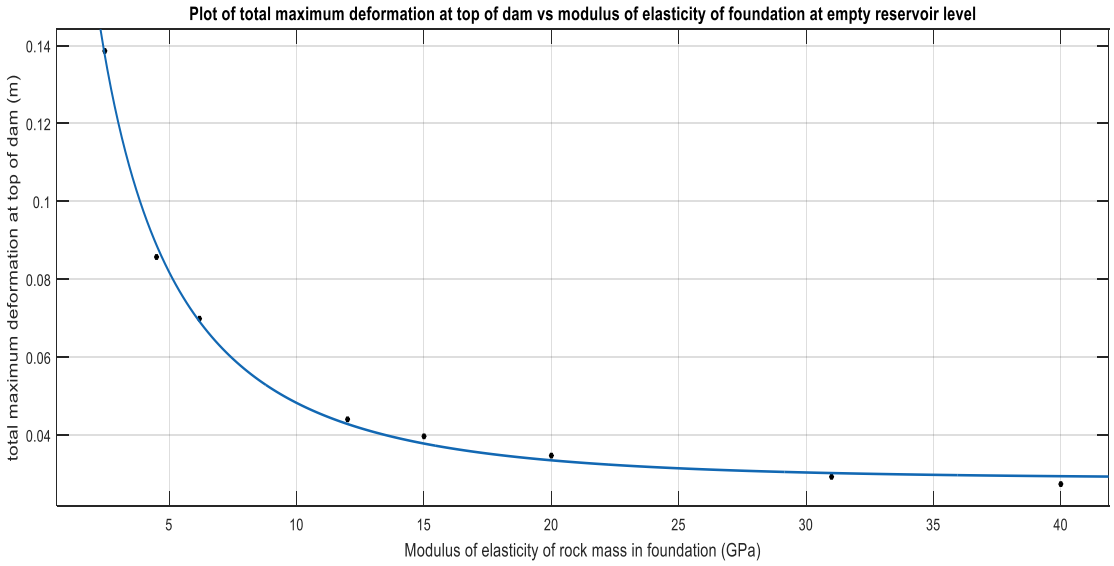

Figure B-1 Plot of total maximum deformation at top of dam vs modulus of elasticity of foundation rock at empty reservoir level (self-weight of dam).

- At reservoir depth 112m

  d= 0.3056*$e^{-0.8561*E_r^{0.5}}$+0.01974

  R-squared value =0.999

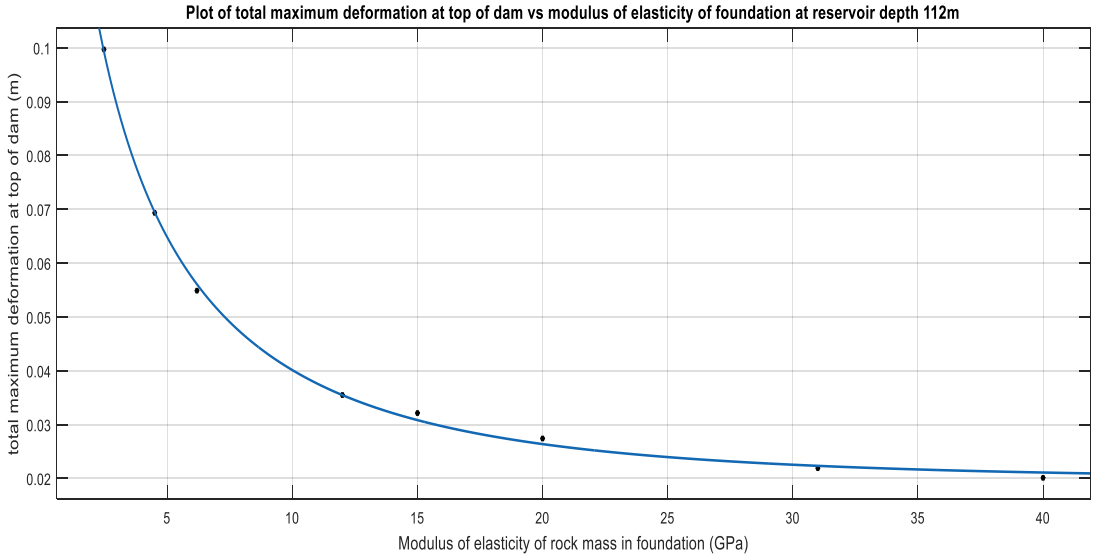

Figure B-2 Plot of total maximum deformation at top of dam vs modulus of elasticity of foundation rock at reservoir depth 112m.

- At reservoir depth 162m

  d= 0.9642*$e^{-1.091*E_r^{0.5}}$+0.02926

  R-squared value =0.999

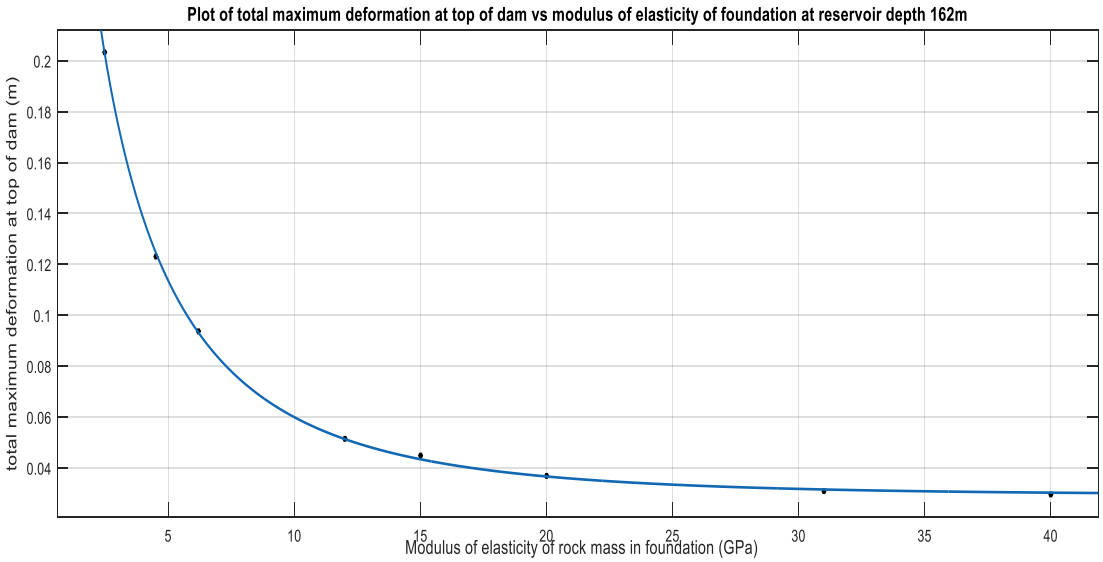

Figure B-3 Plot of total maximum deformation at top of dam vs modulus of elasticity of foundation rock at reservoir depth 162m.

- At reservoir depth 187m

  d= 1.629*$e^{-1.259*E_r^{0.5}}$+0.04706

  R-squared value =0.9997

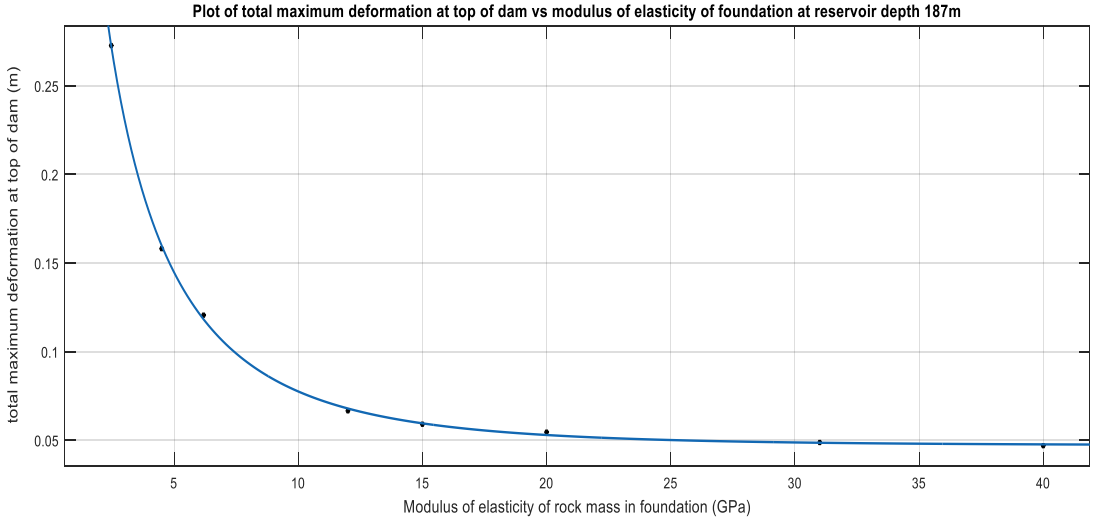

Figure B-4 Plot of total maximum deformation at top of dam vs modulus of elasticity of foundation rock at reservoir depth 187m.

- At reservoir depth 212m

  d= 2.649*$e^{-1.464*E_r^{0.5}}$+0.07996

  R-squared value =0.9987

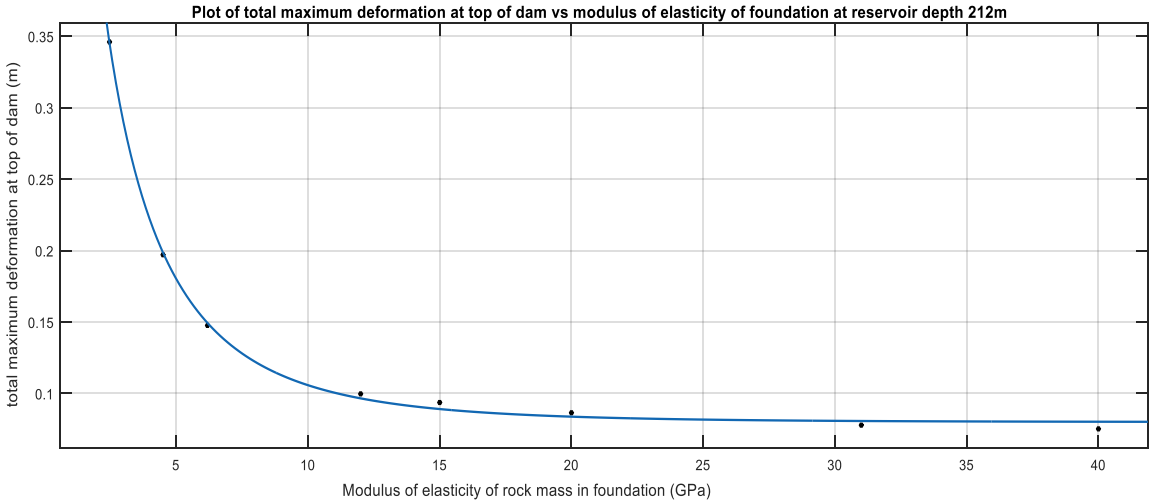

Figure B-5 Plot of total maximum deformation at top of dam vs modulus of elasticity of foundation rock reservoir depth 212m.

Relation between total maximum deformations in foundation vs modulus of elasticity of foundation rock.

- At empty reservoir level

  d= 0.6869*$e^{-0.8661*E_r^{0.5}}$+0.01771

  R-squared value =0.9975

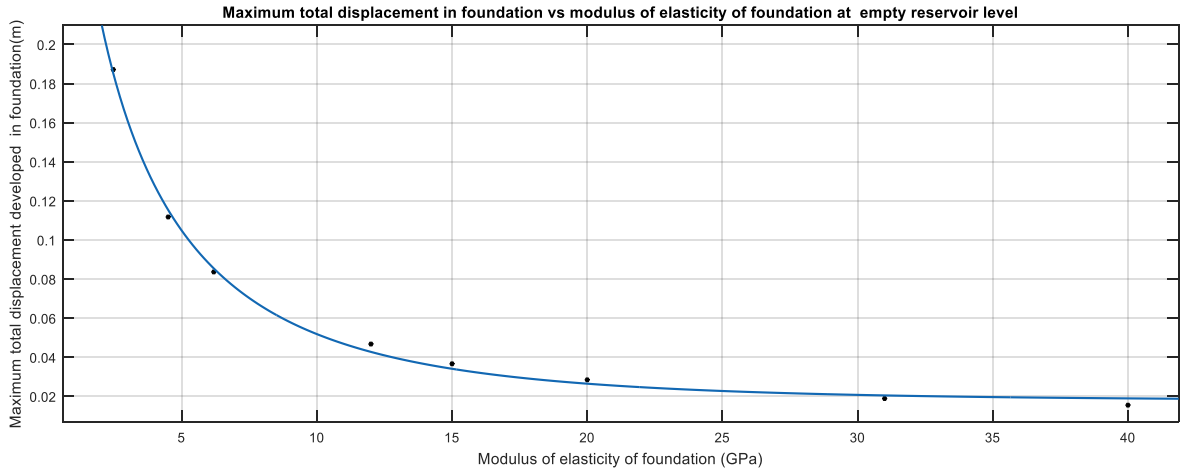

Figure B-6 Plot of total maximum deformation in foundation vs modulus of elasticity of foundation rock at empty reservoir level (self-weight of dam).

- At reservoir depth 112m

  d= 0.6844*$e^{-0.9663*E_r^{0.5}}$+0.0157

  R-squared value =0.998

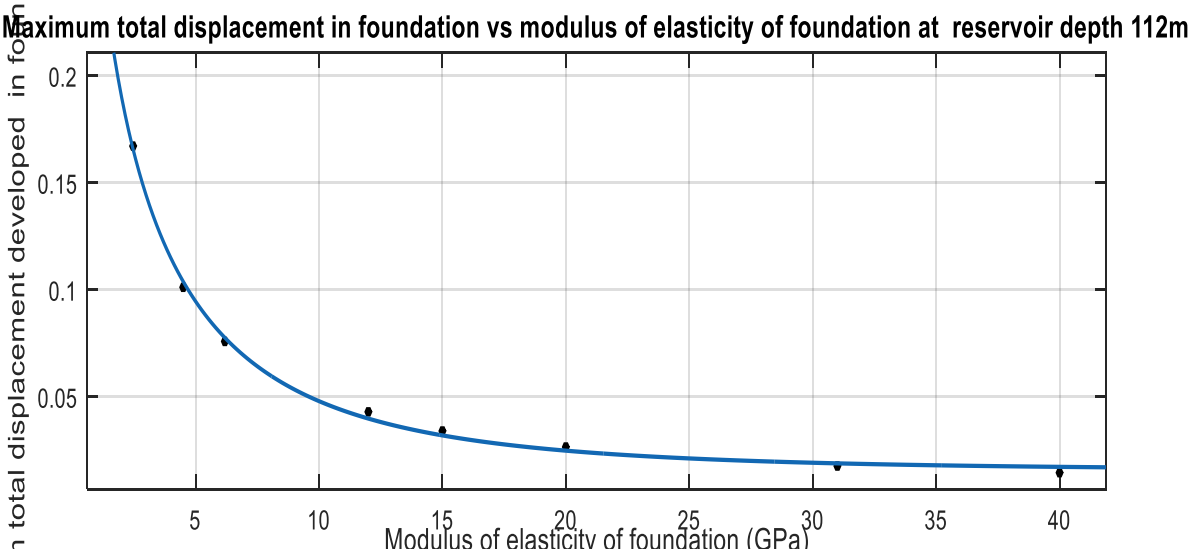

Figure B-7 Plot of total maximum deformation in foundation vs modulus of elasticity of foundation rock at reservoir depth 112m.

- At reservoir depth 162m

  d= 0.536*$e^{-0.8165*E_r^{0.5}}$+0.01625

  R-squared value =0.9974

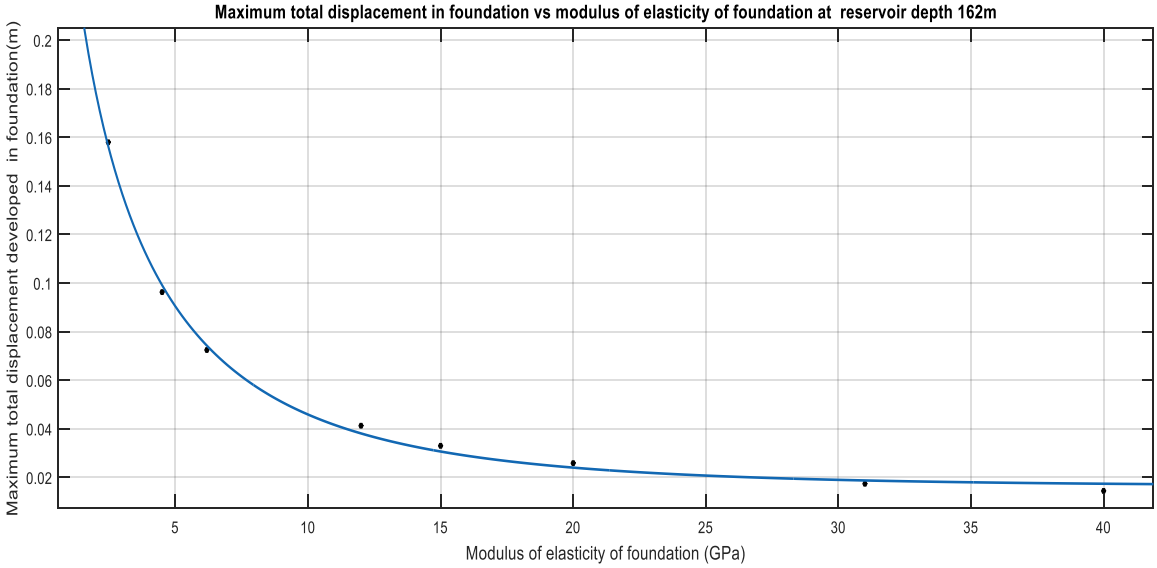

Figure B-8 Plot of total maximum deformation in foundation vs modulus of elasticity of foundation rock at reservoir depth 162m.

- At reservoir depth 187m

  d= 0.6832*$e^{-0.9746*E_r^{0.5}}$+0.01633

  R-squared value =0.998

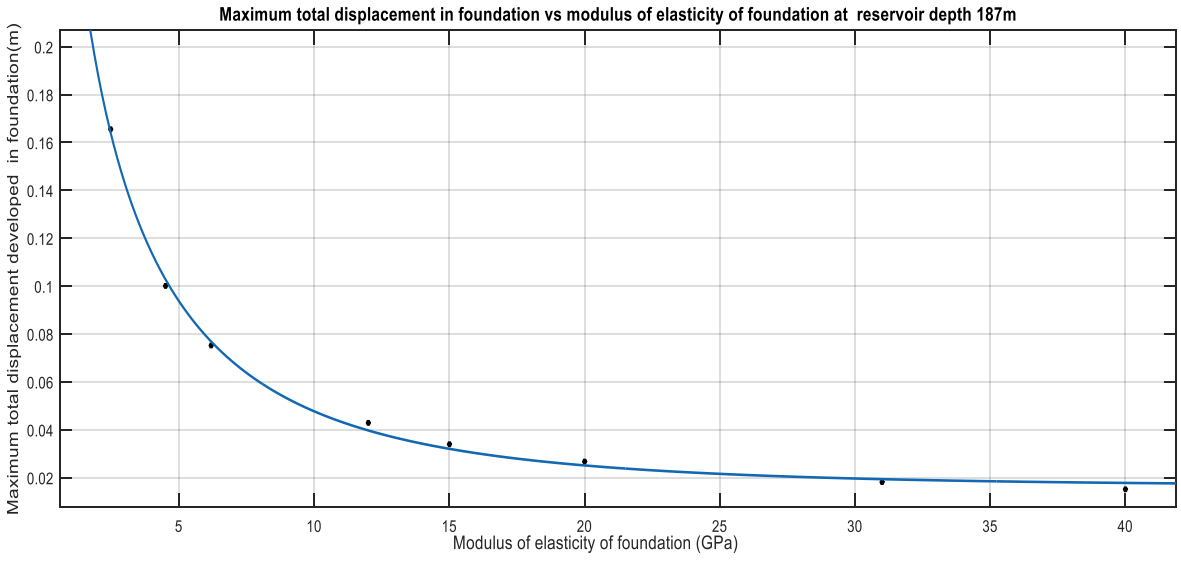

Figure B-9 Plot of total maximum deformation in foundation vs modulus of elasticity of foundation rock at reservoir depth 187m.

- At reservoir depth 212m

  d= 0.8527*$e^{-1.031*E_r^{0.5}}$+0.02027

  R-squared value =0.9963

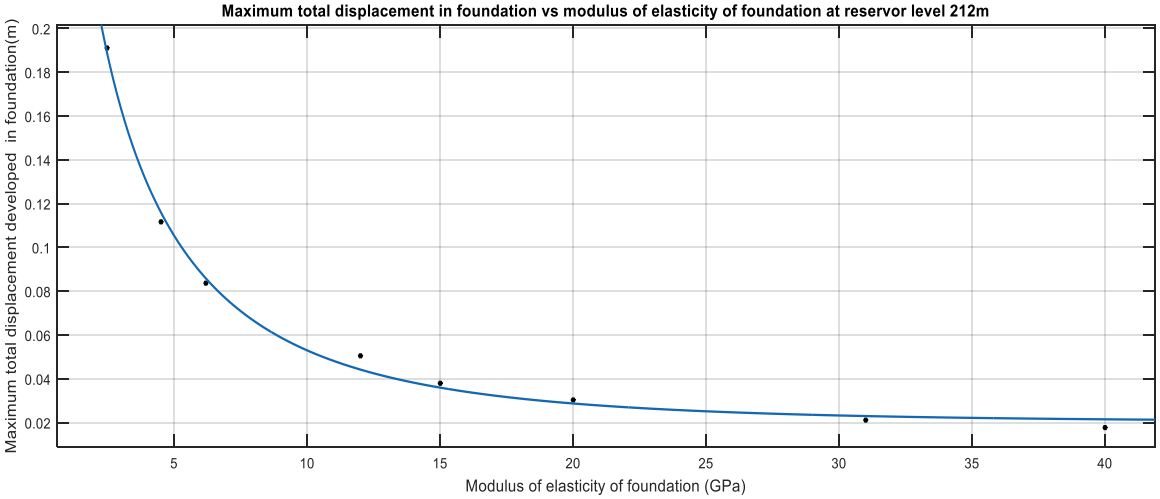

Figure B-10 Plot of total maximum deformation in foundation vs modulus of elasticity of foundation rock at reservoir depth 212m.

Relation between maximum plastic strains in foundation vs modulus of elasticity of foundation rock.

- At empty reservoir level

  ps= 0.02591*$e^{-1.494*E_r^{0.5}}$ + 8.261*10^{-5}

  R-squared value =0.9946

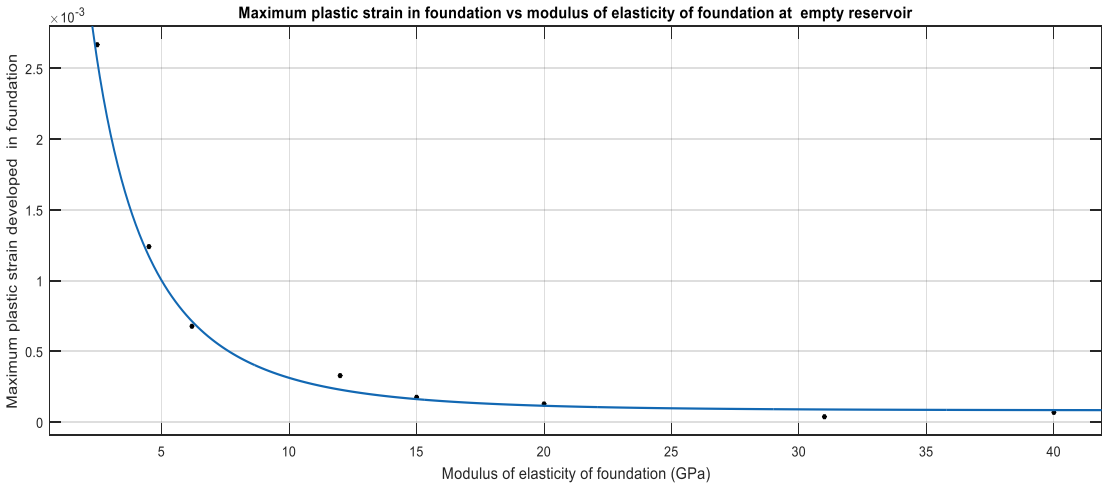

Figure B-11 Plot of maximum plastic strain in foundation vs modulus of elasticity of foundation rock at empty reservoir level (self-weight of dam).

- At reservoir depth 112m

  ps= 0.02202*$e^{-1.424*E_r^{0.5}}$ +14.56*10^{-5}

  R-squared value =0.9903

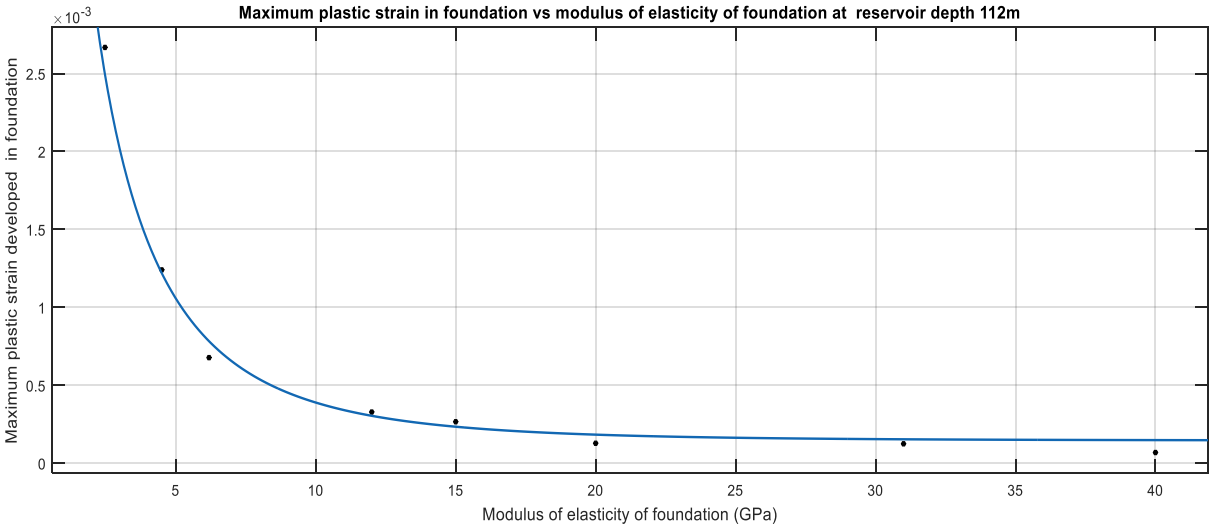

Figure B-12 Plot of maximum plastic strain in foundation vs modulus of elasticity of foundation rock at reservoir depth 112m.

- At reservoir depth 162m

  ps= $0.02834*e^{-1.541*E_r^{0.5}}+12.4*10^{-5}$

  R-squared value =0.9966

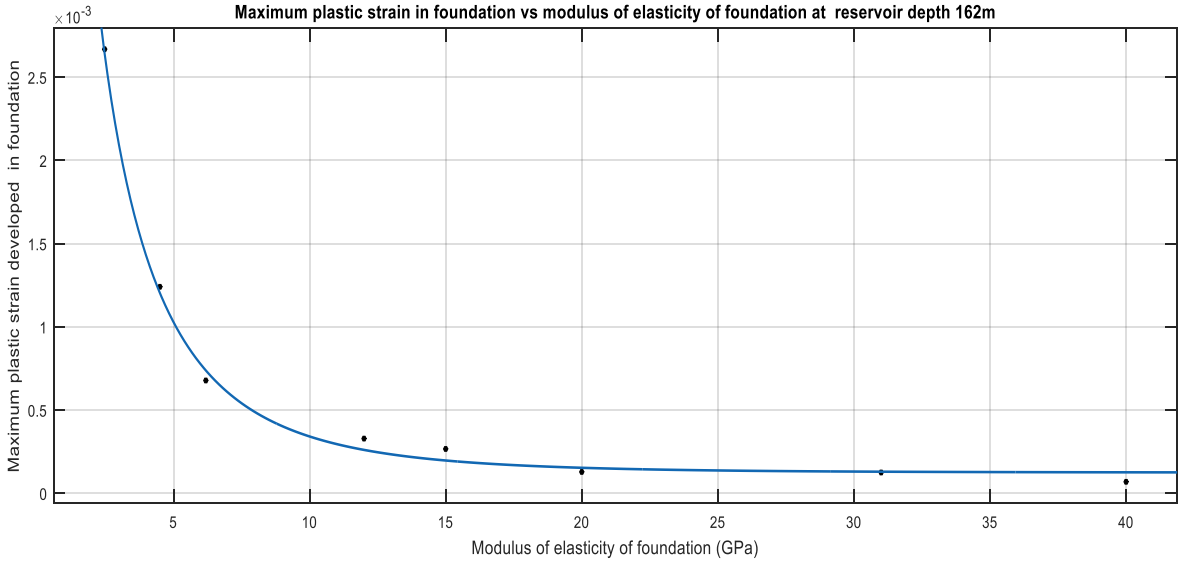

Figure B-13 Plot of maximum plastic strain in foundation vs modulus of elasticity of foundation rock at reservoir depth 162m.

- At reservoir depth 187m

  ps= $0.01569*e^{-1.118*E_r^{0.5}}+4.424*10^{-5}$

  R-squared value =0.9575

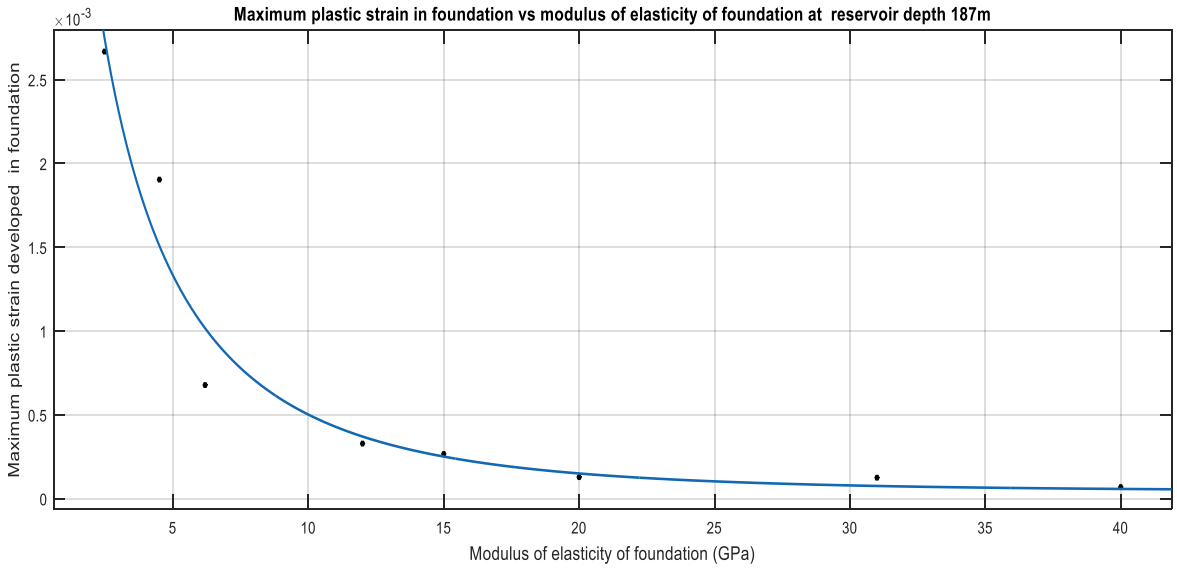

Figure B-14 Plot of maximum plastic strain in foundation vs modulus of elasticity of foundation rock at reservoir depth 187m.

- At reservoir depth 212m

  ps= 0.01561*$e^{-1.118*E_r^{0.5}}$ +4.866*10^{-5}

  R-squared value =0.9574

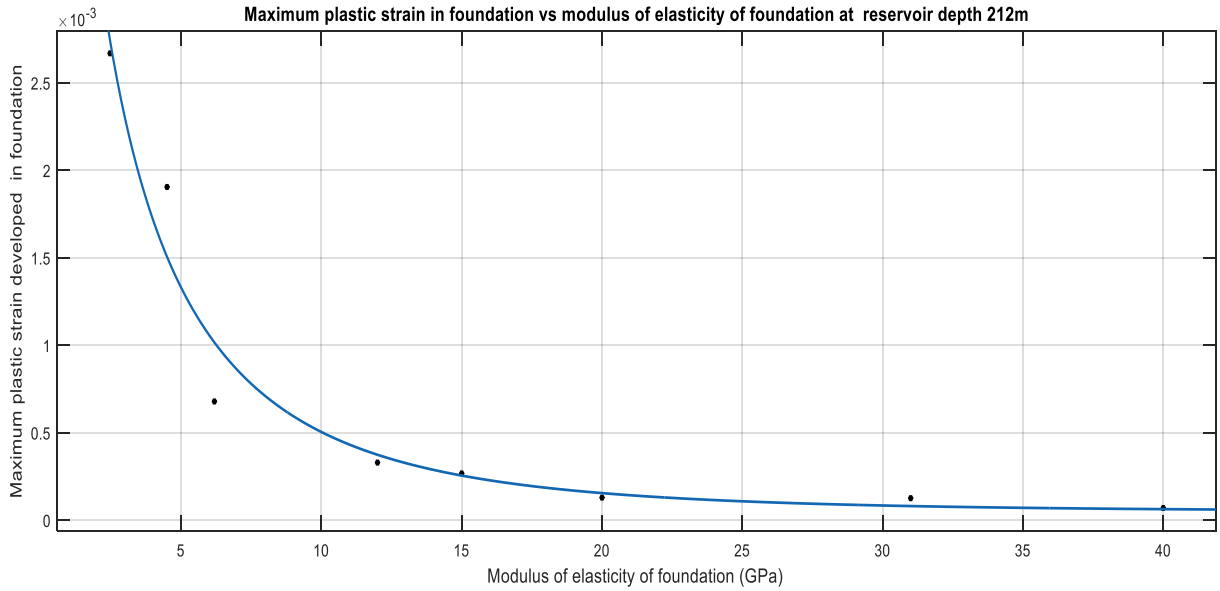

Figure B-15 Plot of maximum plastic strain in foundation vs modulus of elasticity of foundation rock at reservoir depth 212m.

APPENDIX C: SAMPLE FOR CALCULATION OF VECTOR METHOD FOR WEDGE STABILITY ANALYSIS

Vector analysis of Wedge stability					
Joint Properties					
Friction angle of plane1(φr1)=		20			
Friction angle of plane2(φr2)=		18			
Type of rock in wedge is Nourpul Quartzite					
Unit weight of rock=		2.6	gm/cm3		
Volume of wedge=		2.99E+06	m3		
Area of contact 1		2764.981542			
Area of contact 2		26985.69732			
Joint Wall Compressive strength					
Of joint 1	JCS1(kN/m2)=	60000			
Of joint 2	JCS2(kN/m2)=	60000			
Joint Roughness Cofficent					
Of Joint 1	JRC1=	2			
Of Joint 2	JRC2=	2			
Vector Properties of joints					
Direction cosine of normal to the plane 1(w1)					
-0.3021	-0.2359	0.9236			
Direction cosine of normal to the plane 2(w2)					
-0.502	0.4524	0.7371			
Direction cosine of intersection line of two plane(X12)					
-0.7498	-0.548	-0.3708			
Direction cosine of line perpendicular to intersection line and parallel to plane 1(S12a)					
0.5937	-0.8046	-0.0113			
Direction cosine of line perpendicular to intersection line and parallel to plane 1(S12b)					
-0.2387	0.7467	-0.6209			
Total load vector R					
579083.9209	-2578445.396	-7.05E+07			
Check either uplift occurs on surface					
on surface 1					
R.w1=	-6.47E+07	No uplift			
on surface 2					
R.w2=	-5.35E+07	No uplift			

For sliding direction					
Along surface 1					
R.S12a=	3.22E+06				
R.S12b=	4.17E+07				
As both R.S12a and R.S12b are positive so sliding will not occur on any one plane only					
AS sliding occurs at intersection line					
For direction of sliding					
R.X12=	2.71E+07	Downward			
As sliding occurs on intersection line					
Tangential force T12 (kN)=		2.71E+07			
Vector of tangential force T12=		-2.03E+07	-1.49E+07	-1.01E+07	
Normal to intersection N12=		2.09E+07	1.23E+07	-6.05E+07	
Normal force acting on plane 1(N1)=		61304527.14			
Normal force acting on plane 2(N2)=		59139293.4			
F.O.S=	1.53E+00				